SINTEF/NTNU

Design of 100 kW R744 compressor and plate heat exchanger test facility

Project work

Trondheim 2010

Author **Moo-Gyn Kim**

Supervisor **Dr.-Ing Armin Hafner**

PROJECT WORK
for
Moo-Gyn KIM

Design of 100 kW R744 compressor and plate heat exchanger test facility

Background and objective

Research on novel industrial refrigeration systems using natural refrigerants: To release the potential of refrigeration systems based on natural refrigerants, novel components ensuring high performance and maintainability are required. On a path to a sustainable energy future, energy systems applying natural working fluids represent a sustainable solution in many regions on earth. Oil-free compressors for natural working fluids like carbon dioxide, ammonia and hydrocarbons can change the refrigeration world completely.

In the near future a test facility will be build at SINTEF/NTNU to evaluate the performance of oil-free R744 compressors and plate heat exchangers in the power range of 100 kW (200-300 kW heat exchangers).

The following questions should be considered in the project work:

1. Literature survey on available test facility setups
2. Define layout of test circuits (P&ID)
3. Evaluate measurement equipment and data logging systems which could be applied for the test facility
4. Define support systems (external cooling system, etc) which are necessary to perform the experiments
5. Uncertainty analysis of the expected measurement results
6. Summary of the findings, draft version of a scientific paper
7. Further work

Acknowledgments

For the warm welcome at SINTEF and for the supervision and overall support for my bachelor's thesis I like to show my gratitude to Dr. Armin Hafner. I like to thank also Dr. Trond M. Anderson for assisting me with the design process of the plate heat exchangers and Dr. Håvard Rekstad for his support for the pressure vessel design.

I would also like to thank Selma M. Sveberg for helping me out with all the registration and application matters in Norway and the overall support.

Finally I like to thank my parents, Kim Young-Bok and Son Soo-Hwi and my two older brothers, Kim Moo-Jung and Moo-Song for their everlasting encouragement.

Table of Contents

I. Summary

In the near future a test facility will be build at SINTEF/NTNU to evaluate the performance of oil-free R744 compressors and plate heat exchangers in the power range of 100 kW (200kW heat exchangers). For the test facility a design concept has been proposed with the necessary plate heat exchangers and pressure vessel in detail. The design process has been documented with all equations listed. The calculated parameters with appropriate equipment lists are showcased in the appendix with a summarization and recommendation of available commercial equipments represented in the chapter *V Final recommended design with appropriate data*. Besides the thesis several *excel* modules programmed with *visual basic for application* are provided showcasing the design process in a deeper manner.

The present work has been carried out at SINTEF Energy and the Norwegian University of Science and Technology (NTNU), Trondheim in 2010.

II. Introduction

A. The development of carbon dioxide in the refrigeration industry

The use of carbon dioxide as a refrigerant has been done in 1866[1], 32 years after the invention of a close cycle refrigeration machine[2]. The main use of machines with carbon dioxide as a refrigerant was to transport frozen food overseas. Carbon dioxide has been favoured in the marine market to ammonia as a refrigerant and open air circuit cycles due to the small sizes of the machineries. The problem at that time was and still is the required high pressures for the use of carbon dioxide in a closed vapour compression cycle. First steps to cope with the problem have been made by introducing compressors[3] for the use with carbon dioxide in the 1890s.

However instead of further focusing in the design of compatible components, investigation in new synthetic refrigerants has been done by research programmes from General Motors and DuPont. As a result in the mid-50s, the Chloro-Fluoro-Carbon (CFC) and Hydoro-Chloro-Fluoro-Carbon (HCFC) were introduced as refrigerants. In a direct comparison to artificial refrigerants, carbon dioxide was and still is inefficient mainly due to the high evaporating and cooling pressures for commercial applications. As a result of a market-driven economy these synthetic refrigerants have almost completely supplanted carbon dioxide in the marine market due to less machinery costs.

Meanwhile their negative impact on the ozone and their global warming potential (GWP) caused by chemical reactions in the atmosphere encouraged the politics to restrict the use of synthetic refrigerants. The Montreal Protocol and the Kyoto Protocol are few examples of the political effort to encourage the industry in developing nature friendly solutions. One is the use of natural gases as refrigerant.

The recent development of pressure resistant components and political restrictions once more justifies the development in carbon dioxide refrigeration systems. Gustav Lorentzen published a report[4] which confirms the recent activities in the carbon dioxide

[1] Statement claimed on a patent by Thaddeus Lowe (23)
[2] Statement claimed on a patent by Jacob Perkins (20)
[3] Franz Windhausen patented an improved carbon dioxide compressor in 1886, followed by a compound compressor for CO2 by Everard Hesketh of J&E Hall in 1889
[4] Taken from Lorentzen, Gustav(17)

component research. They are mostly for transportation systems and only few are directed for industrial use however this seems quick to change. “Safety awareness backed by appropriate codes and legislation” [5] are the premise to carry over environment friendly systems to industrial level of HVAC systems in the future.

[5] Quoted from Pearson (19)

III. General design

A. General overview & process creation

The facility is to be designed to operate in different conditions as it is meant for the use of testing purposes. The goal is to research the potential of carbon dioxide as a refrigerant in high power ranges. Power is defined as the product of enthalpy difference and mass flow. To obtain wide ranges of power, different ranges of pressure, temperature and mass flow have to be achieved. Furthermore the behavior of the heat exchangers is investigated through parallel arrangement with equivalent divided mass flow on both streaming sides.

In this chapter the thermodynamic properties and transport properties of carbon dioxide will be introduced. The refrigeration process will be specified with the given boundary conditions in mind. With the circuit defined, the necessary components and instrumentals will be discussed. The layout of the test circuit will be defined through a P&ID.

Last but not least the thermo dynamic requirements and conditions for the equipment will be discussed. The final recommended design backed up with the appropriate data is done in Chapter V.

B. Thermodynamic properties of carbon dioxide

For the design process an excel library with the thermodynamic properties of carbon dioxide was provided by Sintef. Some important constants are listed in Table 1.

Table 1 Carbon dioxide - important datas and constans

Molecular formula/Refrigerant code	$CO_2/R744$
Molar mass	$M_{CO2} = 44{,}011\ kg/kmol$
Molar Normvolume	$V_{mn} = 22{,}263\ m^3/kmol$
Special gas constant	$R_{CO2} = 0{,}1889\ kJ/kgK$
Critical temperature	$t_{crit} = 31\ °C$
Critical pressure	$p_{crit} = 73{,}83\ bar$
Sublimations point	$t_s = -78{,}9\ °C$ at $0{,}981\ bar$
Tripel point	$t_T = -56{,}6\ °C$ at $5{,}18\ bar$

As commonly known the critical temperature of carbon dioxide is very low, resulting in a trans-critical cycle to achieve reasonable heating applications for heat rejection.

As it can be seen from the p,h-diagram in the appendix Figure 29, changes in temperature results in high pressure differences. This is one of the main reason carbon dioxide wasn't able to establish itself in commercial refrigeration applications.

The small density ratio of carbon dioxide results in a high refrigeration capacity which is defined as the product of the condensation enthalpy and the gas density. This fact also results in a more homogeneous two-phase flow thus increasing the heat transfer coefficient.

In general the heat coefficients in the different phases are high because of the favourable viscosity attributes thus prandl numbers of carbon dioxide in comparison to most artificial refrigerants.

C. The refrigeration process

The typical closed refrigeration process is done by compression, cooling, expansion and evaporation of the refrigerant. To keep the heat inside the system, the rejected heat can be used to evaporate the refrigerant. This is done by two external ethylene glycol circuits, as shown in Figure 1. The use of ethylene glycol instead of water was necessary because of the high temperature ranges of the heat rejection. The heat rejection will be in temperatures above 100°C and under 0°C. Ethylene glycol with a minimum of 50% concentration by volume should cope with these temperatures without freezing or evaporating.

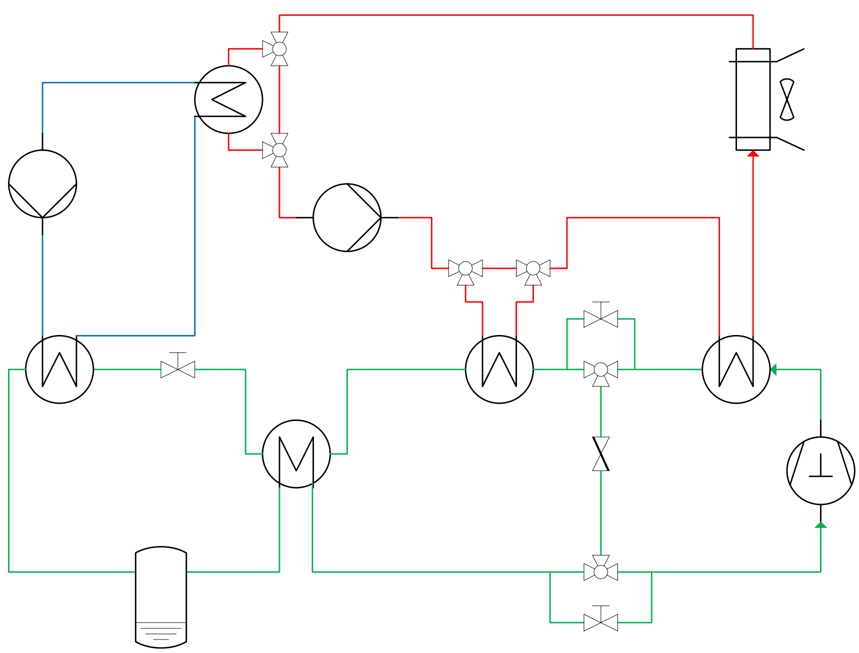

Figure 1 Process flow diagram with basic operation units. Green lines is indicate the carbon dioxide circuit, blue and red lines indicate the ethylene glycol circuits.

The heat created by the compressor will be rejected by an external air cooler. For testing purposes the compression enthalpy will first be transferred to the ethylene glycol circuit. Not shown in Figure 1 is that each heat exchanger for evaporating and heating purposes will be arranged in parallel order with split flow on each refrigeration side. For testing purposes the circuit has been divided through valves to test only the compression capacities.

The requested boundary conditions are summed up as follows:

- Shaft power 100kW
- Isentropic efficiency 0,8
- Compressor inlet temperatures from -40°C to 0°C
- Outlet pressures up to 130bar
- Duties of plate heat exchanger 200kW, accomplished in parallel order of a 100kW heat exchanger and two 50kW heat exchanger respectively

Following assumption have been made to calculate the process:

- The inlet temperatures results after a second overheating process of about 10K
- The overheating process is without pressure loss, thus the required pressures are taken directly from the outlet temperature of the evaporator and enthalpy
- The compression head is adiabatic and only the isentropic efficiency will be taken into account. The value is assumed to be 80%
- Pressure losses in all apparatus have been neglected
- All apparatus including pipes and instruments have been assumed to work adiabatic
- The compressibility factor has been neglected in trust on the provided carbon dioxide library
- The mass flow through the heat exchanger system is split in 1:2, 1:4, 1:4 relations
- The carbon dioxide will leave the pressure vessel without any liquid droplets
- A constant refrigeration charge is provided by the pressure vessel

With the given boundary conditions and made assumptions the adiabatic head for the compressor can be calculated through:

$$w_s = \frac{\kappa_{CO2}}{\kappa_{CO2} - 1} v_1 p_1 \left(\left(\frac{p_2}{p_1} \right)^{\frac{\kappa_{CO2}-1}{\kappa_{CO2}}} - 1 \right) \qquad \text{(III.D.1)}$$

With the purposed isentropic efficiency taken into account the mass flow rate is expressed by:

$$\dot{m} = \frac{P \cdot \eta_s}{w_s} \qquad \text{(III.D.2)}$$

To state every conditions of the carbon dioxide during the circuit a table has been created and put in the appendix Table 11 to indicate the calculation processes made. The complete result can be seen in the appendix Table 12 with the p,h-diagram showcasing the trans -critical circuit for the boundary design conditions.

The desired inlet temperatures are achieved by varying the mass flow through the compressor's rotation speed. This leads to two different boundary operation conditions. The conditions are showcased in the appendix Table 12 and Table 13 . If R744 is to have a compressor inlet temperature of $-50°C$ the heat rejection capacities are to reduce to 100kW for the cooling and the evaporating process as the efficiency would suffer.

D. Necessary equipments, instruments and plant layout

With the circuit defined, the necessary design parameters for the main components will be discussed.

Major operational variables for the compressor design are the compression ratio and the flow rate. This is also the case for the pumps in use. The main characterisation variable is their power input.

The heat exchangers are designed firstly after the type of heat exchangers in use; here plate heat exchanger with the inlets in counter current arrangement. The operation variables are the inlet temperatures, desired outlet temperatures and the mass flow. These variables are backed up by the thermodynamic attributes like density, vapour quality, viscosity and thermal conductivity of the fluid. The major variable characterizing the heat exchangers are their heat transfer area.

For the low-side liquid separator and receiver column it’s necessary to calculate the volume needed to secure constant refrigeration charge in the components at all times. After determining a reasonable maximum permissible pressure the thickness of the shell can be designed. The pressure vessel is characterized by its size and thickness.

The pipes are designed after reasonable assumptions and empirical data for the velocity. In general a permissible maximum pressure loss will be specified and the diameter will be designed after these values.

To obtain the necessary data to calculate the capacities of each apparatus, appropriate instrumentation have to be done. In interest of cost reduction unnecessary instrumentation has to be avoided.

E. Table of nomenclature - III General design

Symbol	Unit	Description
$\dot{m}$	kg/s	Mass flow
v	m^3/kg	Specific volume
p	Pa	Pressure
P	W	Power
w	kg/s	
η	$-$	Efficiency coefficient
κ	$-$	Specific heat ratio

Subscripts

$CO2$		Carbon dioxide
s		Isentropic

IV. Equipment design

A. General overview

The components will be discussed in this chapter, with the brazed plate heat exchangers, the pressure vessel and the instruments discussed in detail. This chapter has the purpose to show with which equations the design decision were justified. The results with appropriate data are stated in chapter V and in the tables listed in the appendix.

B. Heat exchanger

1. General description

Since the plate heat exchanger was introduced in the 1930s[6], the development has been continuously going forward to satisfy industrial requirements, from larger capacities for the use in the oil and gas industry to compact solutions for transportation systems. Today plate heat exchangers have a leading role in certain industrial applications. Due to the complex geometry high turbulence attributes can be achieved, hence they achieve good heat transfer rates. The high values of heat transfer results in a small required heat transfer area. Because of the possibility to achieve high heat fluxes a compact design of the plate heat exchanger can be accomplished.

One advantage is the modular design. Plate heat exchanger can be easily disassembled and then cleaned. The sacrifice for this modular construction is that those plate heat exchangers can't operate in high process pressures. To achieve high operating pressures meant to discharge the modular concept and to braze the plates together. One important reason for this facility is to investigate the possible capacities of these brazed plate heat exchangers in high operating pressures.

In this part of the thesis, the influence of the geometrical parameters on the heat transfer will also be investigated. The concept of brazed plate heat exchangers and thus the capability to achieve heat transfer processes in reasonable temperatures is relatively new. Hence only few methods are published to design plate heat exchanger for this application. Thus the design choices are all based on theoretical approaches and the geometrical parameters were modified upon existing brazed plate heat exchangers. The

[6] 1923 by Richard Seligman

presented correlations are also based on different facility set-ups and are only used to determine a vague design recommendation for the heat exchanger.

2. Design parameters

There are a quite amount of geometrical parameters to design a plate heat exchanger. The important parameters to calculate the required heat transfer area for the plate heat exchanger are shown in Figure 2.

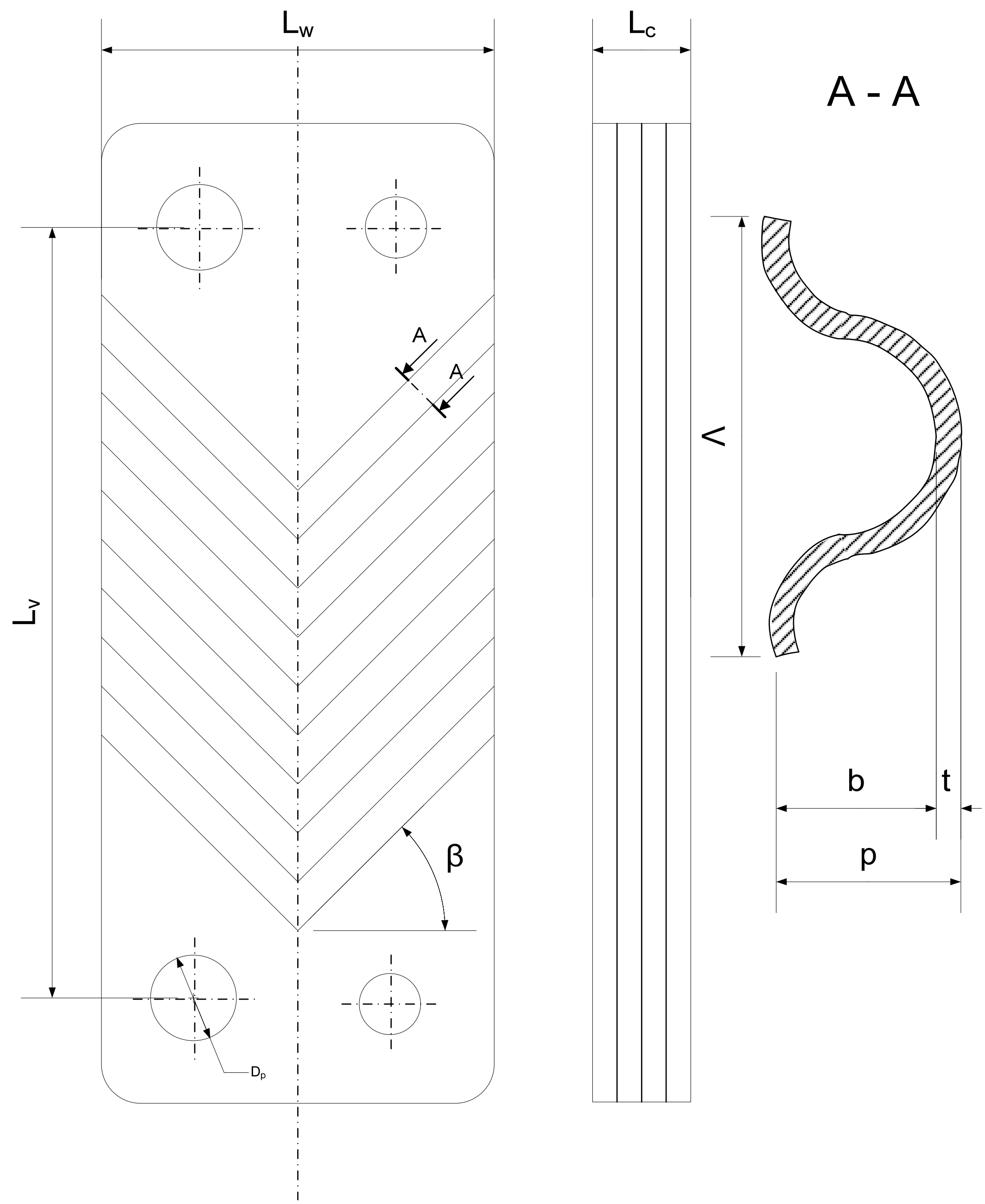

Figure 2 Geometry parameters of an brazed plate heat exchanger.

For all fluid transport parameters the hydraulic diameter is defined as:

$$d_h = \frac{b}{\Phi} \tag{IV.B.1}$$

where the mean channel spacing is illustrated in Figure 2. is determined as follows:

$$b = p - t \tag{IV.B.2}$$

with p being the plate pitch and t the thickness of the plate. The plate pitch can also be calculated as

$$p = \frac{L_c}{N_t - 1} \tag{IV.B.3}$$

where N_t is the amount of plates. The area enlargement factor for a sinusoidal corrugation on a plate can be calculated after H. Martin (1) as follows:

$$\Phi \approx \frac{1}{6}\left(1 + \sqrt{1 + X^2} + 4\sqrt{1 + \frac{X^2}{2}}\right) \tag{IV.B.4}$$

With the use of a dimensionless corrugation parameter, where Λ is the wavelength of the sinusoidal corrugated plate.

$$X = \frac{\pi \cdot b}{\Lambda} \tag{IV.B.5}$$

Usually the enlargement factor is given by the manufacturer. The value ranges from 1.77 to 1.22. For further calculation the value 1.22 has been taken Lower values means that the mean channel spacing is shorter while the corrugation form will be more flat.

The fluid transport parameters common in each heat transfer process are listed here. If the thermodynamic attributes are different because the fluid is to be assumed in a two-phase legion the equation will be shown separated. All thermodynamic attributes are assumed in a specific interval defined later on in this chapter.

Equivalent mass flux through the channel is defined as

$$G_{eq} = \frac{\dot{m}}{N_{cp} \cdot b \cdot L_w} \tag{IV.B.6}$$

with N_{cp} being the number of channel per pass. The equivalent mass flux is defined differently in the boiling process as the influence of the vapor quality must be considered.

The Prandtl number is defined as follows:

$$Pr = \frac{\eta \cdot c_p}{\lambda} \tag{IV.B.7}$$

The Reynold number is calculated as follows:

$$Re = \frac{G_{eq} \cdot d_h}{\eta} \tag{IV.B.8}$$

a) *Influence of geometry parameters on overall heat transfer capacity*

In this part of the chapter the influence of the geometrical parameters is investigated. One of them is the corrugated form on the plates. The most common corrugated pattern in use is of chevron design as indicated in Figure 2. The chevron angle β has a significant influence on the heat transfer coefficient and the frictional pressure loss. During the design process it is of great importance to know of its influence on the overall design. During this work a program was written in *visual basic for application* to calculate the overall heat transfer capacity of a plate heat exchanger with variable geometric parameters as input.

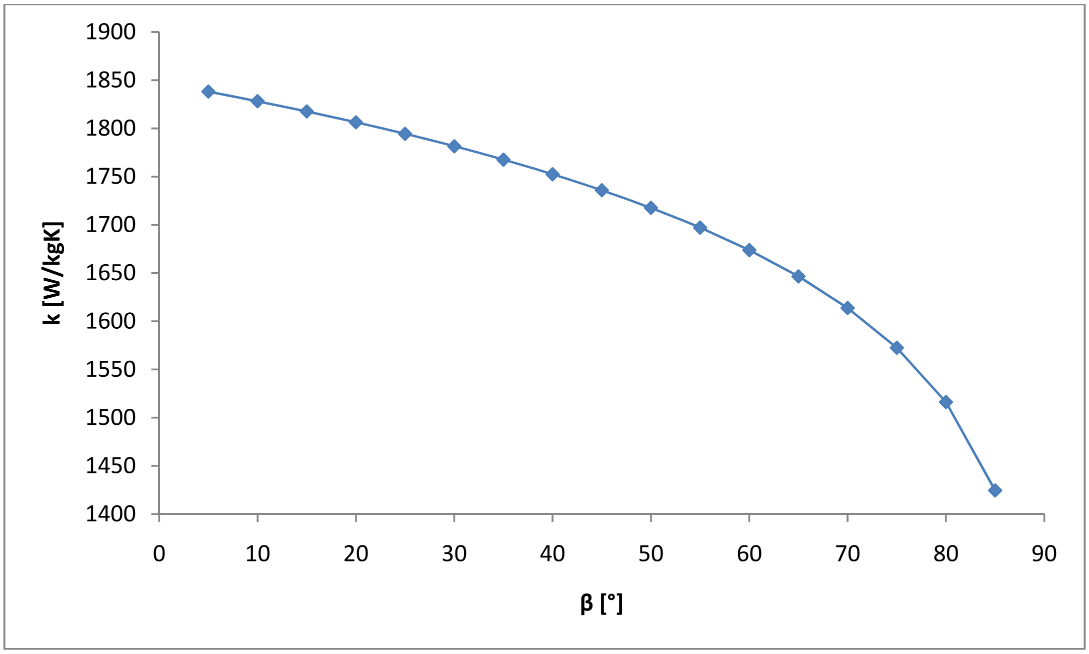

Figure 3 Influence of the chevron angle on the heat transfer coefficient.

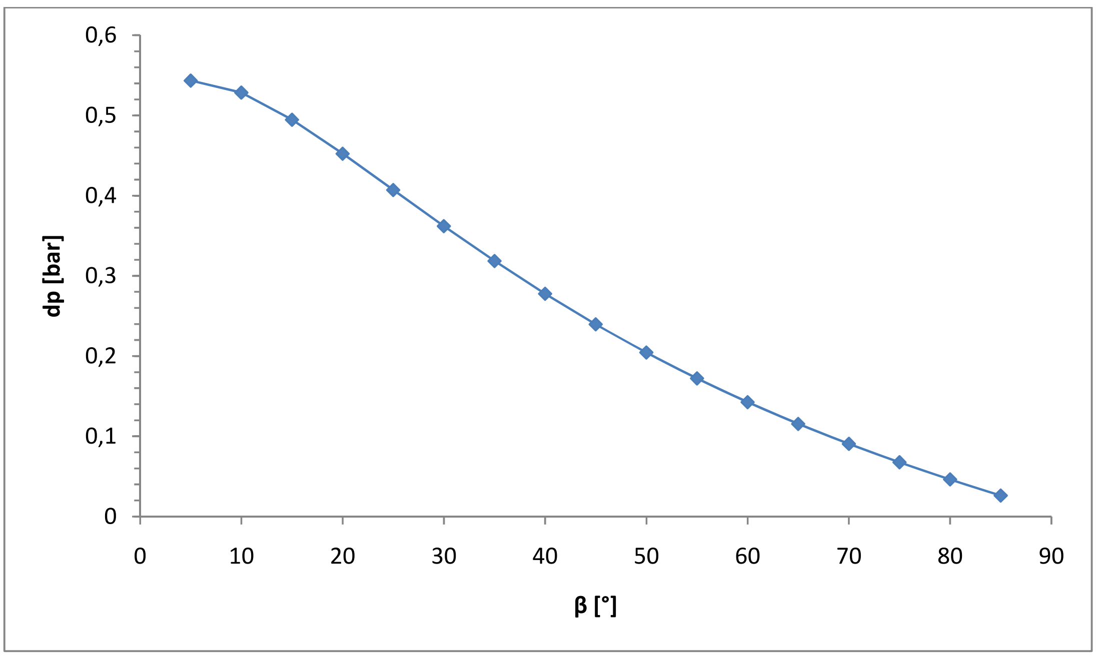

Figure 4 Influence of the chevron angle on the pressure loss.

Figure 3 shows the Influence of the chevron angle on the heat transfer coefficient. The overall heat transfer coefficient decreases with higher chevron angle. Figure 4 shows the Influence of the chevron angle on the frictional pressure loss. A higher chevron angle will reduce the frictional pressure loss in the plate heat exchanger. It can be seen that design decision has to be made by comparing the required transfer area resulting in material costs versus the pressure loss resulting in higher process costs. As many previous works have been made with plate heat exchangers with an chevron angle of 45° it seems to be on the safe side to follow the trend an also recommended a chevron angle of 45°.

The test facility will be operating with a high mass flow. That means that the flow channel has to be increased to reduce frictional pressure losses in the plate heat exchanger. One efficient way is to increase the geometric values defining the hydraulic diameter namely the mean channel spacing as shown in equation III. Another way is to increase the general width of the corrugated plates L_w. Both values reduce the mass flux thus decreasing the pressure loss as showcased in equation III.

To decide which way would be more efficient in regards on mainly the thermodynamic attributes the influences of both geometric parameters on the required heat transfer area and the pressure lost has been compared.

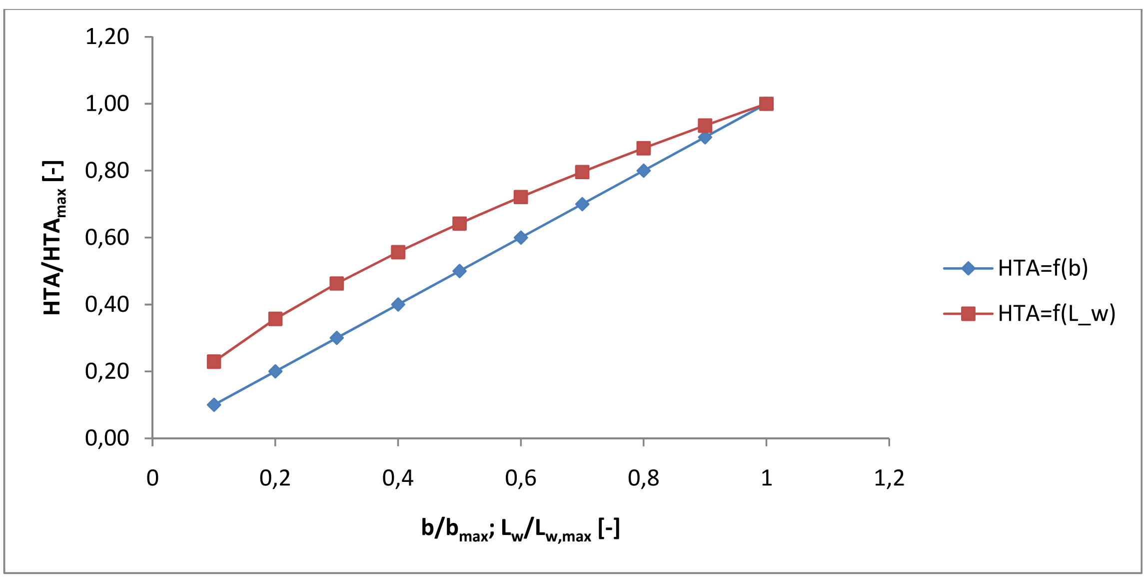

Figure 5 influence of mean channel spacing and the general width on the required heat transfer area. All values are normalized. The enlargement factor Φ has been hold constant at all times.

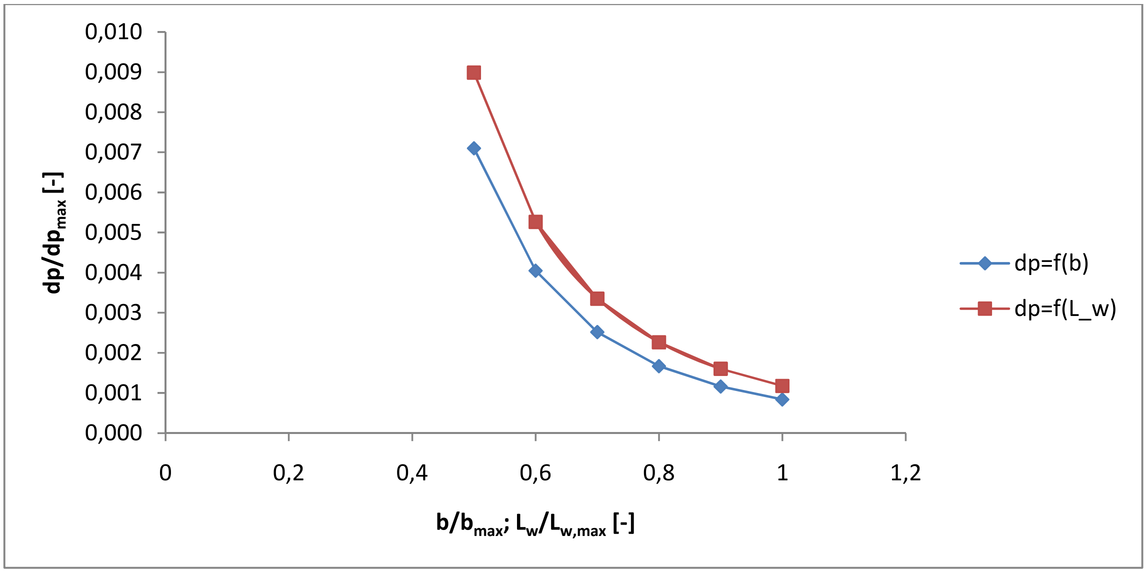

Figure 6 influence of mean channel spacing and the general width on the pressure loss in the plate heat exchanger. All values are normalized. The enlargement factor Φ has been hold constant at all times.

Figure 5 and Figure 6 shows the influence of b and L_w on the required heat transfer and the pressure loss respectively. Therein the values from $\mathrm{b_{max}}$ and $\mathrm{L_{w,max}}$ has been normalized by 10mm and 247mm respectively. Increasing the mean channel spacing b results in a lower heat transfer area and lower pressure losses as increasing the plate width L_w does. It shows that increasing the mean channel spacing by holding the enlargement factor constant seems to be more efficient then increasing the overall width.

3. Heat transfer coefficient

To determine the heat transfer coefficient in plate heat exchangers for special conditions during the heat transfer process the scientific report from García-Cascales, et al. (2) proved to be very helpful. They compared the different available equations with each other and listed them in their paper. Figure 7 shows the different equations in comparison. It has been decided to be on the save side to use the equation with the most stable curves and with a relative small heat transfer coefficient especially in the design of a test facility operating in dimensions there empirical information is missing. The used equations will be highlighted in the specified chapters.

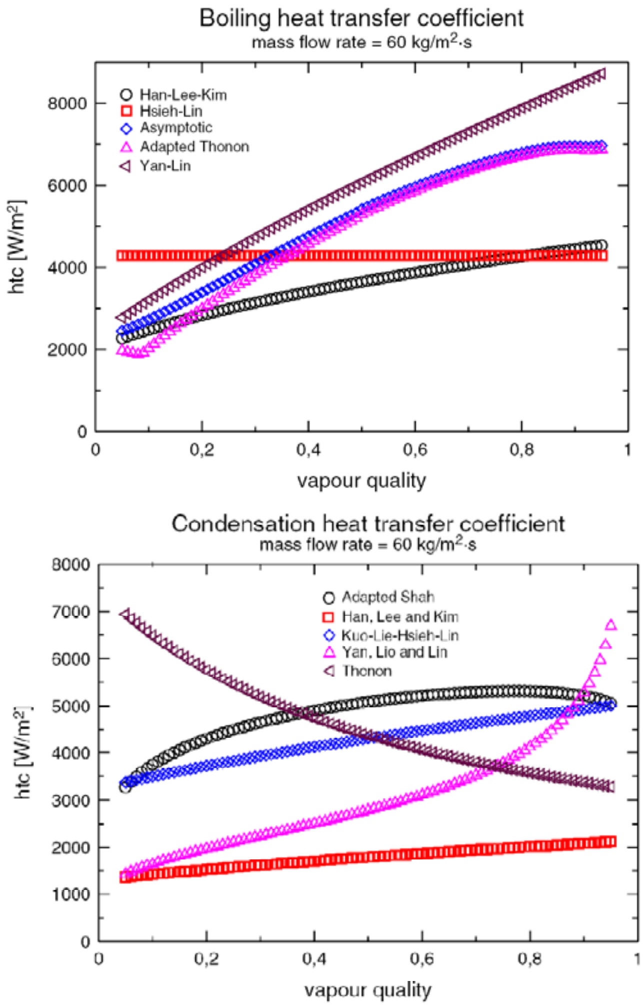

Figure 7 Comparison of the different equation in use taken from García-Cascales, et al. (3)

a) Single phase

To calculate the Nusselt number for single phase flow the equation from Y.-S. Kim, et al (3) has been taken. This equation considers the influence of the chevron angle.

$$\mathrm{Nu} = 0{,}295 \cdot \mathrm{Re}^{0{,}64} \cdot \mathrm{Pr}^{0{,}32} \cdot \left(\frac{\pi}{2} - \beta\right)^{0{,}09} \qquad \text{(IV.B.9)}$$

The heat transfer coefficient has been calculated as follows.

$$\alpha_{CO2} = \frac{\mathrm{Nu} \cdot \lambda}{d_h} \qquad \text{(IV.B.10)}$$

b) Condensation

Based on the experimental data of D.-H. Han, et al. (4) the following equations are used to calculate the heat transfer during condensation phase. During the calculation the vapor quality had to be taken into account. This is done by taking the thermo dynamical attributes of the liquid and gas phases in each calculation interval into consideration.

$$\mathrm{Pr_G} = \frac{\eta_G \cdot c_{pG}}{\lambda_G} \tag{IV.B.11}$$

$$\mathrm{Pr_L} = \frac{\eta_L \cdot c_{pL}}{\lambda_L} \tag{IV.B.12}$$

$$\mathrm{Pr} = x \cdot \mathrm{Pr_G} + (1 - x) \cdot \mathrm{Pr_L} \tag{IV.B.13}$$

The Nusselt number is calculated after the following equation:

$$\mathrm{Nu} = G_{e1} \cdot \mathrm{Re}_h^{G_{e2}} \cdot \mathrm{Pr}^{\frac{1}{3}} \tag{IV.B.14}$$

For each iteration step the heat transfer coefficient has been calculated to take the change of vapour quality into account.

$$\alpha_{CO2} = \frac{\mathrm{Nu} \cdot (x \cdot \lambda_G + (1 - x) \cdot \lambda_L)}{d_h} \tag{IV.B.15}$$

c) Evaporation

The evaporation process in general can be investigated by separating the convective boiling, the nucleate boiling, flow boiling, vapour heat and wet wall heat transfer processes. Usually heat transfer coefficients of these different conditions during the evaporation process are calculated separately and then super positioned together. The equation presented by D.-H. Han, et al. (5) simplifies the correlation by using a single phase correlation with an enhancement factor.

$$g = \frac{\dot{m}}{N_{cp} \cdot b \cdot L_w} \tag{IV.B.16}$$

$$G_{e1} = 2{,}81 \cdot \left(\frac{\lambda}{d_h}\right)^{-0{,}041} \cdot \left(\frac{\pi}{2} - \beta\right)^{-2{,}83} \tag{IV.B.17}$$

$$G_{e2} = 0{,}746 \cdot \left(\frac{\lambda}{d_h}\right)^{-0{,}082} \cdot \left(\frac{\pi}{2} - \beta\right)^{0{,}61} \tag{IV.B.18}$$

$$G_{eq} = g \cdot \left(1 - x + x \cdot \left(\frac{\rho_l}{\rho_g}\right)^{\frac{1}{2}}\right) \tag{IV.B.19}$$

$$q_w = q_{w,i} \tag{IV.B.20}$$

$$B_{oeq} = \frac{q_w}{G_{eq} \cdot q_h} \tag{IV.B.21}$$

With the heat flux q_w iterative determined. The Prandtl number is calculated as in equation (IV.B.13). The Nusselt number is determined as follows:

$$Nu = G_{e1} \cdot Re^{G_{e2}} \cdot B_{oeq}^{0{,}3} \cdot Pr_c^{0{,}4} \tag{IV.B.22}$$

$$\alpha_{CO2} = \frac{Nu \cdot (x \cdot \lambda_G + (1 - x) \cdot \lambda_L)}{d_h} \tag{IV.B.23}$$

4. Heat transfer area

With the given equation the calculation of the required heat transfer area has been calculated by writing a program in VBA. The simplified program structure can be seen in Figure 8.

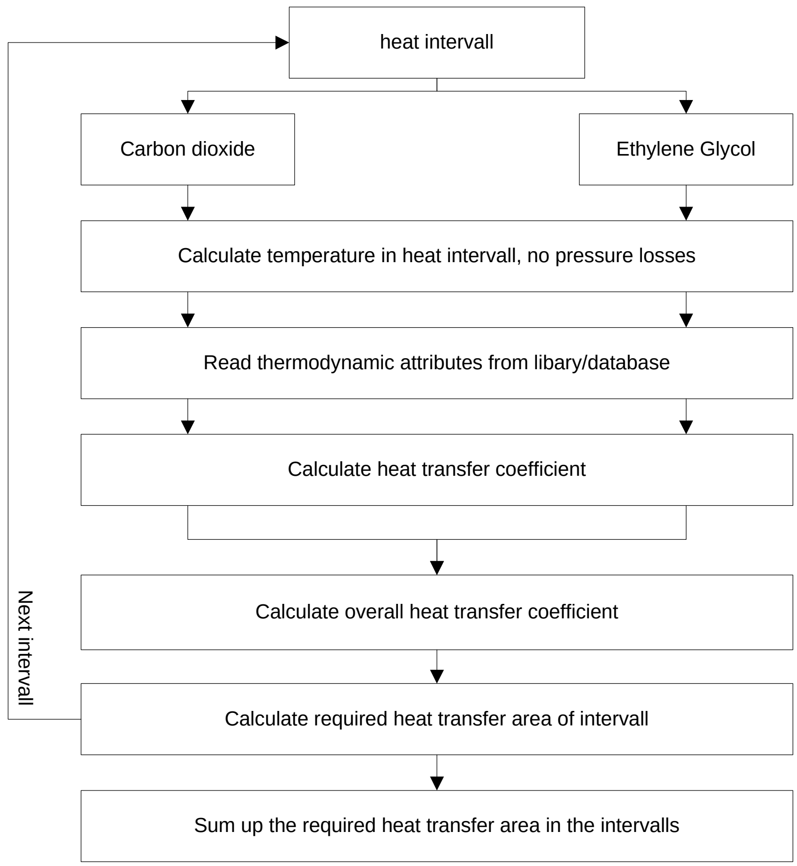

Figure 8 Basic scheme of the program structure used to calculate the required heat transfer area

The heat transfer area in an interval has been calculated with the logarithmic temperature approach. As the overall heat transfer coefficient and the local temperature differs in the heat exchanger the required heat transfer areas has been calculated splitting the calculation process in intervals and summing them together. The required heat transfer area in one interval was calculated as follows:

$$A = \sum dA_i = \sum \frac{q_i}{\dfrac{U_i \Delta T_{i,in} - U \Delta T_{i,out}}{\ln\left(\dfrac{U_i \Delta T_{i,in}}{U_i \Delta T_{i,out}}\right)}} \qquad \text{(IV.B.24)}$$

As shown in Figure 8 the calculation process was done without consideration of the pressure losses.

5. Pressure loss

The total pressure loss consist of the pressure loss through acceleration, static head, pressure drop in the port in- and outlet and the frictional pressure loss. Therein the frictional pressure loss takes the greatest amount of the total pressure loss.

$$\Delta p = \Delta p_{acceleration} + \Delta p_{static} + \Delta p_{port} + \Delta p_{friction} \tag{IV.B.25}$$

The pressure loss through acceleration can be determined as follows:

$$\Delta p_{acceleration} = \left(\frac{G_{eq}^2 \cdot x}{\rho_{fg}}\right)_{out} - \left(\frac{G_{eq}^2 x}{\rho_{fg}}\right)_{in} \tag{IV.B.26}$$

With the mass flux calculated as follows:

$$G_c = \frac{\dot{m}}{N_{cp} \cdot b \cdot L_w} \tag{IV.B.27}$$

$$G_{eq} = G_c \left(1 - x + x\left(\frac{\rho_l}{\rho_g}\right)^{\frac{1}{2}}\right) \tag{IV.B.28}$$

The static pressure loss is determined by the height of the plate heat exchanger

$$\Delta p_{static} = \rho_m g L_v \tag{IV.B.29}$$

The pressure loss created by the port in- and outlet of the plate heat exchanger ports can be determined by after S.Kakac, et al.(6)

$$\Delta p_{port} = 1{,}4 \frac{G_p^2}{2\rho_m} \tag{IV.B.30}$$

Where the port mass flux can be determined as follows:

$$G_p = \frac{\dot{m}}{\pi \cdot \frac{D_p^2}{4}} \tag{IV.B.31}$$

with D_p as the diameter of the inlet or outlet.

a) frictional pressure loss

The frictional pressure loss is usually determined by measuring the total pressure loss and calculates it after equation (IV.B.25). For design purposes it is important to know the frictional pressure loss beforehand. The equations to calculate the frictional pressure loss has been taken from H. Martin (1).

$$\Delta p_{\mathrm{friction}} = \frac{\xi \cdot \rho \cdot w^2 \cdot L_v}{2 \cdot d_h} \tag{IV.B.32}$$

with w as the volume flow through the channel

$$w = \frac{\dot{m} \cdot \left(\frac{1}{\rho}\right)}{b \cdot L_w} \tag{IV.B.33}$$

The friction factor ξ is a function of the Reynolds number, inclination angle and a number of geometrical parameters. It can be determined by

$$\xi = \left(\frac{\mathrm{Cos}(\phi)}{\left(b \cdot \mathrm{Tan}(\phi) + c \cdot \mathrm{Sin}(\phi) + \frac{\xi_0}{\mathrm{Cos}(\phi)}\right)^{\frac{1}{2}}} + \frac{\left(1 - \mathrm{Cos}(\phi)\right)}{(\xi_1)^{\frac{1}{2}}} \right)^{-2} \tag{IV.B.34}$$

With ϕ is defined as $\pi - \beta$. As stated above the frictional factor is a function of the Reynolds number and the inclination angle. Both are taken into account by the following equations. For $Re_m < 2000$ the frictional factors ξ_0 and ξ_1 respectively are determined by the following equation:

$$\xi_0 = \frac{B_o}{Re_m} \tag{IV.B.35}$$

$$\xi_1 = \frac{B_1}{Re_m} + C_1 \tag{IV.B.37}$$

For the case $Re_m \geq 2000$ the frictional factors have to be calculated as follows:

$$\xi_0 = \left(1{,}8 \cdot \frac{\log(\mathrm{Re_m})}{\log(10)} - 1{,}5\right)^{-2} \tag{IV.B.38}$$

$$\xi_1 = \frac{\mathrm{K_1}}{\mathrm{Re_m^n}} \tag{IV.B.39}$$

For the general design the geometrical parameters can be replaced by empirical values as stated by H. Martins report (1),

- $a = 3{,}8$
- $b = 0{,}18$
- $c = 0{,}36$
- $B_o = 64$
- $B_1 = 597$
- $C_1 = 3{,}85$
- $K_1 = 39$
- $n = 0{,}289$

6. Table of nomenclature – IV.B Heat exchanger

Symbol	Unit	Description
A	m^2	Heat transfer area
b	m	Mean channel spacing
c_p	$J/(kgK)$	Isobaric specific heat capacity
d_h	m	Hydraulic diameter
G_{eq}	$kg/(m^2s)$	Equal mass flux
g	$kg/(m^2s)$	mass flux
L_c	m	Depth of plate heat exchanger
L_v	m	Height of plate heat exchanger
L_w	m	Width of plate heat exchanger
$\dot{m}$	kg/s	Mass flow
N_{cp}	$-$	Number of channels
N_t	$-$	Number of plates
Nu	$-$	Nusselt number
p	m	Plate pitch
Pr	$-$	Prandl number
q_w	W/m^2	Heat flux
Re	$-$	Reynold number
T	$°C$	Temperature
U	W/m^2K	Overall heat transfer coefficient
w	m/s	Velocity
x	$-$	Vapor quality
X	$-$	Dimensionless corrugation parameter
α	W/m^2K	Heat transfer coefficient
β	rad	Chevron angle
Λ	m	Wavelength
λ	W/mK	Thermal conductivity
η	Pas	Dynamic viscosity
Φ	$-$	Area enlargement factor

ϕ	rad	$\pi - \beta$ Chevron angle with vertical root
ξ	$-$	Friction factor

Subscripts

G	Gas
L	Liquid
i	Indices
m	Average

C. Pressure vessel

1. General description

During the start up process the carbon dioxide will be compressed, cooled and then expanded creating a high pressure side and a low pressure side in the circuit as shown in Figure 9. If the total carbon dioxide charge in the circuit would be considered constant the compressor could dry out due to the lack of carbon dioxide charge in the inlet of the compressor. Thus a buffer volume is needed to increase the volume during the start up process. After Pettersen (7) there are two possible locations for the buffer volume to be placed in the carbon dioxide circuit. It can be placed either in the high-pressure system side or low-side pressure system side. Both of them will result in different requirements on the pressure vessel. In this work the low side pressure buffer system arrangement will be considered as shown in Figure 9.

Besides of the task to prevent drying up the compressor, a buffer system is mainly needed for safety reasons. Most of them are directed to the compressor's behaviour. If the compressor stops operating during a fully charged system, the carbon dioxide on the low pressure side can easily build up high pressures due to high ambient temperatures. It can also be avoided by integrating control engineering components in combination with security valves but these are second hand solutions and correct working at all times can't be guaranteed. Another advantage is that the pressure vessel can provide refrigeration charge compensating leakages inside the system.

The low-pressure receiver in use also has the task of liquid/gas separation which will be evaluated later in this chapter.

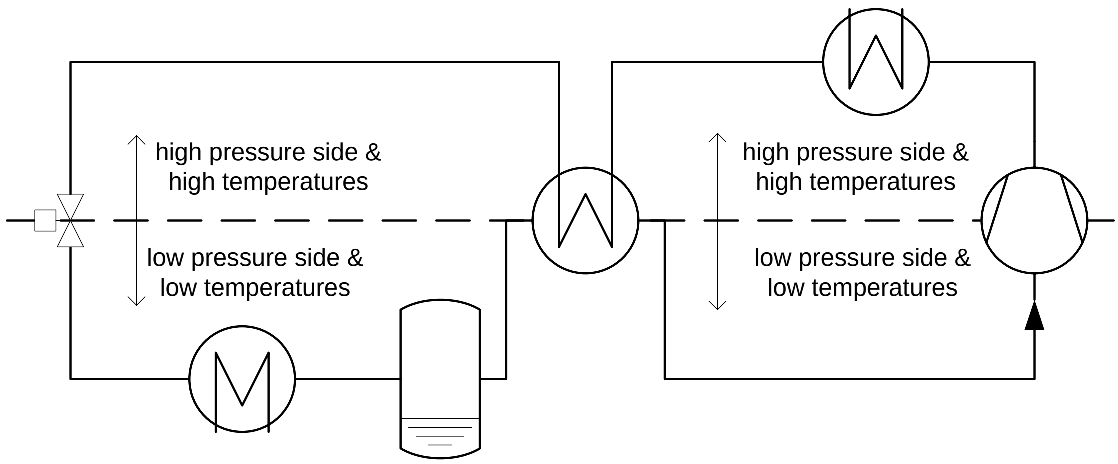

Figure 9 Configuration of a CO2 circuit with the pressure vessel on the low pressure side.

During the designing process of the pressure vessel the boundary conditions have to be calculated after the safety requirements. First a worst case scenario has to be established usually exceeding the operation conditions. The operation conditions on the low pressure side are listed in Table 2 with the chosen design parameters.

Table 2 Operation conditions in the low pressure side and chosen design conditions

	$p_{operating}$ [bar]	p_{design} [bar]	$t_{Operating}$ [°C]	t_{design} [°C]
minimum	6,83	1	-50,00	-50,00
maximum	26,5	100	0	100

The design of the pressure vessel itself has been done in accordance to the pressure directive EN13445. The volume that is needed to feed the carbon dioxide circuit with sufficient refrigerating charge has been calculated as follows:

$$V_{vessel} = \left(m_{HP,operate} - m_{HP;80bar;50°C}\right) \cdot v_{HP;80bar;50°C} + \left(m_{LP,operate} - m_{LP;80bar;50°C}\right) \cdot v_{LP;80bar;50°C} \qquad \text{(IV.C.1)}$$

Therein $v_{HP;operate}$ and $v_{LP;operate}$ are the specific volumes that arise if the compressor is operating. It has been assumed that the carbon dioxide will have a specific volume of

$v_{80bar;50°C} = 0{,}00456 m^3/kg$ equivalent to $\rho_{80bar;50°C} = 0{,}22 kg/l$ before the start up process. The difference of the volumes is the needed buffer volume.

With the necessary height of the cylindrical part of the vessel assumed as $H_{Vessel} = 0{,}4m$ the diameter of the cylindrical shell can be calculated as follows:

$$D_e = \sqrt{\frac{4V_{vessel}}{\pi H_{vessel}}} \tag{IV.C.2}$$

To have extra volume for leakages, the vessel should be of greater volume than needed. This has been taken into account by considering only the cylindrical volume for the needed buffer space as follows:

$$V_{cylindrical\ shell} = V_{vessel} \tag{IV.C.3}$$

The extra volume for free use, result from the hemispherical ends of the vessel which can be approximated as follows:

$$V_{hemispherical\ end} = 0{,}1298 \cdot (D_e - 2 \cdot e)^3 \cdot 2 \tag{IV.C.4}$$

With a design thickness valued:

$$e = 0{,}004 \cdot D_e \tag{IV.C.5}$$

The results are listed in the appendix and in chapter V.

2. Design after pressure directive EN 13445

The design will be according to the pressure directive EN 13445:2002. Designing after pressure directives involves an iterative approach. The engineer assumes certain wall thicknesses for the pressure vessel and then controls if the values can withstand the pressure and stresses inside the used materials. Generally speaking the design parameters are adapted according to the resulting stresses in the materials. Despite of the material data which are listed in several directives the designing process involves the use of many safety coefficients which have been determined through empirical data.

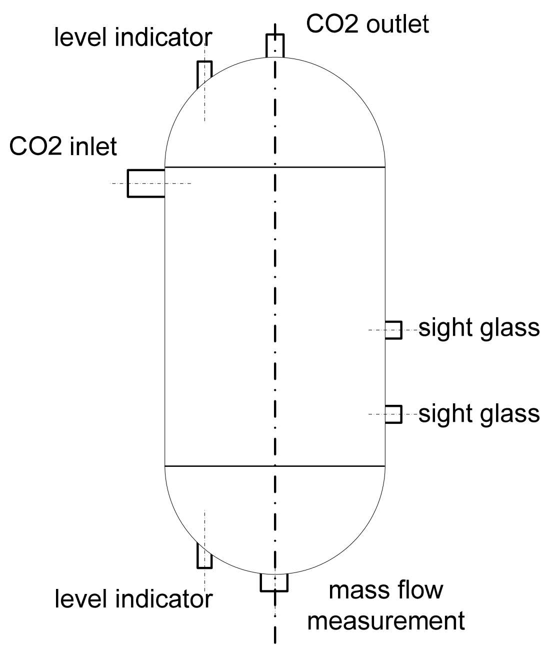

Figure 10 principle sketch of the pressure vessel with the in- and outlets

a) Material choice

The material choice has to be made in consideration with the set boundary conditions of the low pressure side as stated in Table 2. After E.Klapp (8 S. 91) unalloyed steels have a excessive reduction in impact energy attributes when operating in minus temperatures. Either austenitic steels or Ni alloyed steels were recommended. To avoid unnecessary costs for the design of the pressure vessel normalised 12Ni14 steel after EN 10222:1998 with a thickness in the range of $0mm < t_e < 35mm$ has been chosen. This steel falls in the pressure directive EN16445-2 Annex A into the Group 9.2 for nickel alloyed steel.

The nominal design stress f is the minimum of either the testing nominal stress f_{test} or the design stress for normal operating cases f_{dmin}.

$$f = \min(f_{dmin}; f_{test}) \tag{IV.C.6}$$

With the design stress for normal operation cases calculated with safety factors as follows:

$$f_d = \min(\frac{R_{p0,2/t}}{1,5}; \frac{R_{m/20}}{2,4}) \tag{IV.C.7}$$

The design stress for testing and exceptional cases is calculated with the following safety factor and material attributes for 20°C. It can be seen that for testing purposes the safety factor results in a bigger design stress capacity of the material:

$$f_{test} = \frac{R_{p0,2/t_{test}}}{1,05} \tag{IV.C.8}$$

In accordance to the pressure directive the yield strength R_{eH} has been used instead of $R_{p0,2}$ as no values were given in EN10222:1998.

The different definitions for the thickness are shown in Figure 11 and defined as follows:

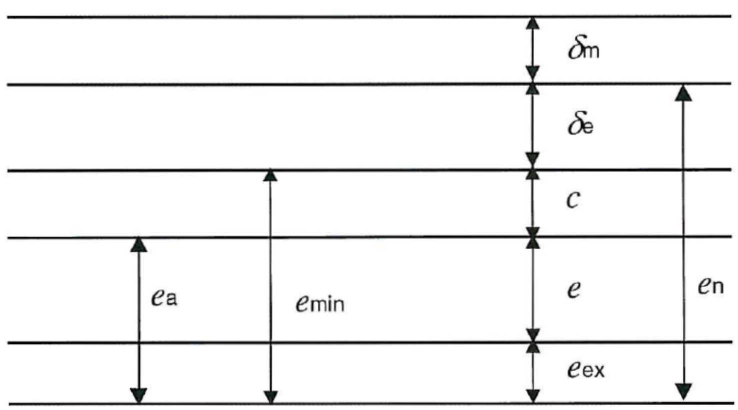

Figure 11 thickness definitions (taken from EN 13445-3)

The thickness definitions are as follow

- e is the required thickness that will be calculated thought the design process
- e_n is the nominal thickness
- e_{min} is the minimum possible fabrication thickness
- e_a is the analysis thickness
- c is the corrosion or erosion allowance, in this case always 1mm is recommended after the German pressure directive AD2000MB0.
- δ_e is the absolute value of the possible negative tolerance on the nominal thickness. The value is taken from EN 10029.
- δ_m is the allowance for possible thinning during manufacturing process
- e_{ex} is the extra thickness to make up to the nominal thickness. This value is mostly results in rounding up the design thickness

The weld joint coefficient for the testing group 3 according to EN 13445-3 – Table 5.6-1 is

- $\mathrm{z} = 0{,}85$

b) Body

The pressure vessel is put together through three parts. One cylindrical shell in the middle and hemispherical ends on both sides. For each part the equation for the required thickness will be presented. The nominal thickness will be calculated with the mentioned considered parameters.

(1) Cylindrical shell

The required thickness of the cylindrical shell has been calculated as follows, with the assumed external diameter.

$$\mathrm{E} = \frac{\mathrm{P} \cdot \mathrm{D_e}}{2 \cdot \mathrm{f} \cdot \mathrm{z} + \mathrm{P}} \qquad \text{(IV.C.8)}$$

The maximum permissible pressure is formulated as follows:

$$\mathrm{P_{max}} = \frac{2 \cdot \mathrm{f} \cdot \mathrm{e_a}}{\mathrm{D_m}} \qquad \text{(IV.C.9)}$$

The maximum permissible pressure for testing load cases has been calculated as follows:

$$P_{max} = \frac{2 \cdot f_{test} \cdot e_{min}}{D_m} \quad \text{(IV.C.10)}$$

With the mean diameter determined as:

$$D_m = D_e - e_n \quad \text{(IV.C.11)}$$

(2) spherical shell/hemispherical end

The required thickness of the hemispherical end has been calculated after:

$$e = \frac{P \cdot D}{4 \cdot f \cdot z + P} \quad \text{(IV.C.12)}$$

It can be seen that the calculated thickness will be smaller than in the cylindrical shell as a result of the geometrical form of a spherical shell. The form allows for a wider stress zone thus decreasing the specific stress on the material. The material for the hemispherical endings is the same as the one in use for the cylindrical shell thus the values are the same as above. This is also the case for the weld joint coefficient.

The maximum permissible pressure is calculated as follows:

$$P_{max} = \frac{4 \cdot f_{test} \cdot e_{min}}{D_m} \quad \text{(IV.C.13)}$$

c) Openings

For all openings a reinforcement check has been made. To meet the requirements, the wall and nozzle thicknesses have been adjusted throughout the calculation process. The thickness of the surrounding areas of an opening had to be increased accordingly to the calculations. Basically the stress resistance in the materials has to be greater than the operating pressure inside the shells as mathematically formulated through:

$$\left(Af_s + Af_w + Af_p + Af_b\right) \cdot (f_s - 0{,}5P) \geq P(Ap_s + Ap_b + 0{,}5Ap_\phi)^7 \quad \text{(IV.C.14)}$$

[7] Equation for the case $f_b > f_s$; reinforced by increased wall thickness has been taken.

With the nominal design stress for the material defined as:

$$\mathrm{f_{op}} = \min(\mathrm{f_s}; \mathrm{f_{op}}) \tag{IV.C.15}$$

The vessel is designed to have the same nozzles in all openings. Thus the following equations are the same for all shell forms. Figure 12 shows the important geometrical parameters appearing in the following equations.

- $Af_s = l_s' \cdot e_{c,s}$; stress loaded cross-sectional area effective as reinforcement in the shell
- $\mathrm{Af_b} = \mathrm{e_b} \cdot (\mathrm{l_b'} + \mathrm{l_{bi}'} + \mathrm{e_s'})$; stress loaded cross-sectional area effective as reinforcement in the nozzle
- $\mathrm{Ap_b} = 0{,}5 \cdot \mathrm{d_{ib}} \cdot \left(\mathrm{l_b'} + \mathrm{e_{a,s}}\right)$ pressure loaded area around the nozzle
- $\mathrm{l_{bi}'} = \min(\mathrm{l_{bi}}; 0{,}5 \cdot \mathrm{l_{bo}})$; protruding length
- $\mathrm{l_{bo}} = \sqrt{(\mathrm{d_{eb}} - \mathrm{e_b}) \cdot \mathrm{e_b}}$; length of the nozzle contributing to the reinforcement
- $\mathrm{l_b'} = \min(\mathrm{l_{bo}}; \mathrm{l_b})$ effective length outside the shell for reinforcement

The max. permissible pressure for the shells is defined as follows:

$$\mathrm{P_{max}} = \frac{\left(\mathrm{Af_s} + \mathrm{Af_w} + \mathrm{Af_b} + \mathrm{Af_p}\right) \cdot \mathrm{f_s}}{\left(\mathrm{Ap_s} + \mathrm{Ap_b} + 0{,}5\mathrm{Ap_\phi}\right) + 0{,}5\left(\mathrm{Af_s} + \mathrm{Af_w} + \mathrm{Af_b} + \mathrm{Af_p}\right)} \tag{IV.C.16}$$

(1) Cylindrical shell with isolated opening, increased wall thickness and set-in nozzle

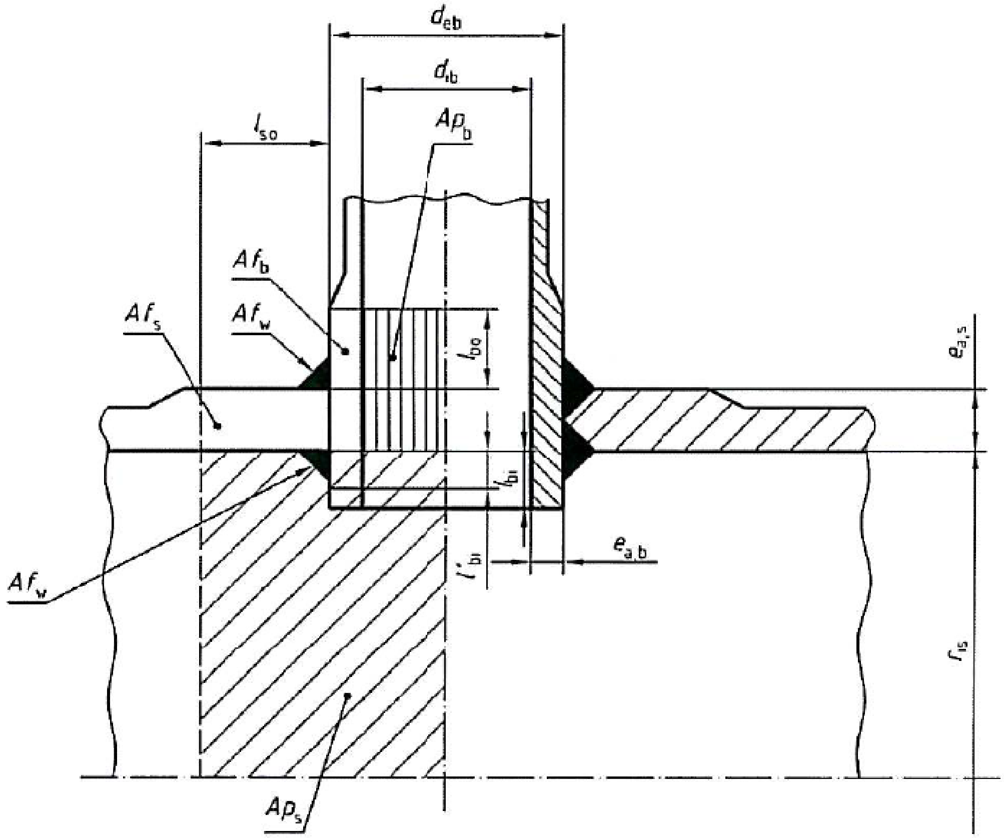

Figure 12 cylindrical shell with isolated opening, increased wasll thickness and set-in nozzle (taken from EN 13445-3)

Figure 12 shows some of the important geometrical parameters and the stress loaded area and the pressure loaded area respectively.

Despite from the general equations given above the pressure loaded area around the shell has been calculated as:

$$Ap_s = r_{is} \cdot (l'_s + a) \qquad \text{(IV.C.17)}$$

With the inside radius of curvature of the shell at the opening centre

$$r_{is} = \frac{D_e}{2} - e_{a,s} \qquad \text{(IV.C.18)}$$

$$a = \frac{d}{2} \tag{IV.C.19}$$

l_s' is the effective length of the shell for opening reinforcement

$$l_s' = \min(l_{so}; l_s) \tag{IV.C.20}$$

$$l_{so} = \sqrt{\left((D_e - 2 \cdot e_{a,s}) + e_{c,s}\right) \cdot e_{c,s}} \tag{IV.C.21}$$

(2) spherical shell with isolated opening, increased wall thickness and set-in nozzle

For the carbon dioxide outlet and the pipe for the mass flow measurement the opening at the hemispherical ends are calculated as follows. Chapter 0 shows that no further increase of the shell thickness had to be done. It has been stated before this is because of the advantageous hemispherical form.

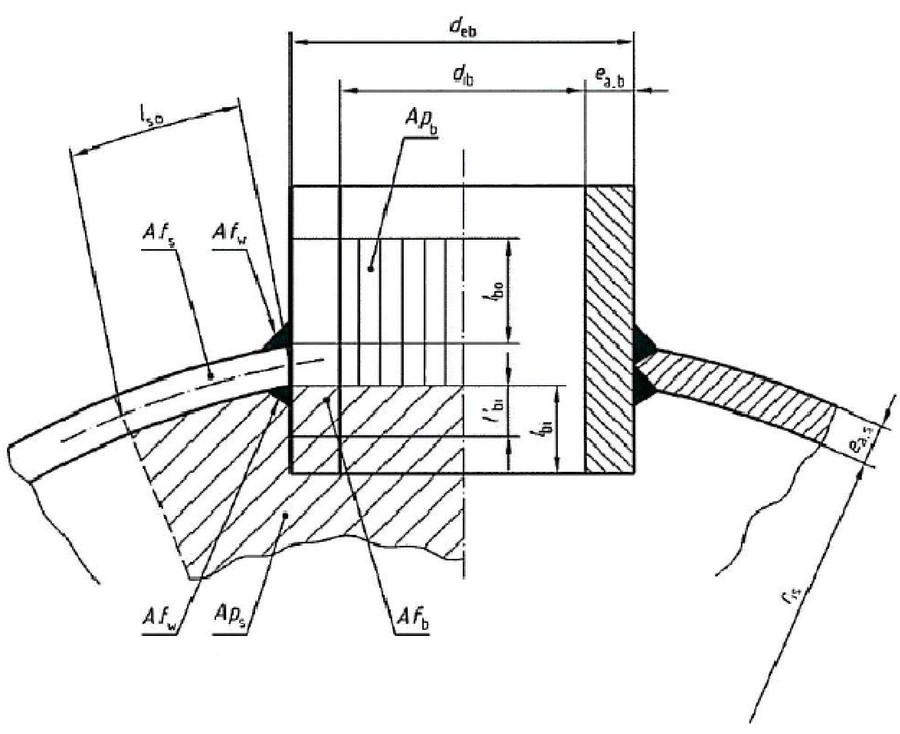

Figure 13 Spherical shell with isolated opening, increased wasll thickness and set-in nozzle (taken from EN 13445-3)

The pressure loaded area for a spherical shell can be calculated through:

$$Ap_s = 0{,}5 \cdot r_{is}^2 \cdot \frac{l_s' + a}{0{,}5 \cdot e_{a,s} + r_{is}} \qquad \text{(IV.C.22)}$$

With the inside radius of curvature of the shell at the opening centre

$$r_{is} = R \qquad \text{(IV.C.23)}$$

$$a = r_{ms} \cdot \arcsin(\delta) \qquad \text{(IV.C.24)}$$

$$\delta = \frac{d_{eb}}{2 \cdot r_{ms}} \qquad \text{(IV.C.25)}$$

The mean spherical radius:

$$r_{ms} = (r_{is} + 0{,}5 \cdot e_{a,s}) \qquad \text{(IV.C.26)}$$

The length of spherical shell contributing to the opening reinforcement is defined as:

$$l_s' = \min(l_{so}; l_s) \qquad \text{(IV.C.27)}$$

$$l_{so} = \sqrt{(2 \cdot r_{is} + e_{c,s}) \cdot e_{c,s}} \qquad \text{(IV.C.28)}$$

(3) oblique nozzles in spherical shells and dished ends

For the level measurement, openings on the hemispherical ends are required.

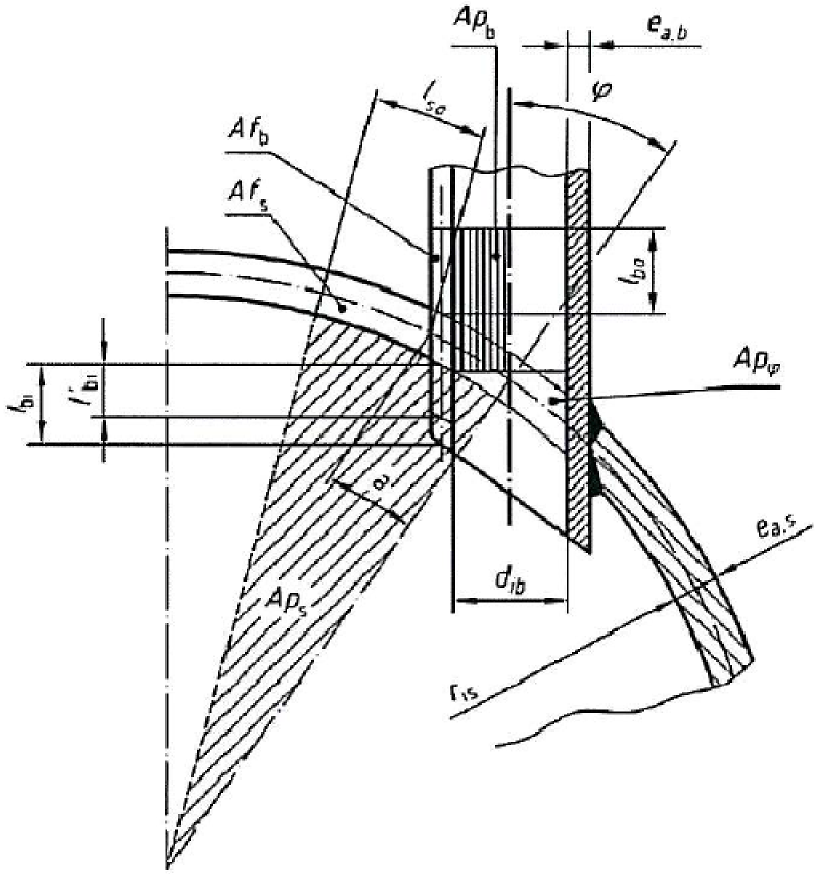

Figure 14 oblique nozzle in spherical shells and dished ends

The pressure loaded area for a spherical shell has been already stated with the inside radius of curvature of the shell at the opening centre. Different is the distance taken along the mid-thickness of the shell between the centre of the opening and the external edge of the nozzle. With a given angle it can be calculated as follows:

$$a = 0{,}5 \cdot r_{ms} \cdot \left(\arcsin\left(\delta + \sin(\phi)\right) + \arcsin\left(\delta - \sin(\phi)\right)\right) \qquad \text{(IV.C.29)}$$

$$\delta = \frac{d_{eb}}{2 \cdot r_{ms}} \qquad \text{(IV.C.30)}$$

The additional pressure loaded area due to the obliquity of the nozzle has been calculated as follows:

$$Ap_{\phi} = \frac{d_{ib}^{2}}{2}\tan(\phi) \tag{IV.C.31}$$

After the pressure directive the equation is only valid if following requirement is satisfied:

$$\Phi < arcsin(1-\delta) \tag{IV.C.32}$$

d) Distance between openings and shell discontinuity

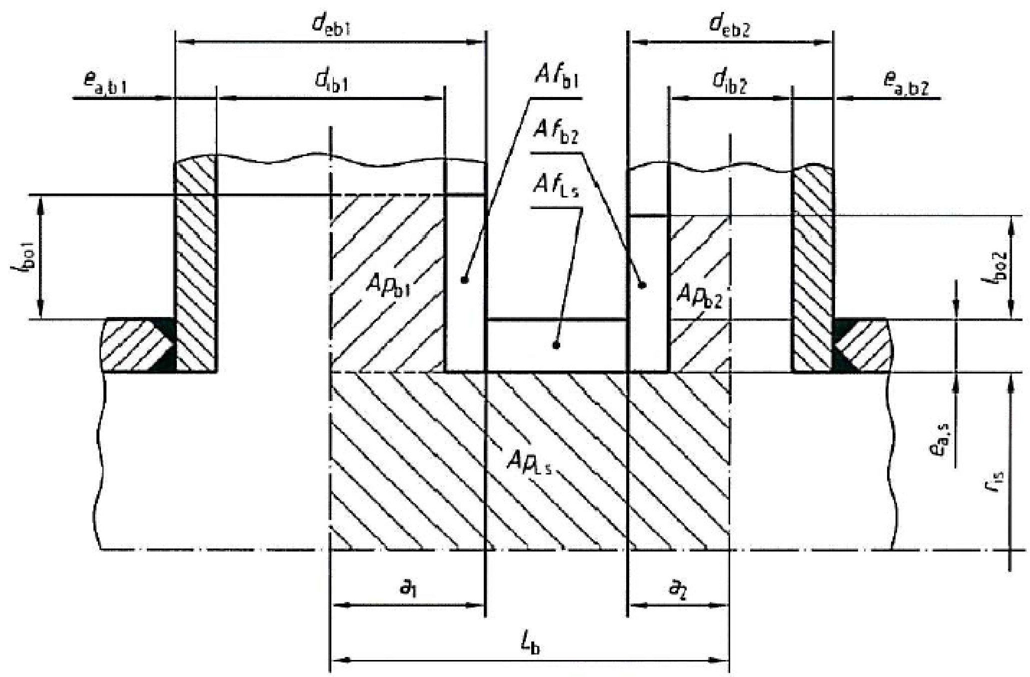

Figure 15 distance parameters for multiple openings

For isolated openings no ligament check for multiple openings has to be done. For an opening to be considered isolated following equations have to be satisfied.

$$L_b \geq a_1 + a_2 + l_{so1} + l_{so2} \tag{IV.C.33}$$

$$l_{so} = \sqrt{(2r_{is} + e_{c,s}) \cdot e_{c,s}} \tag{IV.C.34}$$

These lengths have to be considered especially for the two sight glasses on the cylindrical shell and on the hemispherical endings where the openings for the level indicators are close to the opening for the CO_2 outlet and the flow measurement pipe respectively as shown in Figure 10.

3. Gas/liquid separator

To avoid liquid drops reaching in the suction line of the compressor an evaluation on gas/liquid separation principles has been made which can be applied on the pressure vessel. Different concepts will be shown, which were taken from existing patents. The different concepts will be discussed and the most fitting one will be recommended.

Separation of the liquid drops in the gas happens automatically through gravitation. To speed up the process, different methods are employed. One efficient way is to utilize centrifugal force on the entrained droplets for separation. If the mixture is in a circular flow the liquid droplets have a greater inertia than the gas and consequently flow in contact with the outer surface.

This method is usually combined with an obstruction placed in the flow path of the stream.

Either method inherits complicated forms and surface structures. The following methods utilizes these principles.

a) Separator principles

Moore (9) invented a centrifugal separator for gas/liquid mixtures as shown in Figure 16.

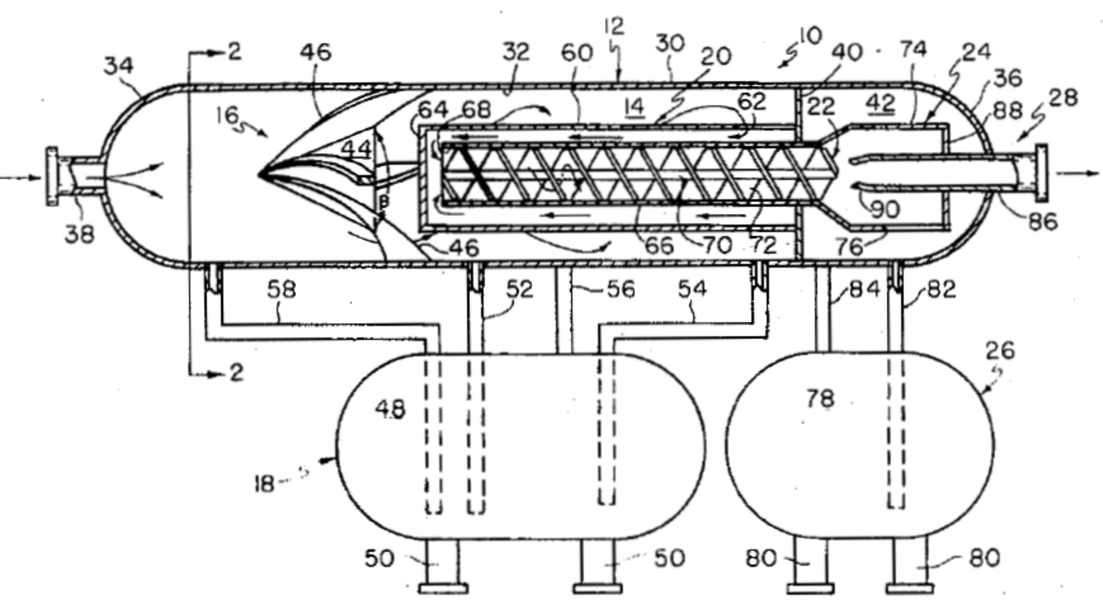

Figure 16 gas-liquid separator

The gas-liquid mixture enters the vessel in point 38 and is guided through the conival deflector which acts as an obstruction to deflect the stream on the interior vessel wall. The pathway redirects the flow in the opposite direction and then redirects it again to the original flow direction to increase the transit length of the gas-liquid stream. Then flowing in the original direction the pathway is formed like a helical screw, forcing the stream to swirl around the construction thus increasing the centrifugal force on the stream. Several outlets inside the tubes carry the liquid drops outside the pathway of the stream.

Another principle utilizing the concept of the centrifugal separation has been patented by Beattie (10). Figure 17 shows the vessel with the construct.

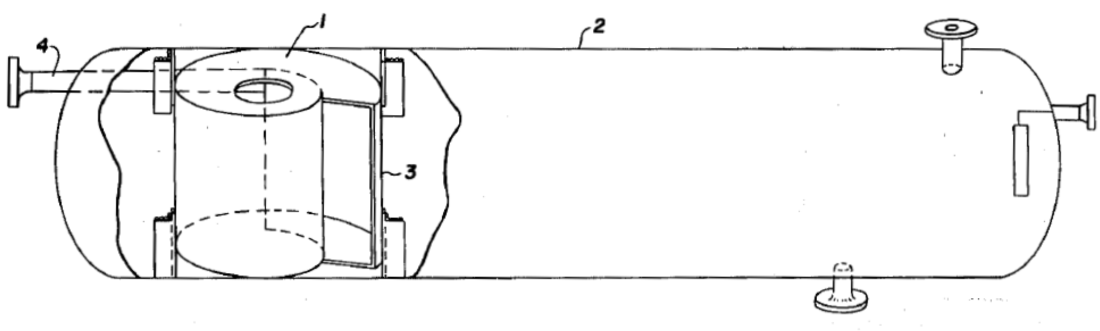

Figure 17 inlet assambly for an oil seperator

This invention has the task to separate gas from gas- liquid mixture with high density as for example oil-water mixtures. The mixture enters from a pipe 4 into the construct 1. From there the mixture rotates outwardly from the inside to the outside of the construct till it reaches point 3. Gas is separated by centrifugation in the smaller radius central portion of the housing and then the liquid flow velocity is reduced by expansion of the stream in the larger radius outer portion. The separated gas streams outside through the hole in the inner radius of the construct.

Figure 18 shows a construct of a separator patented by Reed (11). The invention inherits different principles of separating gas-liquid mixtures.

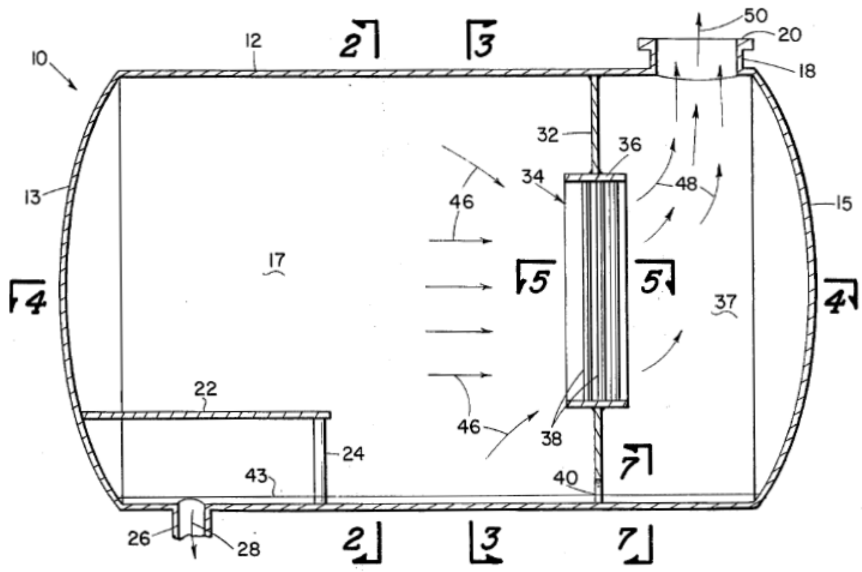

Figure 18 Gas liquid separator for flare systems

Figure 19 shows how the mixture enters the vessel sideways on the level 17. As the pipe is attached tangentional to the zylindrical vessel, the stream flows along the inner surface of the vessel thus creating a centrifugal force on the liquid droplets.

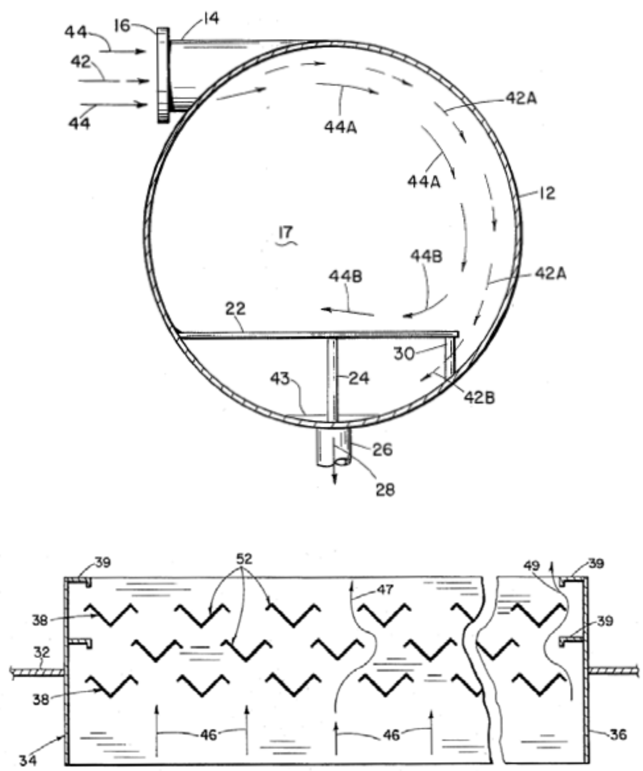

Figure 19 centrifugal separation(above) and separation through an obstacle with specified surface pattern(below)

The second principle utilized to separate the gas-liquid mixture is the separation through an obstacle or demister as shown in Figure 19. The stream is supposed to stream upwards hitting the chevron formed surface pattern on the way. The liquid droplets impinge on the obstacles and attach themselves to it.

b) Recommendation

The carbon dioxide stream goes in the inlet with a velocity of 22m/s. To keep the volume of the vessel as small as possible the separation construct has to be compact to fit in. The principle of Moore seems to satisfy most of the requirements. The helical screw form must be adapted to the vessel form. The necessary boundary parameters for the separator can be taken from the technical drawing of the vessel in the appendix.

To ensure that liquid is separated through gravity and that the upward stream doesn't incorporate any liquid a minimum permissible diameter can be calculated after M. Souder, et al. (12). The length of the vessel is to be three to four times larger than the vessel diameter. The permissible velocity w_{max} is calculated as follows:

$$w_{max} = k\sqrt{\frac{(\rho_L - \rho_G)}{\rho_G}} \qquad \text{(V.E.35)}$$

with $k(26{,}50bar) = 0{,}147$ being an empirical value taken from the Gas Processing Suppliers Association Book (13). The inside area can be calculated as follows:

$$A_{min} = \frac{\dot{m}v_{gas}}{w_{max}} \qquad \text{(V.E.36)}$$

Lastly the minimum permissible diameter inside the cylindrical shell is determined as follows:

$$D_{min} = \left(\frac{4A_{min}}{3.1416}\right)^{0.5} \qquad \text{(V.E.37)}$$

The calculated values can be found in Table 16 in the appendix.

Figure 20 shows principle sketches of different separator concepts. On the left figure a demister is installed in front of the outlet. If a demister is installed the k value in equation (V.E.35) will be $k = 0{,}098$ instead of $k = 0{,}147$ meaning the necessary diameter will be shorter. The principle after Moore has been applied in the middle figure. The right figure shows the vessel relying only on the gravity principle. Then the stream flows on the way upside the diameter difference shouldn't be more than D_{min} to ensure separation through gravity.

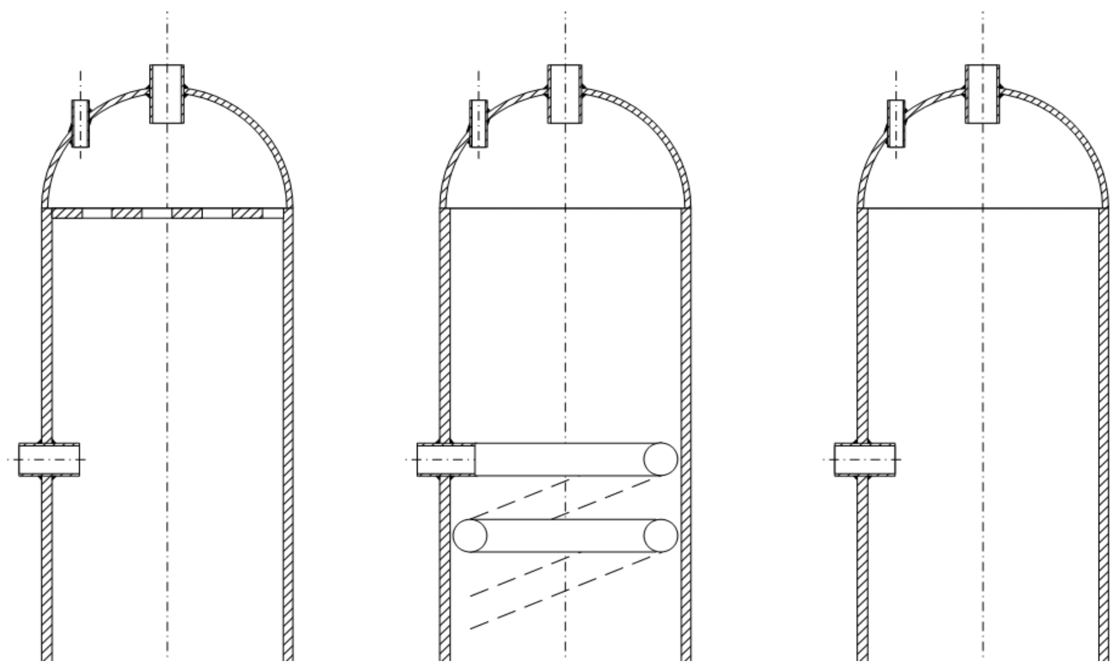

Figure 20 separator concepts for the pressure vessel

4. Table of nomenclature - IV.C Pressure vessel

Symbol	Unit	Description
a	m	distance between mid-thickness of a shell and an opening
A	m^2	Area
d	m	Width of an opening
D	m	Diameter
e	m	Thickness
f	Pa	Design Stress
H	m	Height
k	m	empirical value after Souders
l	m	Length
m	kg	mass
P	Pa	Pressure
r	m	Radius of an opening
R	m	Radius
v	m^3/kg	Specific volume
V	m^3	Volume
w	m/s	Velocity
z	$-$	Weld joint coefficient
ρ	kg/m^3	Specific volume
ϕ	rad	obliquity angle

Subscripts

Symbol	Description
a	Analysis
b	Nozzle
c	Calculated
e	External
G	Gas phase
HP	High pressure side
i	Internal
L	Liquid phase

LP	Low pressure side
m	Average
max	Maximum cases
min	Minimum cases
n	Nominal
o	Max/min value
op	Operational
p	Reinforcement
s	Shell
$test$	Test cases
w	Weld
ϕ	Oblique arrangement

D. Pump and Compressor

1. General description

The pumps for the use in the facility will be listed and it will be discussed in which way the pumps seem to fit in the test facility. During the design process the 100kW oil free compressor is designed specifically for the test facility and was considered in the boundary conditions stated in chapter III.A. Thus the compressor design won't be discussed here.

2. Pump

The pumps have the task to transfer the ethylene glycol through the circuit. This is accomplished by increasing the pressure of the fluid to overcome frictional pressure losses throughout the circuit. For the testing facility the power for the pump is supplied electrically. As there are many types of pumps the design choices should be made considering the type of fluid, capacity and the needed increase in head or pressure respectively. Figure 21 shows typical operation areas of commonly used pump types. The red solid line and broken line respectively indicate the operational point. Looking at the Figure the range of applicable pumps is quite large.

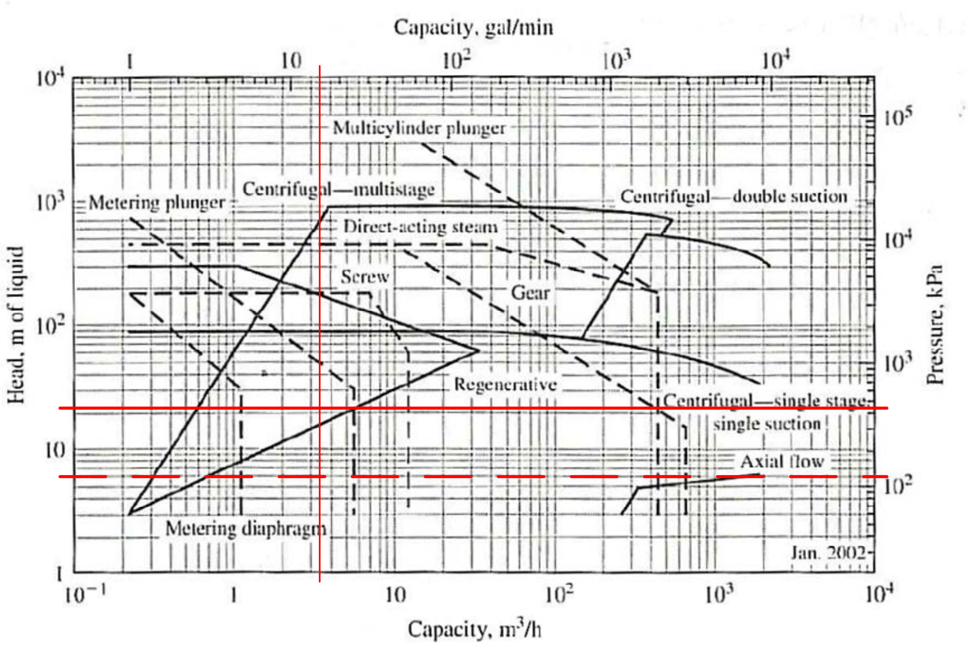

Figure 21 Operating areas of different types of pumps. Solid lines for the left ordinate and broken lines for the reight ordinate. Red lines indicates the operation capacity, pressure and head respectivly. Taken from (12)

Figure 21 can be used as guidance. Knowing from existing test facility that usually centrifugal pumps worked well with ethylene glycol and similarly operation conditions, the design choice has been made in favor on empirical bases.

Usually manufacturers of pumps are listening characteristic curves of their product. Figure 22 shows such a characteristic curve with the operational point indicated though red lines and the possible design points indicated through blue lines.

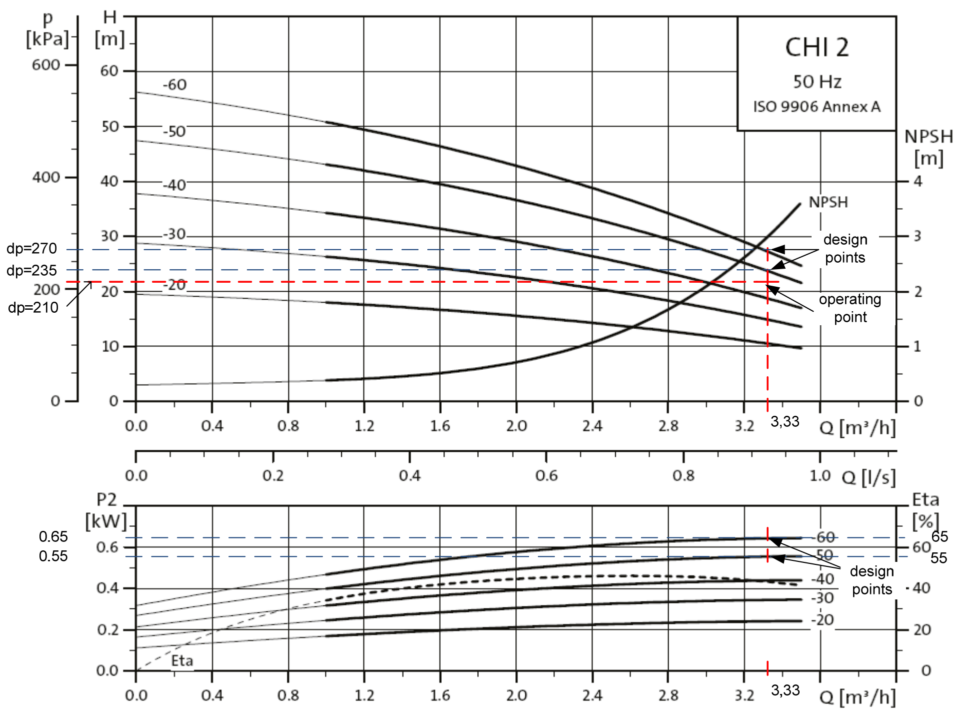

Figure 22 characteristic curves with operation point and possible design points for the centrifugal pump CHI 2 from the manufacture Grundfos

The choice of the pump has to be made by comparing the different prices of the pumps operating in the possible design points. It's recommended to choose the pump with more power to be on the safe side. Also Figure 22 shows that the capable pressure differences of the pumps in sight are only 35kPa. As the pressure loss of the circuit has been calculated with approximations[8] the pump with more power should be chosen.

[8] See Chapter IV.B - Heat exchanger and Chapter IV.E - Pipes

E. Pipes

1. General description

This part of the chapter will show how the diameter design choices have been carried out and how the pressure has been calculated. Also the meaning of the pipe arrangement during the design process will be discussed.

2. Arrangement

As pipes are usually available in standardized sized and pressures, the design of the pipes has been more in regards of the arrangement. For the arrangement it was important that the design itself is compact for transportability purposes. It also should be easy to install and to follow the flow of the circuits for quick measurability and orientation. The final result is shown through an isometric drawing in the appendix Figure 31.

The arrangement also played a huge role in dimensioning the vessel. As the necessary buffer volume in the circuit has been influenced by the pipe length.

3. Diameter

For the design, diameter of the pipes has been choosen after Klapp (8) and the Table 3 seen below.

Table 3 recommended velocities for sizing steel pipes, taken from (Peters, et al., 2003)

Turbulent flow	
Type of fluid	**Recommended velocity range, m/s†**
Water or fluid similar to water	1–3
Low-pressure steam (250 kPa)	15–30
High-pressure steam (750 kPa)	30–60
Air (250–500 kPa)	15–30

Viscous flow			
	Recommended velocity range, m/s†		
Nominal pipe diameter, m (in.)	**$\mu = 50$ cP**	**$\mu = 100$ cP**	**$\mu = 1000$ cP**
0.0254 (1)	0.5–1	0.3–0.6	0.1–0.2
0.0508 (2)	0.75–1.07	0.5–0.75	0.15–0.24
0.102 (4)	1.07–1.5	0.75–1.07	0.24–0.36
0.203 (8)	—	1.2–1.5	0.4–0.55

Besides these recommended parameters the diameters have been increased in case the pressure loss of certain piping arrangements have been over 1bar. A list of the piping geometries can be found in the appendix.

4. Pressure loss

The pressure loss has been calculated after Klapp (8) with the following equation.

$$\Delta p = \frac{\rho}{2} \cdot w^2 \cdot \left(\lambda(Re, \epsilon) \cdot \frac{l}{d} + \Sigma\zeta\right) \tag{IV.E.1}$$

The resistance coefficient $\lambda(Re, \epsilon)$ has been iterative calculated after Colebrook and White as this equation covers a great range of streaming conditions:

$$\lambda = \left(-2 \cdot Lg\left(\frac{2{,}51}{Re \cdot \lambda^{\frac{1}{2}}} + \frac{k}{3{,}72 \cdot d}\right)\right)^{-2} \tag{IV.E.2}$$

With the Reynolds number defined as follows:

$$Re = \frac{w \cdot d}{\nu} \tag{IV.E.3}$$

ζ is the resistance coefficient and considers pressure losses caused by elbows and crosses within the pipe arrangements. The values have been taken from a table listed in Klapps “Apparate- und Anlagentechnik (8 S. 574)“. The calculated values can be taken from Table 21 to Table 23 to be found in the appendix.

5. Table of nomenclature - IV.E Pipes

Symbol	Unit	Description
d	m	Pipe diameter
l	m	Pipe length
$\dot{m}$	kg/s	Mass flow
p	Pa	Pressure
Re	$-$	Reynold number
w	m/s	Velocity
v	m^3/kg	Specific volume
ϵ	$-$	Change in pipe elevation
ζ	$-$	Resistance coefficient
λ	$-$	Pipe friction coefficient
ρ	kg/m^3	Density
ν	m^2/s	Kinematic viscosity

F. Instruments

1. General description

The different types of the instruments in use should be briefly introduced and then an uncertainty analysis should be made with the resulting measurement uncertainty of the heat exchanger capacity in detail. In the introduction of the different instruments the given accuracy will be highlighted. The manufactures of instrumental equipment usually specifies accuracy of their devices in +/- deviations. Mostly the accuracy is given as a percentage value meaning the deviation change with the magnitude of the measured value.

2. Instrument types

a) Resistance thermal device (RTD)

The use of resistance thermal devices is recommended for the test facility as they have been proved to be able to operate in a great range of temperatures. They are also easy to install and to replace if necessary. RTDs of the accuracy class B as defined in IEC60751 for film type RTDs operates in temperature from -50 to 500°C. For platinum type RTDs' the resistance temperature relationship is given by the Calendar-Van Dusen equation as follows:

$$R_T = R_0(1 + \alpha t + \beta t^2 + \delta(t - 100)t^3) \qquad \text{(IV.F.1)}$$

Where $= 3{,}9083 \cdot 10^{-3} \cdot [C^{-1}]$, $\beta = -5{,}775 \cdot 10^{-7} \cdot [C^{-2}]$ and $\delta = -4{,}183 \cdot 10^{-12} \cdot [C^{-4}]$ for the RTD in use. R_0 is the nominal resistance at $0°C$. For the configuration of the strain gages the commonly used Wheatstone bridge circuit is recommended. The chosen resistance thermal device is from the company *omegafilm* and has the accuracy class B. The accuracy is given by equation (IV.F.2).

$$\delta T = \pm(0{,}3 + 0{,}005 \cdot T) \qquad \text{(IV.F.2)}$$

b) Pressure transducer

As with the resistance thermal devices a very common and inexpensive device to measure the pressure in the test facility is the piezoelectric transducer. As the instrument for pressure measuring will be a campact solution the strain gage signal conditioning won't be discussed in detail. The pressure transducer systems in use are from the company *Rheonik*. For the *M PMP45* it lists an accuracy value for the pressure transmitter as follows:

$$\delta p = \pm\, p \cdot 0{,}002 \qquad \text{(IV.F.3)}$$

For the differential pressure transmitter from the same company *S PMD75* the accuracy is defined as follows.

$$\delta p_{Delta} = \pm(p \cdot 0{,}00075) \qquad \text{(IV.F.4)}$$

c) Coriolis mass flowmeter

For measuring the mass flow it is recommended to use a coriolis mass flowmeter as it has a reasonable accuracy for the use of gases. The principle of the coriolis effect itself also allows the measurement of the density of the streaming fluid. The accuracy of the RHM12 mass flowmeter from *Rheonik* is given by:

$$\delta m = \pm(m \cdot 0{,}002) \qquad \text{(IV.F.5)}$$

d) Torque and rpm measurement

Equipment to measure the torque and rpm are best be choosen by the engineer who designs the compressor. As the torque measurement equipment can be installed flanged, through a shaft, bearingless etc... . For a complete uncertainty analysis it should include the measurement deviation of the rpm and torque. For the work here the measurement equipment won't be discussed.

e) Data logging systems

Most of the data logging systems have been taken from an existing test facility as they seemed to be reliable. The data logging systems have been listed in the Equipment list.

The signals from the resistance thermal devices will be gathered by a connector block with eight channels. The data from the pressure transducers and mass flow meters will also be taken from a data logging system with eight channels, one channel for each device output. The data will be sent through an ethernet serial interface of the controller to a personal computer there the input signal from the blocks can be converted accordingly.

f) *Pressure indicator*

The pressure indicator will be provided by the company Tempress from Denmark. P1116 Standard Line. The pressure indicator is only for safety proposes.

3. Uncertainty Analysis of Experiments

An important part for the whole design process is the measurability of the test facility. Besides of laying out proper local conditions for the instrumental equipments in the test facility it is important to know what qualities man can achieve from the measurements. During the design process the engineer can have certain influence on the qualities of the conducted experiments in general.

For a facility for testing proposes it is vital to know uncertainties in measurements beforehand. A proper uncertainty analysis will reduce the work of analyzing measured results and avoid unexpected problems that could occur after the test facility has been built.

In general cases uncertainty is estimated with a confidence level of 95%. The confidence level implies that the actual error from all estimated measurements, is under the estimated uncertainty in 95% of the time. Generally speaking the measured result R can be mathematically described as a function of n measurement values x as seen in equation (IV.F.6).

$$R = f(x_1, x_2, \dots, n) \qquad \text{(IV.F.6)}$$

To express the uncertainty of a certain measurement series it is used to express the small changes of the measured result in differential form as shown in equation (IV.F.7). Therein the changes should be infinitesimal to avoid unnecessary approximation of the measured series. If it is not avoidable because of calculation issues, the values should be in a reasonable area of assumption.

$$\delta R = \delta x_1 \frac{\delta R}{\delta x_1} + \delta x_2 \frac{\delta R}{\delta x_2} + \dots + \delta x_n \frac{\delta R}{\delta x_n} \qquad \text{(IV.F.7)}$$

Manufactures of instrumental equipment usually specifies measurement uncertainties or accuracy of their devices in +/- deviations meaning the deviation of a measurement series can be from negative to positive ranges to even zero. To avoid this issue it is in the sense of the experiment to use the root-sum-square method as shown in equation (IV.F.8) therein δx_i is denoted by the uncertainty of the variables w_{x_i} and the uncertainty of the result δR is replaced by the uncertainty of the result w_R.

$$w_R = \sqrt{\sum_{i=1}^{n} \left(w_{x_i} \frac{\delta R}{\delta x_i} \right)^2} \qquad \text{(IV.F.8)}$$

a) Systematic and Random Aspects of Uncertainty

Uncertainty analysis can be separated by investigating systematic and random errors independently.

Random errors depend from the measuring situation. Therein situation means the environmental condition of the testing area and the capability of reading the measured values. Random errors are also referred as variable errors as they change although the measured conditions are the same. Random errors also occur in instruments through the readability of the device. For example after Coleman, et al. (13) the accuracy of reading a digital device results in the amount of digits displayed in the output.

Analog to random errors, systematic errors are referred to fixed errors as they do not change when the test is repeated several times under the same measured conditions. Systematic errors are considered as errors that are known but can’t be eliminated because of lack of instrumental qualities.

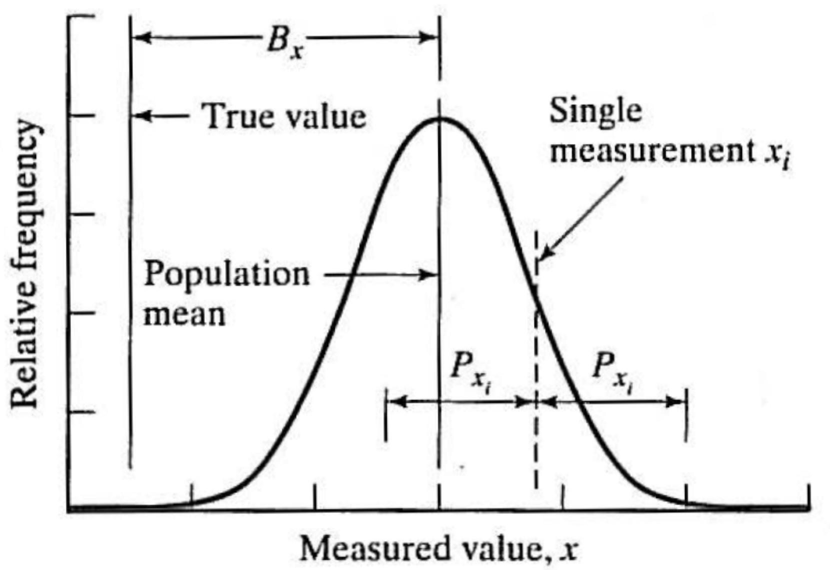

Figure 23 Display of random and systematic uncertainties (taken from Wheeler & Ganji, Introduction to Engingeering Experimentation 2004).

Figure 23 shows the influence of the random uncertainty and systematic uncertainty. Therein the systematic uncertainty is denoted as B_x and the random uncertainty as P_x respectively. The curve takes the typical form of a bell resulting from the gaussian distribution. It is the expected distribution if many measurements were made. As shown most of the measurement values are expected around the range of the systematic uncertainty. The range of the random uncertainties should be around the peak of the curve in 95% of the time if the confidence level is 95%.

b) *Resulting Uncertainty in Heat Exchanger Capacity Measurements*

With the principles of the uncertainty analysis described, the resulting uncertainty of the heat exchanger capacity can be calculated as follows:

$$\delta\dot{Q} = \sqrt{\left(\frac{\delta\dot{Q}}{\delta\dot{m}}\delta\dot{m}\right)^2 + \left(\frac{\delta\dot{Q}}{\delta h}\delta h\right)^2 + \left(\frac{\delta\dot{Q}}{\delta h_0}\delta h_0\right)^2} \qquad \text{(IV.F.9)}$$

Where the individual measurements or terms are defined as:

$$\frac{\delta\dot{Q}}{\delta\dot{m}} = h - h_0 \qquad \text{(IV.F.10)}$$

$$\frac{\delta \dot{Q}}{\delta \dot{h}} = \dot{m} \tag{IV.F.11}$$

$$\frac{\delta \dot{Q}}{\delta \dot{h}_0} = -\dot{m} \tag{IV.F.12}$$

As the enthalpies are deviations from the pressure deviations and temperature deviations themselves they have to be expressed yet through another differential form and summed up with the root-sum-square method. The resulting is shown in equation (IV.F.13).

$$\delta h_i = \sqrt{\left(\frac{\delta h_i}{\delta T_i}\delta T_i\right)^2 + \left(\frac{\delta h_i}{\delta p_i}\delta p_i\right)^2} \tag{IV.F.13}$$

$$\frac{\delta h}{\delta t} = c_p(T_i, p_i) \tag{IV.F.14}$$

$$\frac{\delta h_i}{\delta p_i} = \frac{h(T_i, p_i + \Delta p) - h(T_i, p_i)}{\Delta p} \tag{IV.F.15}$$

The values of the enthalpies can be taken from tables or data bases as in this case. The equation (IV.F.15) is a function of the isobaric heat capacity itself. To simplify the equation it will be approximated. This should be in mind then measurement analyses are going to be made later on.

The measurement deviations for δp_i, δT_i and $\delta \dot{m}_\imath$ can be directly taken from the instrumental manufacturers.

4. Table of nomenclature - IV.F Instruments

Symbol	SI-Unit	Description
c_p	$J/(kgK)$	Isobaric specific heat capacity
h	J/kg	Specific enthalpy
$\dot{m}$	kg/s	Mass flow
p	Pa	Absolute Pressure
p_{Delta}	Pa	Pressure difference
$\dot{Q}$	W	Heat transfer rate
R	$-$	Measured Result
T	$°C$	Temperature
w	$-$	Uncertainty
x	$-$	Measured values
Δ	$-$	Difference
δ	$-$	Deviation

Subscripts

R		Results
x		Values

G. External cooling systems

An external heat exchanger is required to compensate the heat injected through the compressor. This heat can’t be used during the whole operating process and must be rejected outside the operating system boundaries. For the test facility it could be conceivable to use an air cooler. Because the duty has to be around 100kW the power requirement of the fan could be quite high. A recommended air cooled heat exchanger is stated in chapter V.

V. Final recommended design with appropriate data

A. General and description

This chapter mainly lists the specification sheets of the needed equipment with the proposed available equipment listed in the cell “further Description”.

B. Heat exchanger

For the brazed plate heat exchangers only vague recommendations can be done. The recommended products from the company *Haori* are only capatible of operating in pressures up to 30bar and justifies only the required heat transfer area. The avaiable brazed heat exchangers for high operation pressures are small and not capable of handling the required mass flows without high pressure losses. But it is to assume that this will change in the near future as the manufacture announced bigger brazed plate heat exchangers[9] for high pressure uses. The required geometries for each heat exchanger are listed in detail in the appendix.

Heat exchanger			
Identification:	Equipment Code:	HX1	
	required Nr.:	1	
Function:	Rejection of heat due to compressing		
Type:	Brazed plate heat exchanger Heat transfer area: $1{,}6m^2$ Duty: $100kW$		
Hot inlet:		**Cold inlet:**	
Fluid handled	Carbon dioxide	Fluid handled	EG 50% concentration by volume
Flow rate	$1{,}00kg/s$	Flow rate	$1{,}00kg/s$
Pressure	$130bar$	Pressure	$10bar$
inlet Temperature	$t_2 = 131{,}10°C$	inlet Temperature	$t_{3'} = 61{,}75°C$
outlet Temperature	$t_{3'} = 85{,}45°C$	outlet Temperature	$t_3 = 81{,}17°C$
estimated pressure loss	$0{,}71813bar$	estimated pressure loss	$0{,}25180bar$
inside diameter (in/out)	$17{,}30mm/28{,}50mm$	inside diameter (in/out)	$28{,}50mm/28{,}50mm$
Dimensions:	Size (H x W x D) Nr. of plates Material	$0{,}449m\ x\ 0{,}247m\ x\ 0{,}054m$ 15 X5CrNiMo17-12-2	
further Description:	similar available heat exchanger: K215 x 15 from the company Kaori – http://www.kaori-taiwan.com/		

[9] From the K200 series. With LxW (613mm x 186mm) and a heat transfer area of approximately $0.1099m^2$ compared to the K215 with L x W (529mm x 247mm) and a heat transfer area of $0.1103m^2$

Heat exchanger			
Identification:	Equipment Code:	HX2-1	
	required Nr.:	1	
Function:	Heat transfer for testing purposes		
Type:	Brazed plate heat exchanger Heat transfer area: $4{,}11m^2$ Duty: $100kW$		
Hot inlet:		**Cold inlet:**	
Fluid handled	Carbon dioxide	Fluid handled	EG 50% concentration by volume
Flow rate	$0{,}50kg/s$	Flow rate	$0{,}50kg/s$
Pressure	$130bar$	Pressure	$10bar$
inlet Temperature	$t_{3\prime} = 85{,}45°C$	inlet Temperature	$t_2 = 10{,}07°C$
outlet Temperature	$t_{3\prime\prime} = 24{,}54°C$	outlet Temperature	$t_{3\prime} = 61{,}67°C$
estimated pressure loss	$0{,}74573bar$	estimated pressure loss	$0{,}58100bar$
inside diameter (in/out)	$28{,}5mm/17{,}30mm$	inside diameter (in/out)	$28{,}50mm/28{,}50mm$
Dimensions:	Size (H x W x D) Nr. of plates Material	$0{,}449m\ x\ 0{,}247m$ x $0{,}118m$ 37 X5CrNiMo17-12-2	
further Description:	similar available heat exchanger: K215 x 37 from the company Kaori – http://www.kaori-taiwan.com/		

Heat exchanger			
Identification:	Equipment Code:	HX2-2	
	required Nr.:	2	
Function:	Heat transfer for testing purposes		
Type:	Brazed plate heat exchanger Heat transfer area: $4{,}57m^2$ Duty: $50kW$		
Hot inlet:		**Cold inlet:**	
Fluid handled	Carbon dioxide	Fluid handled	EG 50% concentration by volume
Flow rate	$0{,}25kg/s$	Flow rate	$0{,}25kg/s$
Pressure	$130bar$	Pressure	$10bar$
inlet Temperature	$t_{3\prime} = 85{,}45°C$	inlet Temperature	$t_2 = 10{,}07°C$
outlet Temperature	$t_{3\prime\prime} = 24{,}54°C$	outlet Temperature	$t_{3\prime} = 61{,}67°C$
estimated pressure loss	$0{,}46172bar$	estimated pressure loss	$0{,}58100bar$
inside diameter (in/out)	$28{,}5mm/17{,}30mm$	inside diameter (in/out)	$28{,}50mm/28{,}50mm$
Dimensions:	Size (H x W x D) Nr. of plates Material	$0{,}449m\ x\ 0{,}247m$ x $0{,}115m$ 41 X5CrNiMo17-12-2	
further Description:	similar available heat exchanger: K215 x 41 from the company Kaori – http://www.kaori-taiwan.com/		

Heat exchanger			
Identification:	Equipment Code: HX3		
	required Nr.: 1		
Function:	internal R744 circuit heat transfer for overheating		
Type:	Brazed plate heat exchanger Heat transfer area: $0{,}53m^2$ Duty: $15kW$		
Hot inlet:		**Cold inlet:**	
Fluid handled	Carbon dioxide	Fluid handled	Carbon dioxide
Flow rate	$1{,}00kg/s$	Flow rate	$1{,}00kg/s$
Pressure	$130bar$	Pressure	$100bar$
inlet Temperature	$t_{3''} = 24{,}54°C$	inlet Temperature	$t_{1'} = -9{,}93°C$
outlet Temperature	$t_3 = 18{,}65°C$	outlet Temperature	$t_1 = 0°C$
estimated pressure loss	$0{,}07239bar$	estimated pressure loss	$0{,}867299bar$
inside diameter (in/out)	$17{,}30mm/17{,}30mm$	inside diameter (in/out)	$28{,}50mm/28{,}50mm$
Dimensions:	Size (H x W x D) Nr. of plates Material	$0{,}449m\ x\ 0{,}247m$ x $0{,}023m$ 5 X5CrNiMo17-12-2	
further Description:	similar available heat exchanger: K215 x 5 from the company Kaori – http://www.kaori-taiwan.com/		

Heat exchanger			
Identification:	Equipment Code: HX4-1		
	required Nr.: 1		
Function:	evaporation of R744 for testing purposes		
Type:	Brazed plate heat exchanger Heat transfer area: $1{,}83m^2$ Duty: $100kW$		
Hot inlet:		**Cold inlet:**	
Fluid handled	EG 50% concentration by volume	Fluid handled	Carbon dioxide
Flow rate	$0{,}50kg/s$	Flow rate	$0{,}50kg/s$
Pressure	$10bar$	Pressure	$130bar$
inlet Temperature	$t_3 = 52{,}10°C$	inlet Temperature	$t_4 = -10°C$
outlet Temperature	$t_1 = 0{,}26\ °C$	outlet Temperature	$t_{1'} = -10°C$
estimated pressure loss	$0{,}43790bar$	estimated pressure loss	$0{,}64762bar$
inside diameter (in/out)	$28{,}50mm/28{,}50mm$	inside diameter (in/out)	$42{,}50mm/28{,}50mm$
Dimensions:	Size (H x W x D) Nr. of plates Material	$0{,}449m\ x\ 0{,}247m$ x $0{,}050m$ 17 X5CrNiMo17-12-2	
further Description:	similar available heat exchanger: K215 x 17 from the company Kaori – http://www.kaori-taiwan.com/		

Heat exchanger			
Identification:	Equipment Code:	HX4-2	
	required Nr.:	2	
Function:	evaporation of R744 for testing purposes		
Type:	Brazed plate heat exchanger Heat transfer area: 2,66m^2 Duty: 50kW		
Hot inlet:		**Cold inlet:**	
Fluid handled	EG 50% concentration by volume	Fluid handled	Carbon dioxide
Flow rate	0,25kg/s	Flow rate	0,25kg/s
Pressure	10bar	Pressure	130bar
inlet Temperature	$t_3 = 52{,}10°C$	inlet Temperature	$t_4 = -10°C$
outlet Temperature	$t_1 = 0{,}26\,°C$	outlet Temperature	$t_{1'} = -10°C$
estimated pressure loss	0,21497bar	estimated pressure loss	0,11435bar
inside diameter (in/out)	28,50mm/28,50mm	inside diameter (in/out)	42,50mm/28,50mm
Dimensions:	Size (H x W x D) Nr. of plates Material	0,449m x 0,247m x 0,075m 24 X5CrNiMo17-12-2	
further Description:	similar available heat exchanger: K215 x 24 from the company Kaori – http://www.kaori-taiwan.com/		

Heat exchanger			
Identification:	Equipment Code:	HX5-1	
	required Nr.:	1	
Function:	heat transfer between EG circuits		
Type:	Brazed plate heat exchanger Heat transfer area: 8,98m^2 Duty: 100kW		
Hot inlet:		**Cold inlet:**	
Fluid handled	EG 50% concentration by volume	Fluid handled	EG 50% concentration by volume
Flow rate	0,50kg/s	Flow rate	0,50kg/s
Pressure	10bar	Pressure	10bar
inlet Temperature	$t_{1'} = 61{,}72°C$	inlet Temperature	$t_2 = 0{,}25°C$
outlet Temperature	$t_1 = 10{,}16°C$	outlet Temperature	$t_3 = 52{,}10°C$
estimated pressure loss	0,58113bar	estimated pressure loss	0,61771bar
inside diameter (in/out)	28,50mm/28,50mm	inside diameter (in/out)	28,50mm/28,50mm
Dimensions:	Size (H x W x D) Nr. of plates Material	0,449m x 0,247m x 0,262m 81 X5CrNiMo17-12-2	
further Description:	similar available heat exchanger: K215 x 81 from the company Kaori – http://www.kaori-taiwan.com/		

Heat exchanger			
Identification:	Equipment Code:	HX5-2	
	required Nr.:	2	
Function:	heat transfer between EG circuits		
Type:	Brazed plate heat exchanger Heat transfer area: $12{,}49 m^2$ Duty: $50 kW$		
Hot inlet:		**Cold inlet:**	
Fluid handled	EG 50% concentration by volume	Fluid handled	EG 50% concentration by volume
Flow rate	$0{,}25 kg/s$	Flow rate	$0{,}25 kg/s$
Pressure	$10 bar$	Pressure	$10 bar$
inlet Temperature	$t_{1'} = 61{,}72°C$	inlet Temperature	$t_2 = 0{,}25°C$
outlet Temperature	$t_1 = 10{,}16°C$	outlet Temperature	$t_3 = 52{,}10°C$
estimated pressure loss	$0{,}18157 bar$	estimated pressure loss	$0{,}20004 bar$
inside diameter (in/out)	$28{,}50 mm/28{,}50 mm$	inside diameter (in/out)	$28{,}50 mm/28{,}50 mm$
Dimensions:	Size (H x W x D) Nr. of plates Material	$0{,}449 m$ x $0{,}247 m$ x $0{,}366 m$ 113 X5CrNiMo17-12-2	
further Description:	similar available heat exchanger: K215 x 113 from the company Kaori – http://www.kaori-taiwan.com/		

C. Pressure vessel

The designed pressure vessel specification sheet is listed above. It showcases the minimum required/requested specifications like the inlets- and outlets- shell thicknesses. Further details are listed in the appendix.

As stated in Chapter IV.C the required vessel volume is covered through the cylindrical bottom part of the vessel. This allows space for refrigeration charge needed to compensate leakages in the facility. Also enough space should be guaranteed with this configuration to install a liquid/gas separator unit inside.

		Pressure vessel			
Identification:	Equipment Code:	E-1			
	required Nr.:	1			
Function:	provide buffer volume contains gas/liquid separator unit				
Design data:					
	Feed (spherical)		**Bottom (cylindrical)**		**Overhead (spherical)**
Pressure	$100 bar$		$100 bar$		$100 bar$
External diameter	$250 mm$		$250 mm$		$250 mm$
Height	$125 mm$		$2000 mm$		$125 mm$
Volume	$3{,}53 litre$		$83{,}10 litre$		$3{,}53 litre$
Material of construction	12Ni14 +N		12Ni14 +N		12Ni14 +N
thickness of shell	$6 mm$		$10 mm$		$6 mm$
Openings:					
	inlet	**outlet**	**level indicator**	**mass flow indicator**	**sight glass**
location:	Bottom	Overhead	Feed/Overhead	Feed	Bottom
inner diameter:	$28{,}5 mm$	$28{,}5 mm$	$13{,}6 mm$	$28{,}5 mm$	$42{,}5 mm$
required total thickness of shell for reinforcement:	$33 mm$	$9 mm$	$9 mm$	$9 mm$	$34 mm$
required length of shell for reinforcement:	$270 mm$	$140 mm$	$140 mm$	$140 mm$	$274 mm$
further Description:	technical drawing is listed in the Figure 30				

D. Pump

The characteristic curve of the recommended pump has been already shown in chapter IV.D.2.

Pump		
Identification:	Equipment Code:	P-No.
	required Nr.:	2
Function:	transport of ethylene glycol	
Type:	horizontal multistage centrifugal pump Shaft power $= 800W$	
Operation data:	Fluid handled	EG 50% concentration by volume
	mass flow	up to 1kg/s
	pressures	1,00-3,50 bar(abs)
	temperature	-30°C to 20°C
	pipe diameters	28,50mm x 2,60mm
Power supply	$1 \text{ x } 220 - 240\Delta \text{ V}, 50\text{Hz}$	
Dimensions (H x W x D)	184mm x 158mm x 323mm	
further Description:	specification based on Pump: CM3-4, 50Hz from the company *GRUNDFOS* - http://www.grundfos.com/	

E. Instrumentals

The needed instruments are listed in the appendix under "instruments list; uncertainties". The recommended logging systems have been stated in Chapter IV.F.2.e) and are summed up in the equipment list. The main needed instruments are listed here without the RTDs as no further information is needed.

flow meter transmitter		
Identification:	Equipment Code:	FT100-300
	required Nr.:	3
Function:	Measurement of flow, additionally measurement of density possible	
Type:	Coriolis mass flowmeter	
Operation data:	Fluid handled	Carbon dioxide, ethylene glycol 50% concentration by volume
	mass flow	up to 1kg/s
	pressures	up to 290 bar
	temperature	1x -45°C to 210°C 2x -45°C to 120°C
Dimensions (H x W x D)	540mm x 400mm x 70mm	
further Description:	specification based on flow transmitter: RHM 12 - http://www.hi-as.no/ 1x RHM 12 ET1-P1-PM0-M1- G1 2x RHM 12 ET2-P1-PM0-M1- G1	

	pressure transmitter	
Identification:	Equipment Code:	PT100-300
	required Nr.:	4
Function:	Measurement of absolute pressure. Measurement of flow and level possible	
Type:	piezoelectric transducer	
Operation data:	Fluid handled	Carbon dioxide, ethylene glycol 50% concentration by volume
	mass flow	up to 1kg/s
	pressures	up to 700 bar
	temperature	-70°C to 400°C
further Description:	specification based on pressure transmitter: Cerabar S PMP71 from the company *Enress + Hauser* - http://www.endress.com/	

	differential pressure transmitter	
Identification:	Equipment Code:	PDT100-300
	required Nr.:	24
Function:	Measurement of pressure difference.	
Type:	piezoelectric transducer	
Operation data:	Fluid handled	Carbon dioxide, ethylene glycol 50% concentration by volume
	mass flow	up to 1kg/s
	pressures	up to 160 bar
	temperature	-40°C to 120°C
further Description:	specification based on pressure transmitter: Deltabar-S PMD75 from the company *Enress + Hauser* - http://www.endress.com/ Is should be conidered to choose a transmitter capatible of temperature ranges(-50°C to 150°C)	

F. External air cooling

For the air cooled heat exchanger the required specification are listed in this sheet.

	Air cooled heat exchanger	
Identification:	Equipment Code:	HX-A
	required Nr.:	1
Function:	heat rejection in the ethylene glycol circuit	
Type:	heat exchange through thinned coil Duty: $\approx 100kW$	
Liquid inlet:		
	Fluid handled	EG 50% concentration by volume
	Flow rate	$1kg/s$
	Pressure	$3{,}50bar$
	inlet Temperature	$t_3 = 73{,}15°C$
	outlet Temperature	$t_{1'} = 32{,}88°C$
	inside diameter (in/out)	$28{,}50mm/28{,}50mm$
Power supply	$1 \text{ x } 230\Delta \text{ V}, 50\text{Hz}$	
further Description:	similar available liquid air cooler: (SPOLAR Junior G) SJGE-30-6-630-1400-1/230/50-7 from the company *AlfaLaval* – http://www.alfalaval.com/	

B. P&ID

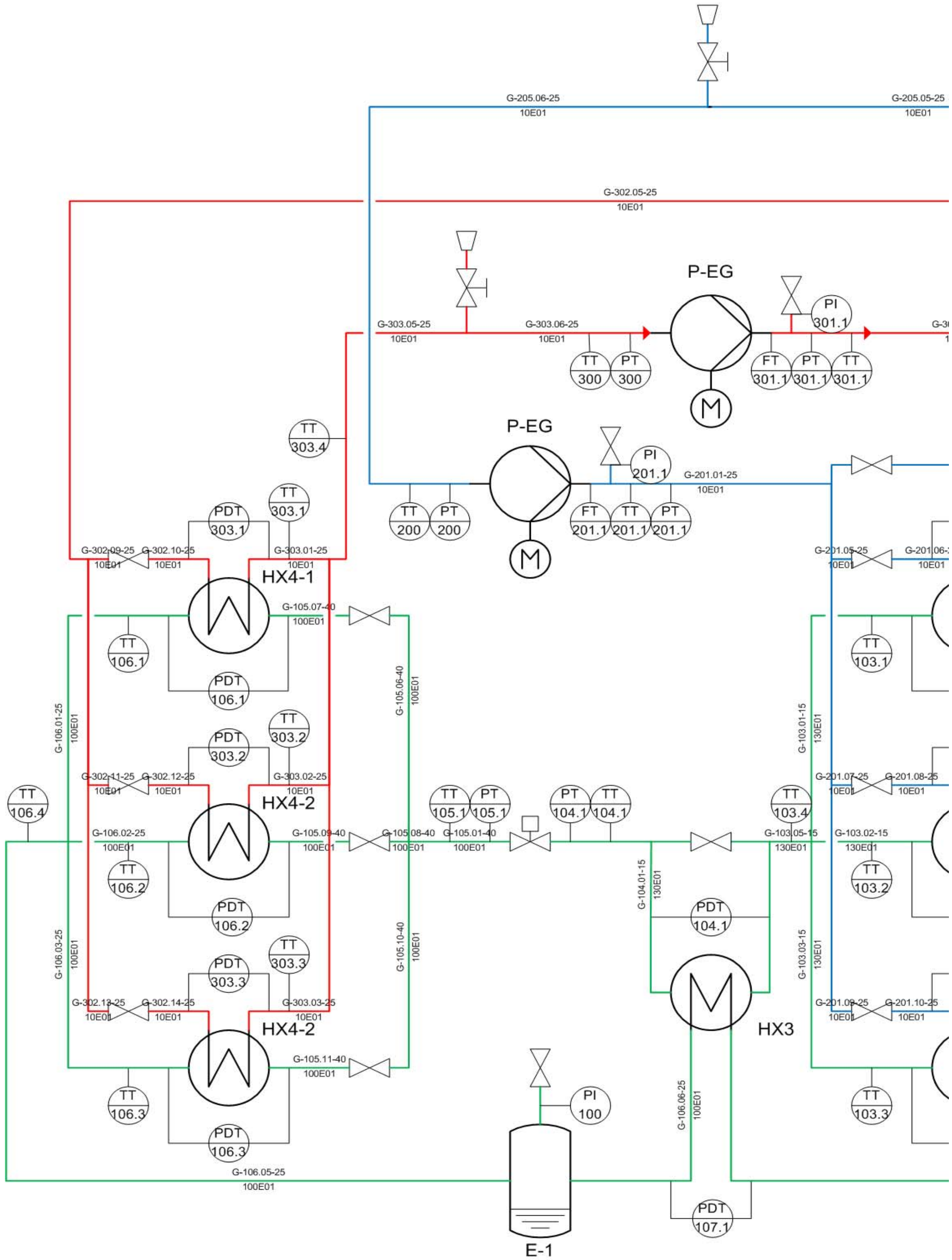

Figure 24 P&ID of the test facility

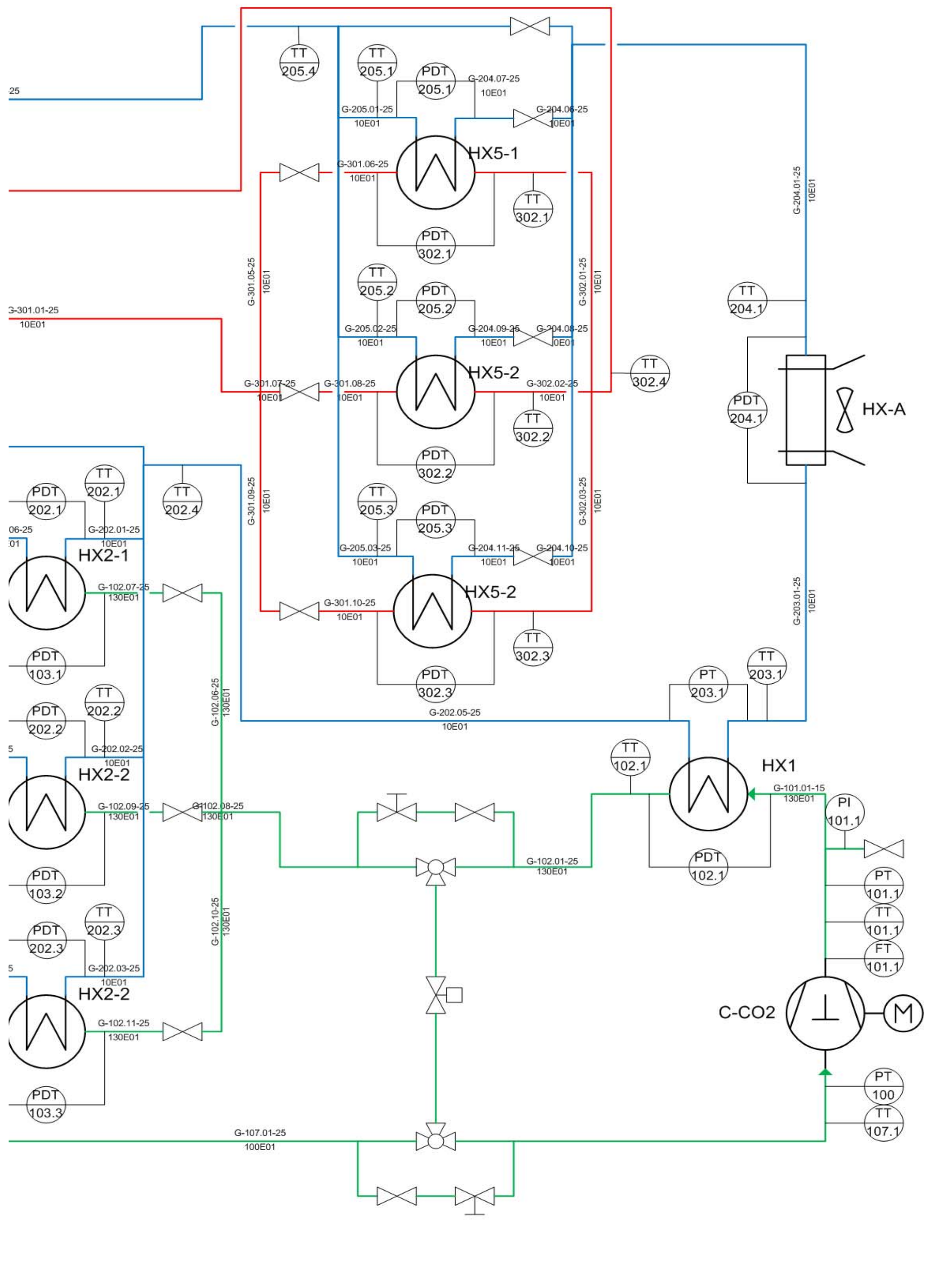

HX5-1
HX5-2
HX5-2
HX-A
HX2-1
HX2-2
HX2-2
HX1
C-CO2
M
TT 205.4
TT 205.1
PDT 205.1
TT 302.1
PDT 302.1
TT 205.2
PDT 205.2
TT 302.2
PDT 302.2
TT 302.4
TT 205.3
PDT 205.3
TT 302.3
PDT 302.3
TT 204.1
PDT 204.1
PT 203.1
TT 203.1
TT 102.1
PDT 102.1
PI 101.1
PT 101.1
TT 101.1
FT 101.1
PT 100
TT 107.1
PDT 202.1
TT 202.1
TT 202.4
PDT 103.1
PDT 202.2
TT 202.2
PDT 103.2
PDT 202.3
TT 202.3
PDT 103.3
G-204.07-25 10E01
G-205.01-25 10E01
G-204.06-25 10E01
G-301.06-25 10E01
G-204.01-25 10E01
G-301.05-25 10E01
G-302.01-25 10E01
G-301.01-25 10E01
G-205.02-25 10E01
G-204.09-25 10E01
G-204.08-25 10E01
G-301.07-25 10E01
G-301.08-25 10E01
G-302.02-25 10E01
G-301.09-25 10E01
G-302.03-25 10E01
G-202.01-25 10E01
G-205.03-25 10E01
G-204.11-25 10E01
G-204.10-25 10E01
G-203.01-25 10E01
G-102.07-25 130E01
G-301.10-25 10E01
G-102.06-25 130E01
G-202.05-25 10E01
G-202.02-25 10E01
G-101.01-15 130E01
G-102.09-25 130E01
G-102.08-25 130E01
G-102.01-25 130E01
G-102.10-25 130E01
G-202.03-25 10E01
G-102.11-25 130E01
G-107.01-25 100E01

C. Equipment list

Equipment code	No	Equipment function/description	Equipment specification				Material of construction	Dimensions
Heat exchangers or evaporators/condensers								
			calculation pressure [bar]	**calculation temperature [°C]**	**transfer area [m^2]**	**Nr. Plates**		**H x W x D [mm]**
HX1	1	first stage CO_2 cooler	130	140	1,6	15	X5CrNiMo17-12-2	247 x 320 x 54
HX2-1	1	second stage CO_2 cooler, 100kW	130	100	4,11	37	X5CrNiMo17-12-2	449 x 247 x 118
HX2-2	2	second stage CO_2 cooler, 50kW	130	100	4,57	41	X5CrNiMo17-12-2	449 x 247 x 115
HX3	1	internal heat transfer, CO_2 overheater	130	from -50 to 30	0,53	5	X5CrNiMo17-12-2	449 x 247 x 23
HX4-1	1	evaporation of CO_2, 100kW	100	from -50 to 10	1,83	17	X5CrNiMo17-12-2	449 x 247 x 50
HX4-2	1	evaporation of CO_2, 50kW	100	from -50 to 10	2,66	24	X5CrNiMo17-12-2	449 x 247 x 75
HX5-1	1	heat transfer between EG circles, 100kW	10	from -30 to 70	8,98	81	X5CrNiMo17-12-2	449 x 247 x 262
HX5-2	2	heat transfer between EG circles, 50kW	10	from -30 to 60	12,49	113	X5CrNiMo17-12-2	449 x 247 x 366
Compressor								
			max. outlet pressure [bar]	**inlet pressure [bar]**				**H x W x D [mm]**
C-CO2	1	oil-free piston CO_2 compressor	130	5			-	900 x 700 x 2500
Pumps								
			operational pressure difference [bar]	**standard voltage**	**Power [kW]**			**H x W x D [mm]**
C-EG	2	CHI2-40 60Hz	5,5	1 x 115/230V, 60Hz	0,55		X5CrNiMo17-12-2	242 x 253 x 437
Vessels								
			calculation pressure [bar]	**calculation temperature [°C]**	**total Volume [litre]**			**ø x l [mm]**
E-1	1	buffer volume, seperator	100	from -50 to 30	513,68		12Ni14	580 x 1980
Pipes								
			PN	**DN**	**total length [m]**			**ø x e [mm]**
100-300			130	15	4,75			17,30 x 1,80
100-300			130	25	24,25			28,50 x 2,60
100-300			130	40	1,55			42,50 x 2,90

			DN	min/max permissable pressure [bar]	min/max permissable temperature [°C]	
Fittings						
Elbow						
100-300	16	Hy-Lok	15	from 365 bar	from -198 to 648	G-X 6 CrNiMo 18-10
100-300	68	Hy-Lok	25	from 365 bar	from -198 to 649	G-X 6 CrNiMo 18-11
100-300	4	Hy-Lok	40	from 365 bar	from -198 to 650	G-X 6 CrNiMo 18-12
Cross						
100-300	2	Hy-Lok	15	from 365 bar	from -198 to 648	G-X 6 CrNiMo 18-10
100-300	14	Hy-Lok	25	from 365 bar	from -198 to 649	G-X 6 CrNiMo 18-11
100-300	1	Hy-Lok	40	from 365 bar	from -198 to 650	G-X 6 CrNiMo 18-12

Valves

Ball valve						
100-300	4	Hy-Lok	15			G-X 6 CrNiMo 18-10
100-300	15	Hy-Lok	25			G-X 6 CrNiMo 18-11
100-300	1	Hy-Lok	40			G-X 6 CrNiMo 18-12

Instuments

TT	33	RTD Sensor, omegafilm
PT	4	pressure transmitter, M PMP45
PI	3	Pressure indicator
PDT	24	differential pressure transmitter, S PMD75
FT	3	Coriolis Mass Flowmeter, RHM12

Data logging systems

cFP-CB-3	5	Thermocouples connector block, National Instruments
cFP-CB-1	5	pressure instruments connector block, National Instruments
cFP-1808	2	backbone for connectorblock, National Instruments

D. Cost evaluation

Pricing information for all equipment couldn't be obtained at the time the thesis was written. Thus pricing assumption had to be made after tables provided by Peters, et al. (14). Following are figures with the used parameters and resulting pricings marked with a cross. It should be considered that similar equipment has been chosen, if tables for the needed equipment were not available. All approximated prices have been marked grey in Table 4. Prices for the compressor and the vessel have not been considered as they are designed at *Sintef*.

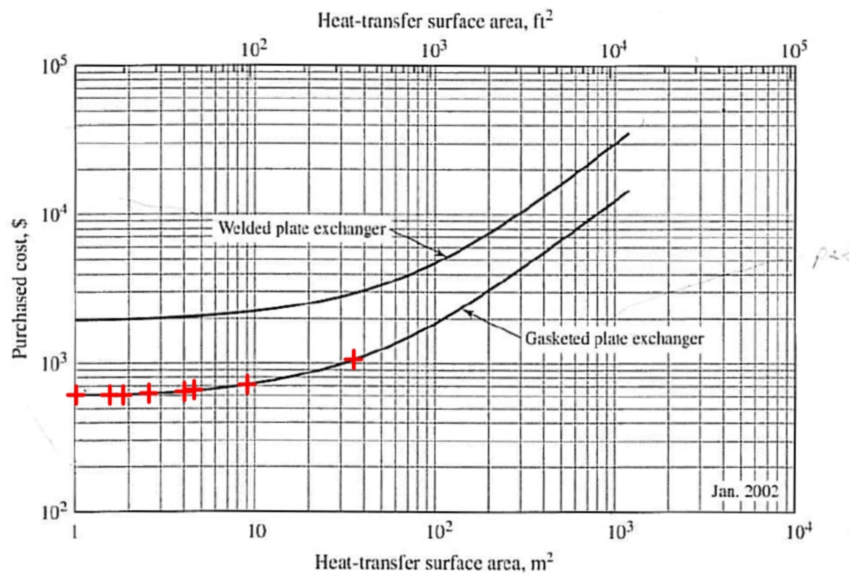

Figure 25 Price assumption for the BPHX. (because of the similarity gasketed plate exchanger have been chosen as replacement)

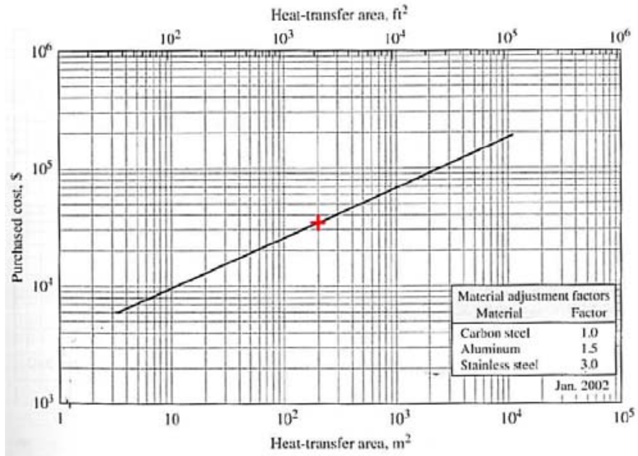

Figure 26 Price assumption for the air-cooled-heat exchanger

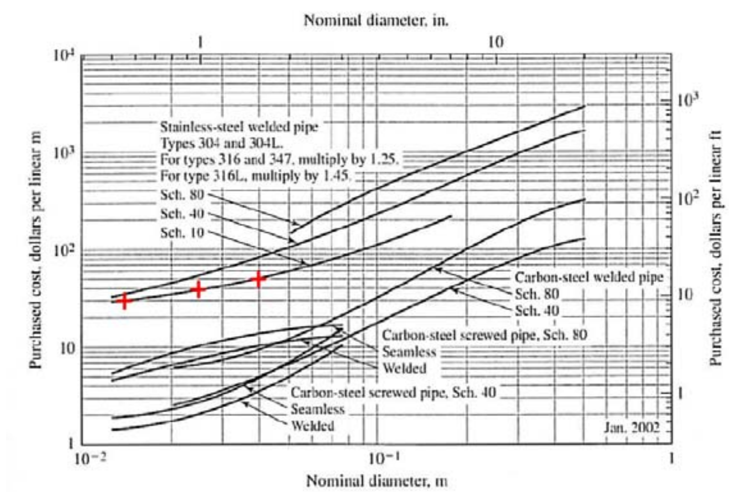

Figure 27 Price assumption for piping material

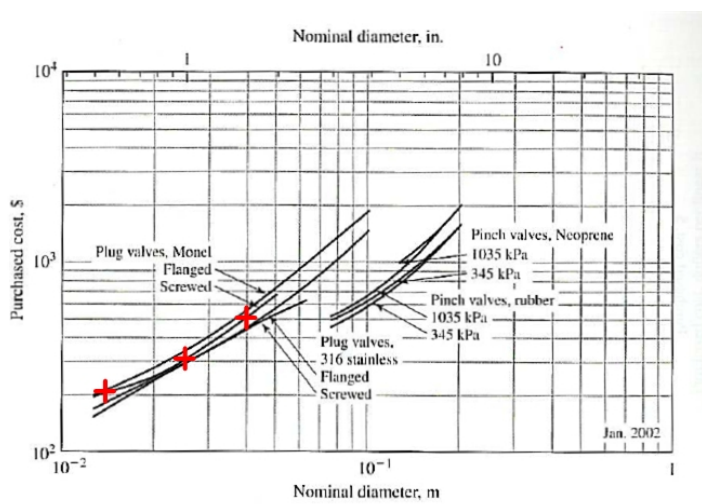

Figure 28 Price assumption for valves

Table 4 Equipment list with prices and ordering code. Assumed prices are grey.

Equipment code	No	Ordering code	price inc. taxes		total price inc. taxes	
Heat exchangers or evaporators/condensers						
HX1	1	K215 x 15 S 1-1/8''	€	451,94	€	451,94
HX2-1	1	K215 x 37 S 1-1/8''	€	489,61	€	489,61
HX2-2	2	K215 x 41 S 1-1/8''	€	508,44	€	1 016,87
HX3	1	K215 x 5 S 1-1/8''	€	451,94	€	451,94
HX4-1	1	K215 x 17 S 1-1/8''	€	459,48	€	459,48
HX4-2	1	K215 x 24 S 1-1/8''	€	467,01	€	467,01
HX5-1	1	K215 x 81 S 1-1/8''	€	527,27	€	527,27
HX5-2	2	K215 x 113 S 1-1/8''	€	828,56	€	1 657,13
HX-A	1	SJGE-30-6-630-1400-1/230/50-7	€	26 363,36	€	26 363,36
Compressor						
C-CO2	1		€	-	€	-
Pumps						
C-EG	2	CM3-4 A-F-G-E AQQE	€	1 125,00	€	2 250,00
Vessels						
E-1	1		€	-	€	-
Pipes						
100-300	4,75		€	22,60	€	107,34
100-300	24,25		€	28,62	€	694,11
100-300	1,55		€	37,66	€	58,38
Fittings						
Elbow						
100-300	16	H-SLA-8N	€	-	€	-
100-300	68	H-SLA-16N	€	-	€	-
100-300	4	H-SLA- #	€	-	€	-
Cross						
100-300	2	H-SXA-8N	€	-	€	-
100-300	14	H-SXA-16N	€	-	€	-
100-300	1	H-SXA- #	€	-	€	-
Valves						
Ball valve						
100-300	4	BV-H-8N-Nil-S316	€	165,71	€	662,85
100-300	15	BV-H-16N-Nil-S316	€	241,04	€	3 615,55
100-300	1	BV-H-#-Nil-S316	€	301,30	€	301,30

Instuments						
TT	33	F2020-100-B	€	20,00	€	660,00
PT	4	PMP71-ABA1WB11AAAA	€	1 167,13	€	4 668,50
PI	3	Pressure indicator			€	-
PDT	24	PMD75-ABA7LB1BAAU	€	1 365,25	€	32 766,00
FT	3	Coriolis Mass Flowmeter, RHM12	€	2 812,50	€	8 437,50
Data logging systems						
cFP-CB-3	5	cFP-CB-3	€	231,13	€	1 155,63
cFP-CB-1	5	cFP-CB-1	€	168,63	€	843,13
cFP-1808	2	cFP-1808	€	1 049,88	€	2 099,75
					€	90 204,62

VI. Conclusion and recommendation

With the equipment specified in chapter V and in the appendix and a layout concept presented through an isometric piping drawing and P&ID, a design concept of a 100kW R744 compressor and plate heat exchanger test facility has been proposed in this thesis.

The brazed plate heat exchangers for the use in this test facility are not commercially available. Thus a design concept of each necessary plate heat exchangers has been made and can be considered as reference values for future development. The used equations have been presented in chapter IV.B.3. As stated before the heat transfer coefficients have been calculated with equations with the lowest promising values. It can be said that the resulting heat transfer capacities are higher than calculated. On the other side the geometrical parameters have been adjusted at will to keep the pressure losses under 1 bar. Experiments with R744 brazed plate heat exchangers have shown that pressure losses are going up to 3 bar with heating duties of 15kW.

As stated in chapter IV.E.2 the arrangement thus the length of the pipes has a not to underestimate influence on the necessary buffer volume. Although extra volume has been considered during the design process the necessary volume in the final design concept should double checked. The gas/liquid separator for the use in the pressure vessel has yet to be designed. Since the general length of the vessel itself is large, the necessary room for the separator should be provided. Further openings on the cylindrical side of the vessel for safety valves and etc. can be added if the necessary space as calculated is provided.

The arrangement proposed in the isometric piping drawing doesn’t consider necessary ventilation ducts for the air cooled heat exchanger.

The measurement and control engineering aspects can be considered after or during building the test facility and are not treated in this work.

VII. References to literature

1. *A theoretical approach to predict the performance of chevron-type plate heat exchangers.* **Martin, Holger.** s.l. : Chemical Engineering and Processing, 1995, Bd. 35.

2. **García-Cascales, J.R., et al.** Assessment of boiling and condensation heat transfer correlations in the modelling of plate heat exchangers. 09. 01 2007, S. 1029-1041.

3. **Kim, Y.S.** An Experimental Study on Evaporation Heat Transfer Characteristics and Pressure Drop in Plate Heat Exchanger. Yonsei University : s.n., 1999.

4. **Han, Dong-Hyouck, Lee, Kyu-Jung und Kim, Yoon-Ho.** The Characteristics of Condensation in Brazed Plate Heat Exchangers with Different Chevron Angles. *Journal of the Korean Physical Society.* 03. 02 2003, S. 66-73.

5. —. Experiments on the characteristics of evaporation of R410A in brazed plate heat exchangers with different geometric configurations. *Applied Thermal Engineering 23.* 16. 10 2002, S. 1209-1225.

6. *Heat exchangers Selection, Rating and Thermal Design.* **Kakac, S. und Liu, H.** s.l. : CRC Press, 1998.

7. **Pettersen, Jostein.** *Trans-critical vapor compression device.* United States of America, 23. 06 1994.

8. **Klapp, Eberhard.** *Apparate- und Anlagentechnik.* Berlin : Springer-Verlag, 1980.

9. **Moore, Lester P.** *3713279* United States of America, 1970.

10. **Beattie, David Lloyd George.** *4070168* Canada, 1976.

11. **Reed, Robert D. und Schwartz, Robert E.** *4035171* United States of America, 1976.

12. *Design of Fractionating Columns.* **Souders, Jr., Mott und Brown, George Granger.** Chicago : s.n., 1933.

13. **GPSA.** *Engineering Data Book 12th Edition.* Oklahoma City : s.n., 2004.

14. **Peters, Max S., Timmerhaus, Klaus D. und West, Ronald E.** *Plant Design and Economics for Chemical Engineers.* New York : McGraw-Hill, 2003.

15. **Coleman, Hugh W. und Steele, W. Glenn.** *Experimentation and Uncertainty Analysis for Engineers.* New York : John Wiley & Sons, 1999.

16. **VDI-Buch.** *Kraftwerkstechnik zur Nutzung fossiler, nuklearer und regenerativer Energiequellen.* s.l. : Springer Berlin Heidelberg, 2006.

17. —. *VDI-Wärmeatlas.* s.l. : Springer Berlin Heidelberg, 2006.

18. **Kim, Man-Hoe, Pettersen, Jostein und Bullard, Clark W.** Fundamental process and system design issues in CO2 vapor compression systems. *Progress in Energy and Combustion Science 30.* 25. 02 2003, S. 119-174.

19. *Revival of carbon dioxide as a refrigerant.* **Lorentzen, Gustav.** 1994, Int. J. Refrig.

20. **Wheeler, Anthony J. und Ganji, Ahmad R.** *Introduction to Engineering Experimentation.* San Francisco : PEARSON, 2004.

21. *Carbon dioxide - new uses for an old refrigerant.* **Pearson, Andy.** s.l. : International Journal of Refrigeration, 2005, Bd. 28.

22. **Perkins, Jacob.** *Improvement in the Apparatus and Means for Producing Ice, and in Cooling Fluids.* London, 1834.

23. **Lowe, Thaddeus.** *Ice-making machine. 952* 1867.

VIII. Appendix

A. Cyclic process

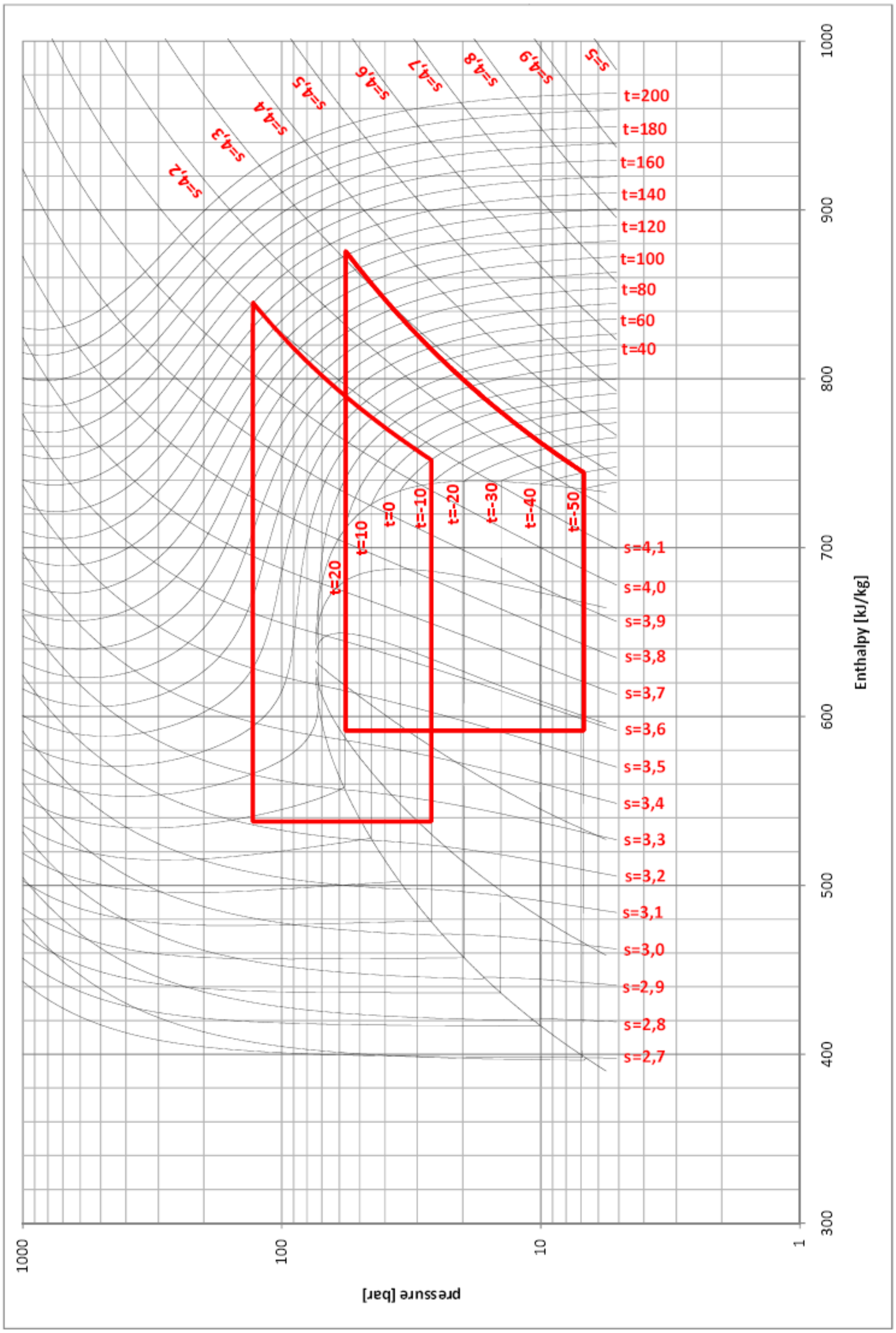

Figure 29 p,h-diagram with two circuit. The compressor inlet temperatures are 0°C and -40°C respectively

Table 5 Calculation process for the conditions in the R744 cyclic process.

Condition	t [°C]	p [Bar]	v [m^3/kg]	c_p [kJ/kgK]	h [kJ/kg]	s [kJ/(kgK)]	x [-]
1	t_1	p_1	$v_1 = f(t_1, p_1)$	$c_{p1} = f(t_1, p_1)$	$h_1 = f(t_1, p_1)$	$s_1 = f(t_1, p_1)$	$x_1 = f(t_1, h_1)$
compression 1-2							
2	$t_2 = f(h_2, p_2)$	$p_2 = p_1 \cdot \left(\frac{w_s}{\frac{\kappa}{\kappa-1} \cdot v_1 \cdot p_1} + 1\right)^{\frac{\kappa}{\kappa-1}}$	$v_2 = f(t_2, p_2)$	$c_{p2} = f(t_2, p_2)$	$h_2 = h_1 + w_s$	$s_2 = f(t_2, p_2)$	$x_2 = f(t_2, h_2)$
cooling 2-3'							
3'	$t_{3'} = f(h_{3'}, p_{3'})$	$p_{3'} = p_2$	$v_{3'} = f(t_{3'}, p_{3'})$	$c_{p3'} = f(t_{3'}, p_{3'})$	$h_{3'} = h_2 - \frac{P}{\dot{m}}$	$s_{3'} = f(t_{3'}, p_{3'})$	$x_{3'} = f(t_{3'}, h_{3'})$
cooling 3'-3''							
3''	$t_{3''} = f(h_{3''}, p_{3''})$	$p_{3''} = p_{3'}$	$v_{3''} = f(t_{3''}, p_{3''})$	$c_{p3''} = f(t_{3''}, p_{3''})$	$h_{3''} = h_{3'} - \frac{Q_{re}}{\dot{m}}$	$s_{3''} = f(t_{3''}, p_{3''})$	$x_{3''} = f(t_{3''}, h_{3''})$
cooling 3''-3							
3	$t_3 = f(h_3, p_3)$	$p_3 = p_{3''}$	$v_3 = f(t_3, p_3)$	$c_{p3} = f(t_3, p_3)$	$h_3 = h_{3''} - \frac{Q_{in}}{\dot{m}}$	$s_3 = f(t_3, p_3)$	$x_3 = f(t_3, h_3)$
expanding 3-4							
4	$t_4 = f(h_4, p_4)$	$p_4 = p_1$	$v_4 = f(t_4, p_4)$	$c_{p4} = f(t_4, p_4)$	$h_4 = h_3$	$s_4 = f(t_4, p_4)$	$x_4 = f(t_4, h_4)$
evaporating 4-1'							
1'	$t_{1'} = f(h_{1'}, p_{1'})$	$p_{1'} = p_{3''}$	$v_{1'} = f(t_{1'}, p_{1'})$	$c_{p1'} = f(t_{1'}, p_{1'})$	$h_{1'} = h_4 + \frac{Q_{re}}{\dot{m}}$	$s_{1'} = f(t_{1'}, p_{1'})$	$x_{1'} = f(t_{1'}, h_{1'})$
evaporating 1'-1							
1	$t_1 = f(h_1, p_1)$	$p_1 = p_{1'}$	$v_1 = f(t_1, p_1)$	$c_{p1} = f(t_1, p_1)$	$h_1 = h_{1'} + \frac{Q_{in}}{\dot{m}}$	$s_1 = f(t_1, p_1)$	$x_1 = f(t_1, h_1)$

Table 6 Calculated values for the R744 circuit. Mass flow 1,00kg/s. Compressor inlet temperature 0°C.

Condition	t [°C]	p [Bar]	v [m^3/kg]	c_p [kJ/kgK]	h [kJ/kg]	s [kJ/(kgK)]	x [-]
1	0,00	26,50	0,01536	1,30	751,95	4,07	1,00
compression 1-2					80,00	0,00	
2	131,10	129,36	0,00461	1,47	831,95	4,07	1,00
cooling 2-3'					-80,00	-0,21	
3'	85,45	129,36	0,00319	2,29	751,95	3,86	1,00
cooling 3'-3''					-200,00	-0,61	
3''	24,54	129,36	0,00116	2,46	551,95	3,25	0,00
cooling 3''-3					-14,10	-0,05	
3	18,65	129,36	0,00112	2,33	537,85	3,21	0,00
expanding 3-4					0,00	0,05	
4	-10,00	26,50	0,00421	2,29	537,85	3,25	0,23
evaporating 4-1'					200,00	0,76	
1'	-9,93	26,50	0,01398	1,50	737,85	4,02	1,00
evaporating 1'-1					14,10	0,05	
1	0,00	26,50	0,01536	1,30	751,95	4,07	1,00

Table 7 Calculated values for the R744 circuit. Mass flow 0,70kg/s. Compressor inlet temperature -40°C.

Condition	t [°C]	p [Bar]	v [m^3/kg]	c_p [kJ/kgK]	h [kJ/kg]	s [kJ/(kgK)]	x [-]
1	-40,00	6,83	0,05917	0,94	744,45	4,26	1,00
compression 1-2					114,29	0,01	
2	117,36	56,72	0,01151	1,13	858,74	4,27	1,00
cooling 2-3'					-114,29	-0,33	
3'	31,65	56,72	0,00665	2,03	744,45	3,94	1,00
cooling 3'-3''				-47,62	-142,86	-0,49	
3''	19,58	56,72	0,00129	4,15	601,59	3,45	0,29
cooling 3''-3					-9,83	-0,03	
3	19,58	56,72	0,00129	4,15	591,76	3,42	0,23
expanding 3-4					0,00	0,15	
4	-50,00	6,83	0,03250	0,99	591,76	3,57	0,57
evaporating 4-1'					142,86	0,64	
1'	-50,02	6,83	0,05504	1,82	734,62	4,21	1,00
evaporating 1'-1					9,83	0,04	
1	-40,00	6,83	0,05917	0,94	744,45	4,26	1,00

Table 8 Calculation process for the conditions in the ethylene glycol cyclic process.

Condition	t [°C]	p [Bar]	v [m³/kg]	c_p [kJ/kg]	h [kJ/kg]
1	t_1	p_1	$v_1 = f(t_1, p_1)$	$c_{p1} = f(t_1, p_1)$	h_1
pumping 1-2					
2	$t_2 = \frac{dh - v_1 \cdot (p_2 - p_1) + c_{p1} \cdot t_1}{c_{p2}}$	p_2	$v_2 = f(t_2, p_2)$	$c_{p2} = f(t_2, p_2)$	$h_2 = h_1 + dh$
heating 2-3'					
3'	$t_{3'} = \frac{dh - v_2 \cdot (p_{3'} - p_2) + c_{p2} \cdot t_2}{c_{p3'}}$	$p_{3'} = p_2$	$v_{3'} = f(t_{3'}, p_{3'})$	$c_{p3'} = f(t_{3'}, p_{3'})$	$h_3 = h_2 + \frac{Q_{in}}{\dot{m}}$
heating 3'-3					
3	$t_3 = \frac{dh - v_{3'} \cdot (p_3 - p_{3'}) + c_{p3'} \cdot t_{3'}}{c_{p3}}$	$p_3 = p_{3'}$	$v_3 = f(t_3, p_3)$	$c_{p3} = f(t_3, p_3)$	$h_3 = h_{3'} + \frac{P}{\dot{m}}$
cooling 3-1'					
1'	$t_{1'} = \frac{dh - v_3 \cdot (p_{1'} - p_3) + c_{p3} \cdot t_3}{c_{p1'}}$	$p_{1'} = p_3$	$v_{1'} = f(t_{1'}, p_{1'})$	$c_{p1'} = f(t_{1'}, p_{1'})$	$h_{1'} = h_{1'} + \frac{Q_{re}}{\dot{m}}$
cooling 1'-1					
1	$t_1 = \frac{dh - v_3 \cdot (p_1 - p_3) + c_{p3} \cdot t_3}{c_{p1}}$	$p_1 = p_{1'}$	$v_1 = f(t_1, p_1)$	$c_{p1} = f(t_1, p_1)$	$h_1 = h_{1'} + \frac{Q_{re}}{\dot{m}}$

Table 9 Calculated values for the ethylene glycol circuit. Mass flow 1,00kg/s. R744 compressor inlet temperature 0°C.

Condition	t [°C]	p [Bar]	v [m³/kg]	c_p [kJ/kg]	h [kJ/kg]
1	10,16	1,00	0,000924	3,20	300,82
pumping 1-2					0,00
2	10,17	5,00	0,000924	3,20	300,82
heating 2-3'					200,00
3'	61,75	4,00	0,000933	3,31	500,82
heating 3'-3					80,00
3	81,17	3,00	0,000938	3,35	580,82
cooling 3-1'					-80,00
1'	61,72	2,00	0,000933	3,31	500,82
cooling 1'-1					-200,00
1	10,16	1,00	0,000924	3,20	300,82

Table 10 Calculated values for the ethylene glycol circuit. Mass flow 0,70kg/s. R744 compressor inlet temperature -40°C.

Condition	t [°C]	p [Bar]	v [m³/kg]	c_p [kJ/kg]	h [kJ/kg]
1	-19,55	1,00	0,000920	3,13	301,42
pumping 1-2					0,00
2	-19,63	5,00	0,000920	3,13	301,42
heating 2-3'					200,00
3'	32,79	4,00	0,000928	3,25	501,42
heating 3'-3					160,00
3	73,15	3,00	0,000936	3,33	661,42
cooling 3-1'					-160,00
1'	32,88	2,00	0,000928	3,25	501,42
cooling 1'-1					-200,00
1	-19,55	1,00	0,000920	3,13	301,42

Table 11 Calculation process for the conditions in the ethylene glycol cyclic process.

Condition	t [°C]	p [Bar]	v [m³/kg]	c_p [kJ/kg]	h [kJ/kg]
1	t_1	p_1	$v_1 = f(t_1, p_1)$	$c_{p1} = f(t_1, p_1)$	h_1
pumping 1-2					
2	$t_2 = \frac{dh - v_1 \cdot (p_2 - p_1) + c_{p1} \cdot t_1}{c_{p2}}$	p_2	$v_2 = f(t_2, p_2)$	$c_{p2} = f(t_2, p_2)$	$h_2 = h_1 + dh$
heating 2-3					
3	$t_{3'} = \frac{dh - v_2 \cdot (p_{3'} - p_2) + c_{p2} \cdot t_2}{c_{p3'}}$	$p_{3'} = p_2$	$v_{3'} = f(t_{3'}, p_{3'})$	$c_{p3'} = f(t_{3'}, p_{3'})$	$h_3 = h_2 + \frac{Q_{in}}{\dot{m}}$
cooling 3-1					
1	$t_1 = \frac{dh - v_3 \cdot (p_1 - p_3) + c_{p3} \cdot t_3}{c_{p1}}$	$p_1 = p_3$	$v_1 = f(t_1, p_1)$	$c_{p1} = f(t_1, p_1)$	$h_1 = h_3 + \frac{Q_{re}}{\dot{m}}$

Table 12 Calculated values for the ethylene glycol circuit. Mass flow 1,00kg/s. R744 compressor inlet temperature 0°C.

Condition	t [°C]	p [Bar]	v [m³/kg]	c_p [kJ/kg]	h [kJ/kg]
1	0,26	1,00	0,000923	3,18	301,22
pumping 1-2					0,00
2	0,25	5,00	0,000923	3,18	301,22
heating 2-3					200,00
3	52,10	3,00	0,000931	3,29	501,22
cooling 3-1					-200,00
1	0,26	1,00	0,000923	3,18	301,22

Table 13 Calculated values for the ethylene glycol circuit. Mass flow 0,70kg/s. R744 compressor inlet temperature -40°C.

Condition	t [°C]	p [Bar]	v [m³/kg]	c_p [kJ/kg]	h [kJ/kg]
1	-29,46	1,00	0,000919	3,11	302,22
pumping 1-2					0,00
2	-29,47	5,00	0,000919	3,11	302,22
heating 2-3					200,00
3	23,40	3,00	0,000926	3,23	502,22
cooling 3-1					-200,00
1	-29,46	1,00	0,000919	3,11	302,22

E. Heat exchanger

Table 14 geometrical design parameters for the heat exchangers in use.

	attribute	HX1	HX2-1	HX2-2	HX3	HX4-1	HX4-2	HX5-1	HX5-2
Design attributes									
Depth	$L_c\ [m]$	0,054	0,118	0,115	0,023	0,050	0,075	0,262	0,366
Width	$L_w\ [m]$	0,247	0,247	0,247	0,247	0,247	0,247	0,247	0,247
Height	$L_v\ [m]$	0,449	0,449	0,449	0,449	0,449	0,449	0,449	0,449
Characterizing values									
heat transfer area	$HTA\ [m^2]$	1,60	4,11	4,57	0,53	1,83	2,66	8,98	12,49
pressure loss	$\Delta p_h\ [bar]$	0,718	0,745	0,461	0,072	0,647	0,214	0,581	0,181
pressure loss	$\Delta p_c\ [bar]$	0,251	0,581	0,430	0,862	0,437	0,114	0,617	0,200
geometric attributes of the plate									
Number of plates	$N_t\ [-]$	12	30	34	4	14	20	66	92
chevron angle	$\beta\ [°]$	45	45	45	45	45	45	45	45
mean channel spacing	$b\ [mm]$	4	2	1,5	6	2	2	2	2
wavelength	$\Lambda\ [mm]$	12,57	6,28	4,71	18,85	6,28	6,28	6,28	6,28
thickness of plate	$t\ [mm]$	2	2	2	2	2	2	2	2
corrugation parameter	$X\ [-]$	1	1	1	1	1	1	1	1
area enlargement factor	$\Phi\ [-]$	1,22	1,22	1,22	1,22	1,22	1,22	1,22	1,22

F. Pressure vessel

Table 15 Volume and mass of the components and piping parts of the test facility

		available Volume V [m³]	pressure [bar]	temperature [°C]	v_{min} $[m^3/kg]$	m_{max} $[kg]$	$v_{80bar,50°C}$ $[m^3/kg]$	$m_{80bar,50°C}$ $[kg]$
HX1	high pressure side	0,0012	129,36	85,45	0,00319	0,38	0,00456	0,27
HX2 (100kW)		0,0028	129,36	24,54	0,00116	2,38	0,00456	0,61
HX2 (50kW)		0,0022	129,36	24,54	0,00116	1,86	0,00456	0,47
HX2 (50kW)		0,0022	129,36	24,54	0,00116	1,86	0,00456	0,47
HX3		0,0004	129,36	18,65	0,00112	0,35	0,00456	0,09
pipes 1		0,0177	129,36	131,10	0,00461	3,83	0,00456	3,87
pipes 2		0,0627	129,36	85,45	0,00319	19,63	0,00456	13,75
pipes 3		0,0340	129,36	24,54	0,00116	29,20	0,00456	7,45
pipes 4		0,0129	129,36	18,65	0,00112	11,55	0,00456	2,83
SUM		**0,136**				**71,04**		**29,81**
HX3	low pressure side	0,000	26,50	-9,93	0,01398	0,03	0,00456	0,09
HX4 (100kW)		0,001	26,50	-10,00	0,00421	0,18	0,00456	0,17
HX4 (50kW)		0,001	26,50	-10,00	0,00421	0,36	0,00456	0,33
HX4 (50kW)		0,001	26,50	-10,00	0,00421	0,36	0,00456	0,33
pipes 5		0,052	26,50	-10,00	0,00421	12,28	0,00456	11,35
pipes 6		0,105	26,50	-9,93	0,01398	7,52	0,00456	23,07
pipes 7		0,036	26,50	0,00	0,01536	2,33	0,00456	7,85
SUM		**0,197**				**23,06**		**43,19**
Required buffer Volume [m³]		**0,096**						

Table 16 minimum permissible diameter for gas/liquid separation

ρ_G $[kg/m^3]$	ρ_L $[kg/m^3]$	$k\ [-]$	w_{max} $[kg/s]$	w_{min} $[m^3/kg]$	$A\ [m^2]$	$D_{min}\ [m]$
97,64	927,41	0,147	0,429	0,0042	0,0098	0,1119

Table 17 Design parameters for the shell thickness

cylindrical shell

		Operational pressure/thickness	Testcase
D_e	$[mm]$	250,00	250,00
P	$[MPa]$	10,00	10,00
$R_{p0,2/t}$	$[N/mm^2]$	335,00	
$R_{m/20}$	$[N/mm^2]$	470,00	
$R_{p0,2/t_{test}}$	$[MPa]$	335,00	335,00
f_{dmin1}	$[N/mm^2]$	223,33	
f_{dmin2}	$[N/mm^2]$	195,83	
f_{dmin}	$[N/mm^2]$	195,83	
f_{test}	$[N/mm^2]$	319,05	319,05
f	$[N/mm^2]$	195,83	
z	$[-]$	0,85	1,00
c	$[mm]$	1,00	
δ_e	$[mm]$	1,00	1,00
e	$[mm]$	7,29	3,86
e_n	$[mm]$	10,00	10,00
e_{min}	$[mm]$	9,00	9,00
e_a	$[mm]$	8,00	
P_{max}	$[N/mm^2]$	12,53	22,97

spherical shell/hemispherical end

D_e	$[mm]$	250,00	250,00
P	$[MPa]$	10,00	10,00
$R_{p0,2/t}$	$[N/mm^2]$	335,00	
$R_{m/20}$	$[N/mm^2]$	470,00	
$R_{p0,2/t_{test}}$	$[MPa]$	335,00	335,00
f_{dmin1}	$[N/mm^2]$	223,33	
f_{dmin2}	$[N/mm^2]$	195,83	
f_{dmin}	$[N/mm^2]$	195,83	
f_{test}	$[N/mm^2]$	319,05	319,05
f	$[N/mm^2]$	195,83	
z	$[-]$	0,85	1,00
c	$[mm]$	1,00	
δ_e	$[mm]$	1,00	1,00
e	$[mm]$	3,70	3,86
e_n	$[mm]$	6,00	6,00
e_{min}	$[mm]$	5,00	5,00
e_a	$[mm]$	4,00	
P_{max}	$[N/mm^2]$	12,53	25,52

Table 18 Design parameters for the shell thickness in the opening areas. For the body.

		cylindrical shell - H1, H2	**cylindrical shell - 106.05**
Geometrical parameter - opening reinforcement			
$e_{c,s}$	$[\,mm]$	10,00	10,00
a		77,05	
l_{so}	$[mm]$	48,99	48,99
l'_s	$[mm]$	13,00	16,00
l'_b	$[mm]$	13,00	16,00
r_{is}	$[mm]$	115,00	115,00
Geometrical parameter - nozzle reinforcement			
d_{ib}	$[mm]$	42,50	28,50
e_b	$[mm]$	2,90	2,60
d_{eb}	$[mm]$	48,30	33,70
l_{bo}	$[mm]$		
l'_{bi}	$[mm]$	11,47	8,99
e'_s	$[mm]$	5,74	4,50

Reinforcement check			
pressure loaded area - round the opening			
Af_b	$[mm^2]$	165,91	139,07
Af_s	$[mm^2]$	159,00	186,00
f_s	$[Mpa]$	335,00	335,00
f_{ob}	$[Mpa]$	335,00	335,00
f_{op}	$[Mpa]$	335,00	335,00
GE_1	$[Mpa]$	108845,95	107272,99
pressure loaded area - due to nozzle			
Ap_b	$[mm^2]$	488,75	370,50
Ap_s	$[mm^2]$	10355,75	10355,75
GE_2	$[Mpa]$	108445,00	107262,50
P_{max}	$[Mpa]$	9,89	10,00

Table 19 Design parameters for the shell thickness in the opening areas. For the feed and overhead.

		hemispherical end - 106.06	hemispherical end - LI1, LI2, FI1
Geometrical parameter - opening reinforcement			
$e_{c,s}$	$[mm]$	6,00	6,00
$e_{a,s}$	$[mm]$	6,00	6,00
l_{so}	$[mm]$	37,63	37,63
l'_s	$[mm]$	37,63	37,63
l'_b	$[mm]$	10,00	10,00
r_{is}	$[mm]$	115,00	115,00
Geometrical parameter - nozzle reinforcement			
d_{ib}	$[mm]$	28,50	13,60
e_b	$[mm]$	2,60	1,80
d_{eb}	$[mm]$	33,70	17,20
r_{ms}	$[mm]$	118,00	118,00
l_{bo}	$[mm]$	8,99	5,26
l'_{bi}	$[mm]$	4,50	2,63

Reinforcement check			
pressure loaded area - round the opening			
Af_b	$[mm^2]$	139,07	139,07
Af_s	$[mm^2]$	186,00	241,38
f_s	$[Mpa]$	335,00	335,00
f_{ob}	$[Mpa]$	335,00	335,00
f_{op}	$[Mpa]$	335,00	335,00
GE_1	$[Mpa]$	107272,99	127450,18
pressure loaded area - due to nozzle			
Ap_b	$[Mpa]$	228,00	108,80
δ		0,14	0,07
a		16,91	8,61
Ap_s	$[Mpa]$	3056,18	2591,06
GE_2	$[Mpa]$	32841,84	26998,58
P_{max}	$[Mpa]$	33,83	45,82

Table 20 Design parameters for the shell thickness in the opening areas. For an oblique opening in the spherical ends.

		oblique nozzles in spherical shells and dished ends
Geometrical parameter - opening reinforcement		
$e_{c,s}$	$[mm]$	6,00
$e_{a,s}$	$[mm]$	6,00
l_{so}	$[mm]$	37,63
l'_s	$[mm]$	37,63
r_{is}	$[mm]$	115,00
Geometrical parameter - nozzle reinforcement		
d_{ib}	$[mm]$	13,60
e_b	$[mm]$	1,80
d_{eb}	$[mm]$	17,20
r_{ms}	$[mm]$	118,00
pressure loaded area - round the opening		
Af_b	$[mm^2]$	139,07
Af_s	$[mm^2]$	186,00
f_s	$[Mpa]$	335,00
f_{ob}	$[Mpa]$	335,00
f_{op}	$[Mpa]$	335,00
GE_1	$[Mpa]$	107272,99
pressure loaded area - due to nozzle		
δ		0,07
Φ	$[rad]$	0,79
$arcsin(1-\delta)$		1,19
a		12,25
Ap_s	$[Mpa]$	2795,21
Ap_ϕ	$[Mpa]$	92,48
GE_2	$[Mpa]$	29502,54
Ap_b	$[Mpa]$	108,80
P_{max}	$[Mpa]$	36,25

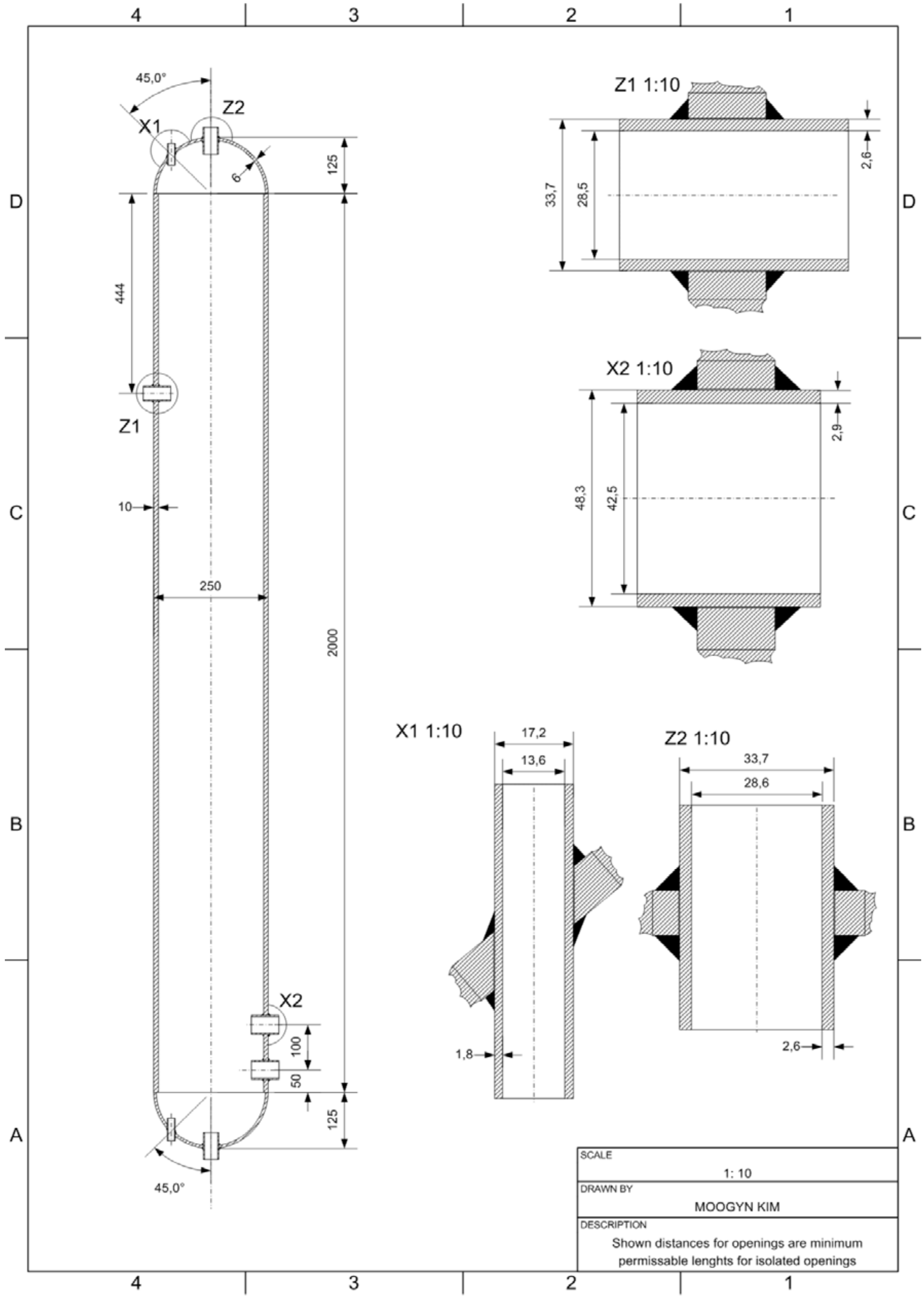

Figure 30 technical drawing of the pressure vessel (image from original file "B1.vsd")

G. Pipes

Table 21 Pipe dimensioning and pressure losses for the R744 circuit.

pipe	$\dot{m}\ [kg/s]$	$w\ [m/s]$	$\rho\ [kg/m^3]$	$PN\ [bar]$	$d_i\ [m]$	$l\ [m]$	$V\ [m^3]$	$\Delta p\ [bar]$
compressing								
101.01	1	19,6302	216,7171	130	0,017	1,3	0,0177	0,5399
						1,3	**0,0177**	**0,5399**
cooling								
102.01	1	5,01	313,1429	130	0,0285	1,5	0,0336	0,0848
102.06	1	5,01	313,1429	130	0,0285	0,45	0,0101	0,1179
102.07	1	5,01	313,1429	130	0,0285	0,1	0,0022	0,0060
102.08	1	5,01	313,1429	130	0,0285	0,1	0,0022	0,1120
102.09	1	5,01	313,1429	130	0,0285	0,1	0,0022	0,0060
102.10	1	5,01	313,1429	130	0,0285	0,45	0,0101	0,1179
102.11	1	5,01	313,1429	130	0,0285	0,1	0,0022	0,0060
						2,8	**0,0627**	**0,4506**
cooling								
103.01	1	4,95	859,6473	130	0,0173	0,45	0,0061	0,2088
103.02	1	4,95	859,6473	130	0,0173	0,1	0,0014	0,0317
103.03	1	4,95	859,6473	130	0,0173	0,45	0,0061	0,0614
103.05	1	4,95	859,6473	130	0,0173	1,5	0,0204	0,4339
						2,5	**0,0340**	**0,7358**
cooling								
104.01	1	4,75	895,0658	130	0,0173	0,95	0,0129	0,0996
						0,95	**0,0129**	**0,0996**
expanding								
105.01	1	2,97	237,4074	100	0,0425	0,25	0,0083	0,0168
105.06	1	2,97	237,4074	100	0,0425	0,45	0,0150	0,0312
105.07	1	2,97	237,4074	100	0,0425	0,1	0,0033	0,0015
105.08	1	2,97	237,4074	100	0,0425	0,1	0,0033	0,0298
105.09	1	2,97	237,4074	100	0,0425	0,1	0,0033	0,0015
105.10	1	2,97	237,4074	100	0,0425	0,45	0,0150	0,0312
105.11	1	2,97	237,4074	100	0,0425	0,1	0,0033	0,0015
						1,55	**0,0517**	**0,1135**
heating								
106.01	1	21,92	71,53	100	0,0285	0,45	0,0101	0,3191
106.02	1	21,92	71,53	100	0,0285	0,1	0,0022	0,0469
106.03	1	21,92	71,53	100	0,0285	0,45	0,0101	0,0787
106.05	1	21,92	71,53	100	0,0285	1,2	0,0269	0,1468
106.06	1	21,92	71,53	100	0,0285	2,5	0,0560	0,2649
						4,7	**0,1052**	**0,8563**
heating								
107.01	1	24,08	65,08	100	0,0285	1,6	0,0358	0,1934
						1,6	**0,0358**	**0,1934**
SUM						**15,4**	**0,3200**	**2,9892**

Table 22 Pipe dimensioning and pressure losses for the ethylene glycol circuit.

pipe	$\dot{m}\ [kg/s]$	$w\ [m/s]$	$\rho\ [kg/m^3]$	$PN\ [bar]$	$d_i\ [m]$	$l\ [m]$	$V\ [m^3]$	$\Delta p\ [bar]$
pumping								
201.01	1	1,45	1081,08	10	0,0285	0,55	0,0123	0,0211
201.05	1	1,45	1081,08	10	0,0285	0,4	0,0090	0,0339
201.06	1	1,45	1081,08	10	0,0285	0,25	0,0056	0,0012
201.07	1	1,45	1081,08	10	0,0285	0,1	0,0022	0,0324
201.08	1	1,45	1081,08	10	0,0285	0,2	0,0045	0,0010
201.09	1	1,45	1081,08	10	0,0285	0,4	0,0090	0,0339
201.10	1	1,45	1081,08	10	0,0285	0,25	0,0056	0,0012
						2,15	**0,0481**	**0,1248**
heating								
202.01	1	1,45	1081,08	10	0,0285	0,45	0,0101	0,0194
202.02	1	1,45	1081,08	10	0,0285	0,1	0,0022	0,0018
202.03	1	1,45	1081,08	10	0,0285	0,45	0,0101	0,0035
202.05	1	1,45	1081,08	10	0,0285	0,9	0,0201	0,0217
						1,9	**0,0425**	**0,0464**
heating								
203.01	1	1,45	1081,08	10	0,0285	0,2	0,0045	0,0060
						0,2	**0,0045**	**0,0060**
cooling								
204.01	1	1,45	1081,08	10	0,0285	1,5	0,0336	0,0296
204.06	1	1,45	1081,08	10	0,0285	0,4	0,0090	0,0339
204.07	1	1,45	1081,08	10	0,0285	0,1	0,0022	0,0017
204.08	1	1,45	1081,08	10	0,0285	0,1	0,0022	0,0324
204.09	1	1,45	1081,08	10	0,0285	0,1	0,0022	0,0017
204.10	1	1,45	1081,08	10	0,0285	0,4	0,0090	0,0339
204.11	1	1,45	1081,08	10	0,0285	0,1	0,0022	0,0017
						2,7	**0,0604**	**0,1351**
cooling								
205.01	1	1,449979	1081,08	10	0,0285	0,5	0,0112	0,0209
205.02	1	1,449979	1081,08	10	0,0285	0,15	0,0034	0,0032
205.03	1	1,449979	1081,08	10	0,0285	0,5	0,0112	0,0050
205.05	1	1,449979	1081,08	10	0,0285	1,1	0,0246	0,0092
205.06	1	1,449979	1081,08	10	0,0285	0,1	0,0022	0,0030
						2,35	**0,0526**	**0,0413**
SUM						**7,4**	**0,1656**	**0,3071**

Table 23 Pipe dimensioning and pressure losses for the ethylene glycol circuit.

pipe	$\dot{m}\ [kg/s]$	$w\ [m/s]$	$\rho\ [kg/m^3]$	$PN\ [bar]$	$d_i\ [m]$	$l\ [m]$	$V\ [m^3]$	$\Delta p\ [bar]$
pumping								
301.01	1	1,45	1084,02	10	0,0285	0,3	0,0067	0,0186
301.05	1	1,45	1084,02	10	0,0285	0,37	0,0083	0,0337
301.06	1	1,45	1084,02	10	0,0285	0,02	0,0004	0,0001
301.07	1	1,45	1084,02	10	0,0285	0,1	0,0022	0,0323
301.08	1	1,45	1084,02	10	0,0285	0,02	0,0004	0,0001
301.09	1	1,45	1084,02	10	0,0285	0,37	0,0083	0,0337
301.10	1	1,45	1084,02	10	0,0285	0,02	0,0004	0,0001
						1,2	**0,0269**	**0,1185**
heating								
302.01	1	1,45	1084,02	10	0,0285	0,45	0,0101	0,0193
302.02	1	1,45	1084,02	10	0,0285	0,1	0,0022	0,0176
302.03	1	1,45	1084,02	10	0,0285	0,45	0,0101	0,0035
302.05	1	1,45	1084,02	10	0,0285	1,35	0,0302	0,0275
302.09	1	1,45	1084,02	10	0,0285	0,37	0,0083	0,0337
302.10	1	1,45	1084,02	10	0,0285	0,02	0,0004	0,0001
302.11	1	1,45	1084,02	10	0,0285	0,1	0,0022	0,0323
302.12	1	1,45	1084,02	10	0,0285	0,02	0,0004	0,0001
302.13	1	1,45	1084,02	10	0,0285	0,37	0,0083	0,0337
302.14	1	1,45	1084,02	10	0,0285	0,02	0,0004	0,0001
						3,25	**0,0727**	**0,1678**
cooling								
303.01	1	1,45	1084,02	10	0,0285	0,4	0,0090	0,0191
303.02	1	1,45	1084,02	10	0,0285	0,05	0,0011	0,0174
303.03	1	1,45	1084,02	10	0,0285	0,4	0,0090	0,0032
303.05	1	1,45	1084,02	10	0,0285	1	0,0224	0,0074
303.06	1	1,45	1084,02	10	0,0285	1,45	0,0325	0,0096
						3,3	**0,0739**	**0,0567**
sum						**7,75**	**0,1735**	**0,3431**

H. instruments list; uncertainties

Table 24 Instrument-list for the R744 circuit.

MSR location/ code	instrument function/ description	operating conditions				pipe dimension	deviation [value]
		flow [kg/s]	pressure [bar]	temperature [°C]	differential pressure [bar]	DN	
F-101							
TT101.1	RTD Sensor, omegafilm	1	129,36	131,10		15	0,955
PT101.1	pressure transmitter, M PMP45	1	129,36	131,10		15	0,259
PI101.1	Pressure indicator	1	129,36	131,10		15	
FT101.1	Coriolis Mass Flowmeter, RHM12	1	129,36	131,10		15	0,002
F-102							
PDT102.1	differential pressure transmitter, S PMD75	1	129,36	85,45	0,65	25	0,259
TT102.1	RTD Sensor, omegafilm	1	129,36	85,45		25	0,727
F-103							
PDT103.1	differential pressure transmitter, S PMD75	1	129,36	24,54	0,79	15	0,259
TT103.1	RTD Sensor, omegafilm	1	129,36	24,54		15	0,423
PDT103.2	differential pressure transmitter, S PMD75	1	129,36	24,54	0,90	15	0,259
TT103.2	RTD Sensor, omegafilm	1	129,36	24,54		15	0,423
PDT103.3	differential pressure transmitter, S PMD75	1	129,36	24,54	0,90	15	0,259
TT103.3	RTD Sensor, omegafilm	1	129,36	24,54		15	0,423
TT103.4	RTD Sensor, omegafilm	1	129,36	24,54		15	0,423
F-104							
PDT104.1	differential pressure transmitter, S PMD75	1	129,36	18,65	0,80	15	0,259
TT104.1	RTD Sensor, omegafilm	1	129,36	18,65		15	0,393
PT104.1	pressure transmitter, M PMP45	1	129,36	18,65		15	0,259
F-105							
TT105.1	RTD Sensor, omegafilm	1	26,50	-10,00		40	0,250
PT105.1	pressure transmitter, M PMP45	1	26,50	-10,00		40	0,053
F-106							
PDT106.1	differential pressure transmitter, S PMD75	1	26,50	-9,93	0,80	25	0,054
TT106.1	RTD Sensor, omegafilm	1	26,50	-9,93		25	0,250
PDT106.2	differential pressure transmitter, S PMD75	1	26,50	-9,93	0,60	25	0,053
TT106.2	RTD Sensor, omegafilm	1	26,50	-9,93		25	0,250
PDT106.3	differential pressure transmitter, S PMD75	1	26,50	-9,93	0,63	25	0,053
TT106.3	RTD Sensor, omegafilm	1	26,50	-9,93		25	0,250
TT106.4	RTD Sensor, omegafilm	1	26,50	-9,93		25	0,250
F-107							
PDT107.1	differential pressure transmitter, S PMD75	1	26,50	0,00	0,63	15	0,053
TT107.1	RTD Sensor, omegafilm	1	26,50	0,00		15	0,300

Table 25 Instrument-list for the ethylene glycol circuit.

MSR location/ code	instrument function/ description	operating conditions				pipe dimension	deviation [value]
		flow [kg/s]	pressure [bar]	temperature [°C]		DN	
F-201							
TT201.1	RTD Sensor, omegafilm	1	5,00	10,17		25	0,351
PT201.1	pressure transmitter, M PMP45	1	5,00	10,17		25	0,010
PI201.1	Pressure indicator	1	5,00	10,17		25	
FT201.1	Coriolis Mass Flowmeter, RHM12	1	5,00	10,17		25	0,002
F-202							
PDT202.1	differential pressure transmitter, S PMD75	1	4,00	61,75	0,29	25	0,010
TT202.1	RTD Sensor, omegafilm	1	4,00	61,75		25	0,609
PDT202.2	differential pressure transmitter, S PMD75	1	4,00	61,75	0,29	25	0,010
TT202.2	RTD Sensor, omegafilm	1	4,00	61,75		25	0,609
PDT202.3	differential pressure transmitter, S PMD75	1	4,00	61,75	0,29	25	0,010
TT202.3	RTD Sensor, omegafilm	1	4,00	61,75		25	0,609
TT202.4	RTD Sensor, omegafilm	1	4,00	61,75		25	0,609
F-203							
PDT203.1	differential pressure transmitter, S PMD75	1	3,00	81,17	0,16	25	0,010
TT203.1	RTD Sensor, omegafilm	1	3,00	81,17		25	0,706
F-204							
PDT204.1	differential pressure transmitter, S PMD75	1	2,00	61,72	0,16	25	0,010
TT204.1	RTD Sensor, omegafilm	1	2,00	61,72		25	0,609
F-205							
PDT205.1	differential pressure transmitter, S PMD75	1	1,00	10,16	0,57	25	0,010
TT205.1	RTD Sensor, omegafilm	1	1,00	10,16		25	0,351
PDT205.2	differential pressure transmitter, S PMD75	1	1,00	10,16	0,56	25	0,010
TT205.2	RTD Sensor, omegafilm	1	1,00	10,16		25	0,351
PDT205.3	differential pressure transmitter, S PMD75	1	1,00	10,16	0,56	25	0,010
TT205.3	RTD Sensor, omegafilm	1	1,00	10,16		25	0,351
TT205.4	RTD Sensor, omegafilm	1	1,00	10,16		25	0,351

Table 26 Instrument-list for the ethylene glycol circuit.

MSR location/ code	instrument function/ description	operating conditions				pipe dimension	deviation [value]
		flow [kg/s]	pressure [bar]	temperature [°C]			
F-301							
TT301.1	RTD Sensor, omegafilm	1	5,00	0,25		25	0,301
PT301.1	pressure transmitter, M PMP45	1	5,00	0,25		25	0,010
PI301.1	Pressure indicator	1	5,00	0,25		25	
FT301.1	Coriolis Mass Flowmeter, RHM12	1	5,00	0,25		25	0,002
F-302							
PDT302.1	differential pressure transmitter, S PMD75	1	3,00	52,10	0,59	25	0,010
TT302.1	RTD Sensor, omegafilm	1	3,00	52,10		25	0,560
PDT302.2	differential pressure transmitter, S PMD75	1	3,00	52,10	0,62	25	0,010
TT302.2	RTD Sensor, omegafilm	1	3,00	52,10		25	0,560
PDT302.3	differential pressure transmitter, S PMD75	1	3,00	52,10	0,62	25	0,010
TT302.3	RTD Sensor, omegafilm	1	3,00	52,10		25	0,560
TT302.4	RTD Sensor, omegafilm	1	3,00	52,10		25	0,560
F-303							
PDT303.1	differential pressure transmitter, S PMD75	1	1,00	0,26	0,60	25	0,010
TT303.1	RTD Sensor, omegafilm	1	1,00	0,26		25	0,301
PDT303.2	differential pressure transmitter, S PMD75	1	1,00	0,26	0,63	25	0,010
TT303.2	RTD Sensor, omegafilm	1	1,00	0,26		25	0,301
PDT303.3	differential pressure transmitter, S PMD75	1	1,00	0,26	0,63	25	0,010
TT303.3	RTD Sensor, omegafilm	1	1,00	0,26		25	0,301
TT303.4	RTD Sensor, omegafilm	1	1,00	0,26		25	0,301

Table 27 Uncertainties of the heat transfer.

Heat exchanger /Flowside	Deviations of thermo dynamical values								calculated heat transfer	fixed deviation	procentual deviation
	$\delta\dot{Q}/\delta\dot{m}$ $[J/kg]$	$\delta\dot{Q}/\delta h$ $[kg/s]$	$\delta\dot{Q}/\delta h_0$ $[kg/s]$	$\delta h/\delta T$ $[J/kg\,K]$	$\delta h/\delta p$ $[m^3/kg]$	δT $[K]$	δp $[bar]$	δh $[J/kg]$	$\dot{Q}$ $[W]$	$\delta\dot{Q}$ $[W]$	%
R744											
HX1	-80000	1	-1	2286	-0,0108	0,73	0,2592	1662	-80000	2180	-2,73
HX1	-80000	1	-1	3307	-0,0074	0,61	0,0101	2012	-80000	3109	-3,89
HX2-1	-200000	0,5	-0,5	2460	-0,0014	0,42	0,2593	1040	-100000	1059	-1,06
HX2-1	200000	0,5	-0,5	3307	-0,0075	0,61	0,0102	2013	100000	1083	1,08
HX2-2	-200000	0,25	-0,25	2460	-0,0014	0,42	0,2594	1040	-50000	477	-0,95
HX3	-14102	1	-1	2332	-0,0010	0,39	0,2587	917	-14102	1387	-9,83
HX4-1	200000	0,5	-0,5	1502	-2,5912	0,25	0,0536	376	100000	637	0,64
HX4-2	200000	0,25	-0,25	1502	-2,5912	0,25	0,0535	376	50000	411	0,82
EG (R744 cooler)											
HX3	14102	1	-1	1300	-0,0185	0,30	0,0535	390	14102	391	2,77
HX2-1	200000	0,5	-0,5	3307	-0,0075	0,61	0,0102	2013	100000	1083	1,08
HX2-2	200000	0,25	-0,25	3307	-0,0075	0,61	0,0102	2013	50000	643	1,29
HX5-1	-200000	0,5	-0,5	3202	-0,0104	0,35	0,0104	1123	-100000	1220	-1,22
HX5-2	-200000	0,25	-0,25	3202	-0,0104	0,35	0,0104	1123	-50000	489	-0,98
EG (R744 evaporator)											
HX4-1	200000	0,5	-0,5	3287	-0,0079	0,56	0,0104	1842	100000	1004	1,00
HX4-2	200000	0,25	-0,25	3287	-0,0079	0,56	0,0105	1842	50000	610	1,22
HX5-1	-200000	0,5	-0,5	3179	-0,0113	0,30	0,0105	958	-100000	1113	-1,11
HX5-2	-200000	0,25	-0,25	3179	-0,0113	0,30	0,0105	958	-50000	655	-1,31

I. Isometric piping

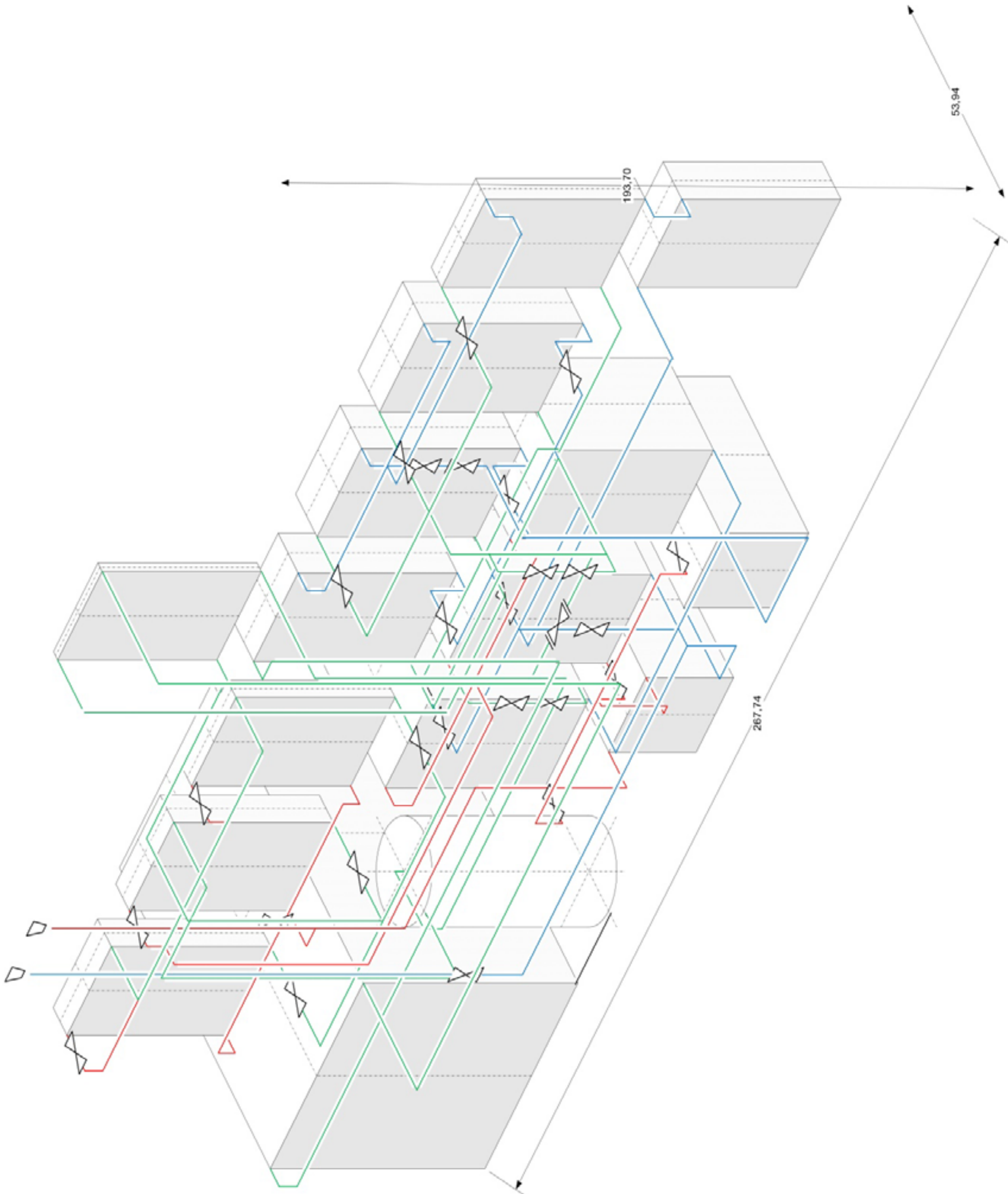

Figure 31 isometric view of the test facility

J. Manual for how to configurate the R744 Library with Microsoft Excel

For the programmed moduls to work probably, the R744 library must be configured with the windows system. Here is a step by step introduction how to do so:

- copy the folder *"kktdlls"* to be found under the path on the cd "*\Bachelorthesis\RN-Linary\"* into the main directory of the system *"C:\"*
- go to the *"system properties"* mostly to be found in *"Control Panel/Performance and Maintance/System"* in the windows configuration as shown in Figure 33
- go to the index tab *"advanced"* and then on *"environment variables"*
- under "System variables" click on the index "Path" and then on "Edit" as showcased in Figure 33
- There type additionally ";C:\kktdlls" and confirm with ok
- under Microsoft Excel go to "Excel options" and then to "Advanced" .
- under "General" – "At startup open all files in:" type in the path "C:\kktdlls" as indicated in Figure 34

To use the moduls the respective macros have to be enabled.

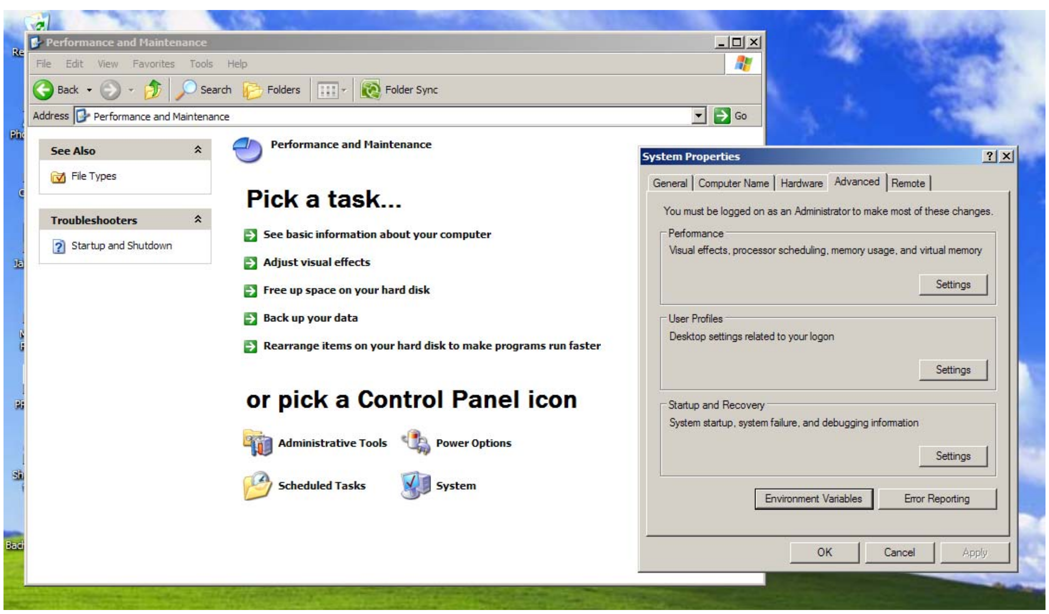

Figure 32 Windows showcasing the place "Enviroment Variables" can be found

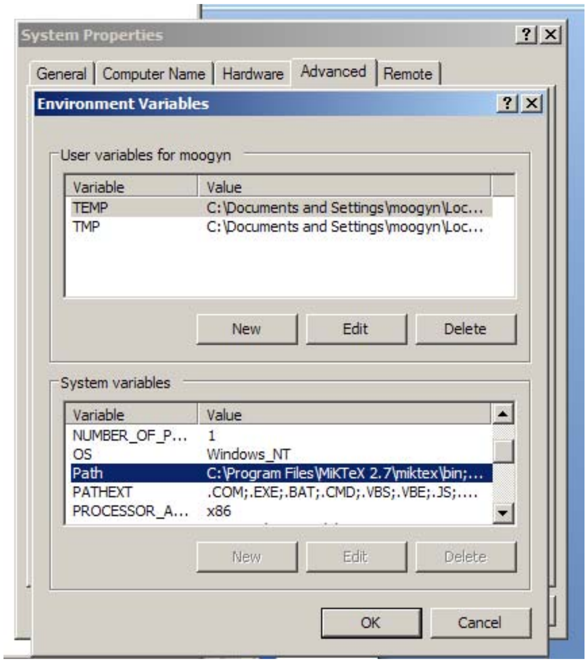

Figure 33 winows showcasing the place “Path” can be found

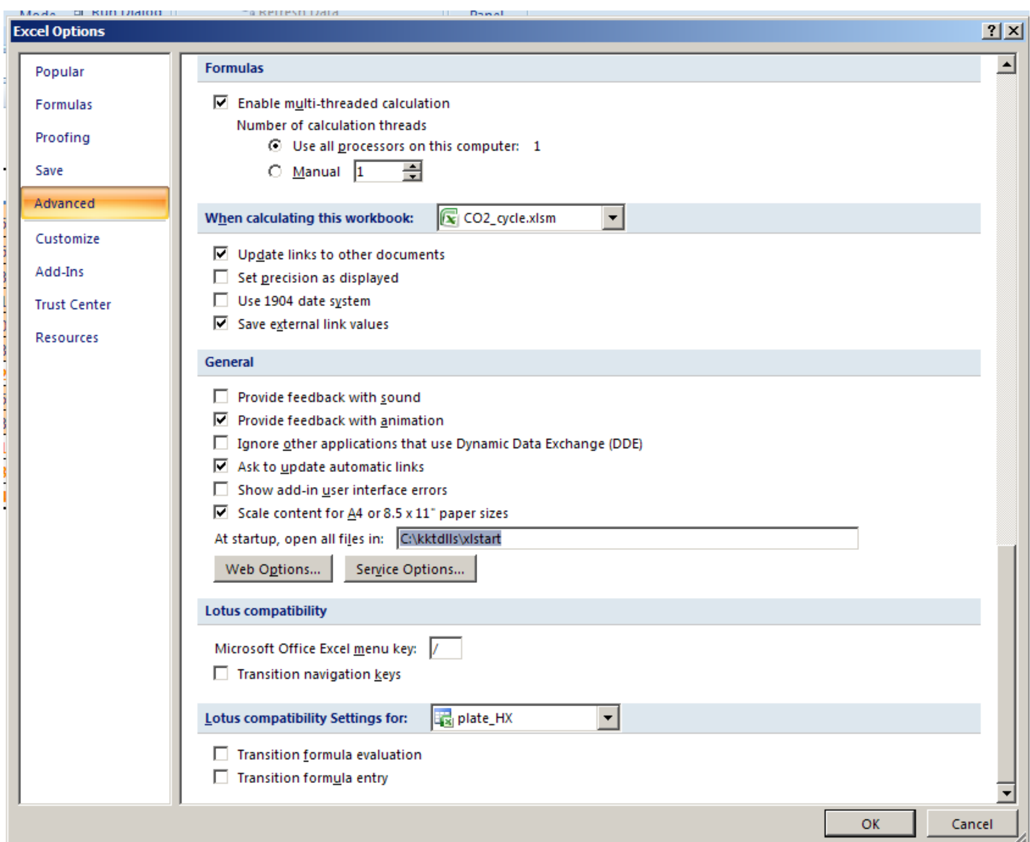

Figure 34 RN-Lib configuration in excel

K. Manual for the use of the refrigeration cycles calculation modul

The modul to create the circuit are devided into files for each used refrigerant, namely:

- *"CO2_cycle.xlsm"* for the R744 circuit
- *"Glycol_cycle.xlsm"* for the ethylene glycol circuit, evaporating R744
- *"Water_cycle.xlsm"* for the ethylene glycol circuit, cooling R744

3	constants						
4	compressor inlet				compression		
5	t_1 [°C]	0		calculate	t_1' [°C]	-10	
6	p_1 [Bar]	26,4983154			p_1' [Bar]	26,4983154	
7	h_1 [kJ/kg]	751,951475			h_1' [kJ/(kgK	737,849054	
8	s_1 [kJ/(kgK)]	4,06900364			s_1' [kJ/(kgK)	4,01628901	
9	v_1 [m^3/kg]	0,01536472			v_1' [m^3/kg	0,01404622	
10	x [-]	1,07861384			x [-]	0,99672618	
11	P_Ku [W]	100000					
12	eta_s [-]	0,8					
13	eta_m [-]	1					
14	kappa [-]	1,3543					
15	gas constant	188,92					
16	flowrate [kg/	1	1	1	Q_in [W]	200000	*R744heating*
17	Q_re [W]	200000	*R744 cooling*		Q_zw [W]	14102,4214	*internal heat transfer*

Figure 35 Interface of CO2_cycle.xlsm - constants

In the sheet *"constants"* for each refrigeration circuit following parameters (indicated by the brown background colour) can be determined as shown in Figure 35:

- the pump/compressor power
- pump/compressor inlet temperatures
- the amount of heat transfer
- the mass flow for each heat exchanging process
- efficiency coefficient

Then putting the parameters in it should be considered that the heat rejection and the inlet heat have the same value.

When pressed on the button *"calculate"* the thermodynamic values for each process will be created in the sheet *"ideal_CP"*. The diagrams on the right hand side are vague presentation of the circuit.

A specific p,h-diagram can be created with the file *"p,h-diagram.xlsm"*, It takes the data from the file *"CO2_cycle.xlsm"* and creates the cyclic process in a p,h-diagramm. As the process can take a long time on standard personal computers the steps (accuracy) of each thermodynamic variable can be changed. Every button indicates what type of data first should be visualized. It is important to create the desired pressure range first by pressing the button "*pressure*" as seen in Figure 36. The p,h-diagram is then showcased in the sheet p,h-diagram.

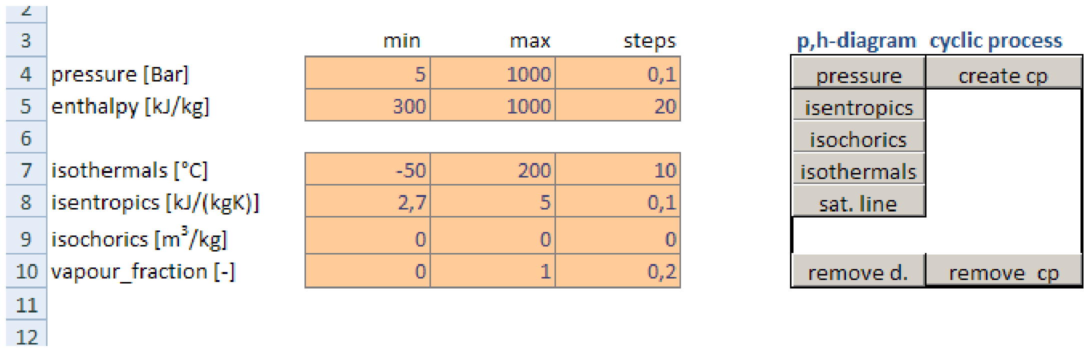

Figure 36 Interface of p,h-diagram.xlsm - layout_data

L. Manual for the use of the plate heat exchangers calculation modul

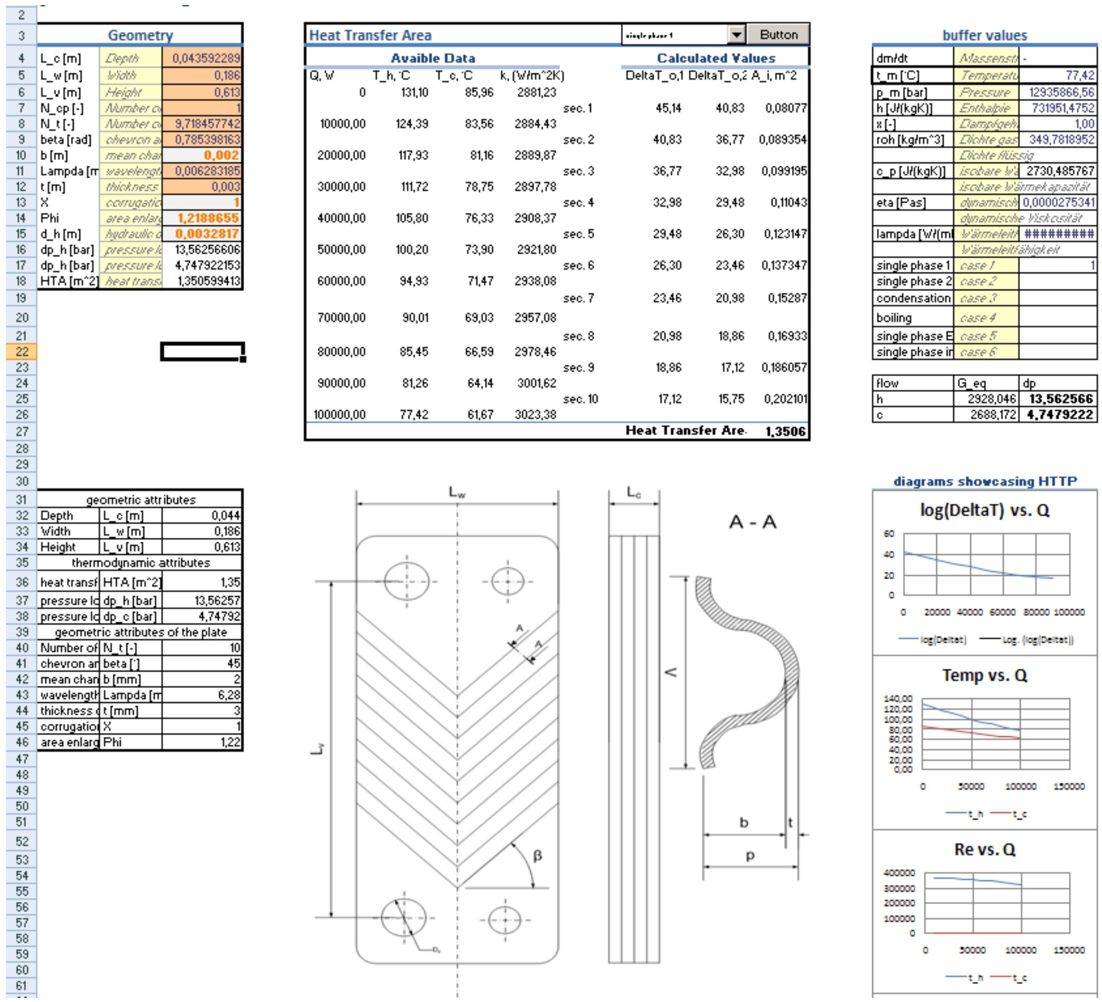

Figure 37 Modul interface for calculating the heat transfer area.

The Modul for calculating the heat transfer area can be found in the file *"CO2_cycle.xlsm"* under the sheet *"plate_HX",* the interface is showcased in Figure 37. On the left hand side the geometrical parameters for the plate heat exchanger can be inserted. The heat transfer area (hta) can be calculated by first choosing the desired heat transfer process in the dropdown list. Each heat transfer process is related to a heat exchanger. Thus the evaporation process indicates that the required hta will be calculated for the evaporating heat exchanger. The values for the process will be taken from the files of each refrigerant. If the values in the circuit are thermodynamically impropriate (e.g. the inlet R744 temperature is lower than the outlet EG temperature during the cooling process of R744) the programme will display an error message and leads the user directly to the programme code. In these cases the error should be neglected and another volume for the circuit should be considered. Diagrams showcase the process of the heat transfer with different values versus the heat transfer. They help to indicate there an impropriate assumption has been made in the cycle of each refrigerant.

M. Manual for the use of the macro to calculate the pressure loss in pipes

The pipe geometries are listed in the file "*pipes.xlsm*". To calculate the pressure loss of the pipes, the pressure resistance coefficient λ has to be determined iteratively. This macro is assigned to the shortcut key "STRG+l". Before pressing the shortcut the cell must be selected as indicated in Figure 38. The values are connected to the file "*pressure_vessels.xlsx*" to determine the necessary buffer volume for the vessel.

2															
3	pipe	dm/dt [kg/	w [m/s]	rho [kg/m^	ny [m^2/s]	PN [bar]	d_i [m]	e [m]	l [m]	V [m^3]	k	Re=f(d,w,ny)	lambda_R=f(k	Zeta_Krümme	Zeta_Fittings/	Deltap [bar]
4	CO2															
5	compressing															
6	101.01	1	19,6302	216,717	1,11E-07	130	0,0173	0,002	1,3	0,0177	2E-06	3059432	0,0128	0,33	0	0,5399
7									**1,3**	**0,0177**						**0,5399**
8	cooling															
9	102.01	1	5,01	313,143	8,3E-08	130	0,0285	0,0026	1,5	0,0336	2E-06	1717363	0,0124	0,11	1,4	0,0848
10																
11																
12																
13																
14	102.06	1	5,01	313,143	8,3E-08	130	0,0285	0,0026	0,45	0,0101	2E-06	1717363	0,0124	0,11	2,7	0,1179
15	102.07	1	5,01	313,143	8,3E-08	130	0,0285	0,0026	0,1	0,0022	2E-06	1717363	0,0124	0,11	0	0,0060
16	102.08	1	5,01	313,143	8,3E-08	130	0,0285	0,0026	0,1	0,0022	2E-06	1717363	0,0124	0,11	2,7	0,1120

Figure 38 pipes – geometries and pressure loss